

**THE EFFECTS OF EARTHQUAKE EXCITATIONS ON RETICULATED DOMES**

**by**

**David A. Uliana**

**Thesis submitted to the Faculty of the  
Virginia Polytechnic Institute and State University  
in partial fulfillment of the requirements for the degree of  
MASTER OF SCIENCE**

**in**

**CIVIL ENGINEERING**

**APPROVED:**

**Dr. S. M. Holzer**

**Dr. A. E. Somers, Jr.**

**Dr. R. H. Plaut**

**February, 1985  
Blacksburg, Virginia**

## ACKNOWLEDGMENTS

The author would like to express his gratitude to Dr. S. M. Holzer for his guidance, unlimited patients, and helpful suggestions throughout the researching and writing of this manuscript. The completion of this thesis would have been impossible without his help. Gratitude is also extended to Dr. A. E. Somers, Jr., and Dr. R. H. Plaut for their helpful comments and for reviewing this thesis.

A special and most sincere thanks is extended to , and for being my family away from home, to for being an exceptional officemate and consultant, and to and for their friendship through the difficult times.

The financial support provided by the Department of Civil Engineering and the use of the Virginia Tech computing facilities are also greatly appreciated.

## TABLE OF CONTENTS

<b>ACKNOWLEDGMENTS . . . . .</b>	<b>ii</b>
<b>LIST OF TABLES . . . . .</b>	<b>v</b>
<b>LIST OF FIGURES . . . . .</b>	<b>vi</b>
<b><u>Chapter</u></b>	<b><u>Page</u></b>
<b>I. INTRODUCTION . . . . .</b>	<b>1</b>
Objectives . . . . .	1
Literature Review . . . . .	3
<b>II. STRUCTURAL MODEL . . . . .</b>	<b>8</b>
Introduction . . . . .	8
The Tangent Stiffness Matrix . . . . .	9
Dome Models . . . . .	12
<b>III. STATIC ANALYSIS . . . . .</b>	<b>17</b>
Introduction . . . . .	17
Newton-Raphson Method . . . . .	20
Convergence Criteria . . . . .	23
Discussion of Stability . . . . .	26
<b>IV. DYNAMIC ANALYSIS . . . . .</b>	<b>31</b>
Introduction . . . . .	31
Modeling Earthquake Excitations . . . . .	32
Damping Matrix . . . . .	34
The Newmark-Beta Method . . . . .	36
Linear Analysis . . . . .	36
Nonlinear Analysis . . . . .	37
Discussion of Time Steps . . . . .	39
<b>V. RESULTS . . . . .</b>	<b>41</b>
The Finite Element Program . . . . .	42
Comparison with Previous Results . . . . .	42
Checks on Some Assumptions . . . . .	58
Small Lamella Dome . . . . .	59
Static Analyses . . . . .	59
Dynamic Analyses . . . . .	66
Large Dome . . . . .	68
Static Analyses . . . . .	68
Dynamic Analyses . . . . .	83

## TABLE OF CONTENTS (continued)

	<u>Page</u>
Comparisons of Stresses for Both Large and Small Domes . . . . .	90
VI. CONCLUSIONS AND RECOMMENDATIONS . . . . .	100
Conclusions . . . . .	100
Recommendations for Future Research . . . . .	101
REFERENCES . . . . .	104
 <u>Appendix</u>	
A. FREQUENCIES OF VIBRATION FOR THE SMALL LAMELLA DOME . . . . .	110
B. FREQUENCIES OF VIBRATION FOR THE LARGE LAMELLA DOME . . . . .	111
C. PROGRAM LISTING . . . . .	114
VITA . . . . .	189
ABSTRACT	

## LIST OF TABLES

<u>Table</u>	<u>page</u>
1. Maximum stresses of static analysis for numbered members of the small dome. . . . .	63
2. Maximum allowable stresses and buckling stresses for numbered members of the small dome. . . . .	64
3. A comparison of maximum stresses in numbered members of the small dome for dead load only. . . . .	75
4. A comparison of maximum stresses in numbered members of the small dome for dead load plus 10 lb./ft. <sup>2</sup> . 76	76
5. A comparison of maximum stresses in numbered members of the small dome for dead load plus 20 lb./ft. <sup>2</sup> . 77	77
6. A comparison of maximum stresses in numbered members of the small dome for dead load plus 30 lb./ft. <sup>2</sup> . 78	78
7. A comparison of maximum stresses in numbered members of the small dome for dead load plus 40 lb./ft. <sup>2</sup> . 79	79
8. Maximum stresses of static analysis for numbered members of the large dome. . . . .	82
9. Maximum allowable stresses and buckling stresses for numbered members of the large dome. . . . .	84
10. A comparison of maximum stresses in numbered members of the large dome for dead load only. . . . .	92
11. A comparison of maximum stresses in numbered members of the large dome for dead load plus 20 lb./ft. <sup>2</sup> . 94	94
12. A comparison of maximum stresses in numbered members of the large dome for dead load plus 40 lb./ft. <sup>2</sup> . 96	96

## LIST OF FIGURES

<u>Figure</u>	<u>page</u>
1. Member end displacements for a typical truss element. . . . .	10
2. Large lamella dome. . . . .	13
3. Small lamella dome . . . . .	15
4. The tributary area for the top node of the domes. . . 19	
5. The Newton-Raphson method for a one degree-of-freedom system. . . . .	22
6. The Modified Newton-Raphson method for a one degree-of-freedom system. . . . .	24
7. Equilibrium path for a one degree-of-freedom system. 29	
8. One degree-of-freedom plane truss presented by Nickell. . . . .	43
9. Displacement vs. load graph for the static analysis of the one degree-of-freedom truss presented by Nickell. . . . .	44
10. Displacement vs. time graph for the dynamic analysis of the one degree-of-freedom truss presented by Nickell. . . . .	45
11. Ten member plane truss presented by Noor and Peters	46
12. Displacement vs. time graphs of joint A for linear and nonlinear analyses of the ten member truss. . . 48	
13. Axial force in member B for the linear analysis of the ten member truss. . . . .	49
14. Axial force in member B for nonlinear analysis of the ten member truss. . . . .	50
15. A comparison of the stress-strain relationships. . . 51	
16. Large ten-bay truss presented by Noor and Peters. . . 53	

17. The displacement of joint A for the linear analysis of the ten-bay space truss. . . . .	54
18. Axial force in member B for linear analysis of the ten-bay space truss. . . . .	55
19. Displacement of joint A for nonlinear analysis of the ten-bay space truss. . . . .	56
20. Axial force in member B for nonlinear analysis of the ten-bay space truss. . . . .	57
21. Small lamella dome with numbered members. . . . .	60
22. Load vs. displacement curves for uniform load on the small dome. . . . .	61
23. Load vs. displacement curves for nonuniform load on the small dome. . . . .	65
24. Accelerations, velocities and displacements for the El Centro earthquake of May 18, 1940. . . . .	67
25. Displacement of joint A for dead load only on the small dome. . . . .	69
26. Displacement of joint A for dead load plus 10 lb./ft. <sup>2</sup> on the small dome. . . . .	70
27. Displacement of joint A for dead load plus 20 lb./ft. <sup>2</sup> on the small dome. . . . .	71
28. Displacement of joint A for dead load plus 30 lb./ft. <sup>2</sup> on the small dome. . . . .	72
29. Displacement of joint A for dead load plus 40 lb./ft. <sup>2</sup> on the small dome. . . . .	73
30. A comparison of the displacements of node A for several live loads on the small dome. . . . .	74
31. Large lamella dome with numbered members. . . . .	80
32. Load vs. displacement curves for uniform load on the large dome. . . . .	81
33. Load-displacement curves for nonuniform load on the large dome. . . . .	86

34. Displacement of joint A for dead load only on the large dome. . . . .	87
35. Displacement of joint A for dead load plus 20 lb./ft. <sup>2</sup> on the large dome. . . . .	88
36. Displacement of joint A for dead load plus 40 lb./ft. <sup>2</sup> on the large dome. . . . .	89
37. A comparison of the displacements of joint A for the two live loads on the large dome. . . . .	91

## Chapter I

### INTRODUCTION

#### 1.1 OBJECTIVES

Dome structures, in particular reticulated domes, have demonstrated their usefulness as strong, light-weight coverings over large areas such as stadiums, industrial buildings and exhibition centers where large, unobstructed areas are required. They enclose a maximum amount of space with a minimum surface and are economical because they require little material as compared to other structures. Several different dome configurations exist. Some of the more popular configurations are the lamella, the geodesic, and the Schwedler domes.

Many studies have been performed by various researchers to analyze these domes under static loads. They have repeatedly demonstrated the domes' strength and economy for Civil Engineering applications. The author found no references, however, that presented results for dynamic analyses of full sized reticulated domes. Due to an increasing interest in earthquake resistant design of structures, dynamic analyses of these domes are definitely needed.

This thesis is a study of the behavior of full sized domes, designed under static criteria and subjected to

earthquake excitations. Static analyses are performed on two lamella domes. The axial stresses and strains in all members are determined for several distributed static loads. Dynamic analyses are then performed on the same structures with the same distributed loads. The dynamic loads are in the form of earthquake excitations to the bases of the domes. Axial stresses and strains in all members are determined and compared to those of the static analyses. The displacements of several nodes for both analyses are given and effects of the earthquake motions on the stability of the domes and their members are determined.

A finite element computer program written by the author (see Appendix C) was used to perform these analyses. The program can analyze geometrically and materially nonlinear behavior of space trusses subjected to static or dynamic loads. The direct integration procedure used is the Newmark-Beta method and the nonlinear solution technique is the Newton-Raphson method. The program can calculate the displacements, velocities, and accelerations of all nodes as well as the axial stresses and strains of all members at each load or time step. The ability to determine if any member reaches its buckling load or if the dome becomes globally unstable is also present in the program.

## 1.2 LITERATURE REVIEW

A literature search revealed that there is little research done on the dynamic analysis of space truss structures. No references were found that addressed the topic of earthquake excitations on reticulated domes. Several references were found that closely relate to this topic, though none use the space truss specifically. Penzien and Liu (43) and Tanabashi (52) address the solution of nonlinear structures subjected to earthquake excitations while Berger and Shore (8) and Carter, Dib and Mindle (10) present the dynamic response of nonlinear structures.

In order to cover the thesis topic more carefully, three subjects were searched for pertinent literature. These subjects are:

1. Analysis of space trusses
2. Methods for structural dynamics solutions
3. Modeling earthquake excitations

A review of these subjects provides a review of the thesis topic.

One method of analysis that is used to model large space trusses, such as reticulated domes, is to replace the truss with a continuum model. The continuum model may then be solved with familiar methods of mechanics. Forman and Hutchinson (16) and Crooker and Buchert (12) present methods

to replace a space truss with a continuous shell. Renton (45) models a repetitive space truss as a continuous beam and Noor, Anderson and Greene (40) offer approximations for beam-like and plate-like lattices. Conventional finite element analyses of large systems would be expensive and time consuming. These methods allow relatively inexpensive analyses of large repetitive structures.

Force and displacement methods are popular for analyzing trusses since a truss model may be defined by a finite number of forces or displacements. Methods such as Maxwell-Mohr and matrix analysis are relatively simple for linear models. Goldberg and Richard (19) and Hensley and Azar (22) derive analyses methods for material nonlinearities while Epstein and Tene (15) and Jagannathan and Epstein (29) consider the geometric nonlinearities. A mixed formulation is provided by Noor (38) who considered both material and geometric nonlinearities, and a geometrically nonlinear stiffness matrix for a space truss element is derived by Baron and Venkatesan (2) with perturbation techniques. Reducing the number of degrees-of-freedom for these nonlinear problems is desirable for many analyses. A discussion on the reduction of the number of degrees-of-freedom of nonlinear problems is given by Noor (39).

For trusses that should be modeled with imperfect members, Rosen and Schmit (47) and (48) have both an accurate and an approximate method to include the imperfections. If the effects of transverse loads are desired, then a frame element is needed. A model for a geometrically nonlinear pin-jointed frame is presented by McConnel and Klimke (33). The pin-jointed frame has the characteristics of a truss but permits bending strains. For dynamic analyses of nonlinear space trusses, which is required for this study, Noor and Peters (41) use a mixed method.

Several techniques exist for the solution of structural dynamics problems. Among some of the less familiar methods are the Finite Strip Method (11), the Runge-Kutta Method (27) and the Fast Fourier Transform Method (20). These methods have not proved to be as popular for solutions of multi-degree-of-freedom systems as modal analysis and direct integration. Der Kiureghian (13) presents a probabilistic approach to linear modal analysis and Nickell (36) presents a deterministic approach to nonlinear modal analysis.

For solution of nonlinear problems like the space truss, direct integration proves to be much more suitable than modal analysis, according to Ref. 18. Several different direct integration procedures exist. Some of these methods are the Central Difference method (42), the Wilson- $\theta$  method

(54), the Newmark method (34) and the method proposed by Ginsburg and Gilbert (18). Two important factors to consider when using direct integration are the stability and accuracy of the solution. Nickell (35), Preumont (44) and Bathe and Wilson (7) discuss stability and accuracy while Hinton, Rock and Zienkiewicz (24) and Bathe and Cimento (6) present methods for increasing the accuracy and economy of a solution. Atalik (1) makes solutions more economical by constructing linear approximations for the element mass, damping and stiffness matrixies for nonlinear problems.

Earthquake excitations may be modeled in two ways. Either an actual digitized accelerogram may be used or an artificial accelerogram may be produced. Real digitized data, such as that given by Haroun (21), are available for many earthquakes. Data in this form, however, may not be useful if it is digitized in time increments that are not appropriate. Liou (32) offers a numerical method for redigitizing seismic data without producing superficial frequencies.

An accelerogram may be generated artificially if it is more desirable than the available digitized data. Earlier methods for producing artificial accelerograms were mostly deterministic. Bernrueter (9) finds maximum acceleration only, St. Balan, et. al. (50) generate an accelerogram as a series of trigonometric functions and Wong and Trifunac (55)

use a Fourier transform method. These and other deterministic methods have been replaced by probabilistic formulations due to an increasing interest and understanding of the variability of earthquake ground motions. Some of the most recent research on this topic is presented by Kubo and Penzien (31), Kameda and Ang (30), Housner and Jennings (27), Trifunac (53) and Iyengar and Iyengar (28). These studies demonstrate how to generate artificial accelerograms through probabilistic methods.

Because of the distinct advantages of reticulated domes and the increasing interest in earthquake resistant design of structures, the thesis topic should be of increasing interest in the future.

## Chapter II

### STRUCTURAL MODEL

In this chapter the tangent stiffness matrix for a geometrically nonlinear space truss element is presented. It is derived by the familiar principle of virtual work. This chapter also presents the domed structures that will be used in the analysis.

#### 2.1 INTRODUCTION

A reticulated dome is a collection of one-dimensional elements assembled in space so that their joints lie on a spherical surface. These one-dimensional elements may be modeled either as truss elements, where only axial elongation and contraction are considered, or frame elements, for which torsion and bending about two axes are also considered. For a space truss each element has six translational degrees of freedom. For a space frame each element has six translational and six rotational degrees of freedom.

A space truss element was chosen for this study for the following reasons:

1. Members of a reticulated dome are usually joined in a fashion that more closely resembles a pinned connection than a rigid connection.

2. Dynamic nonlinear analyses are, by nature, time consuming. The space truss element has fewer degrees of freedom and is more economical.

The geometry of a reticulated dome and slenderness of its members allow for the possibility of large displacements and rotations although the strains that develop can be small. This results in geometrically nonlinear behavior which is the result of a nonlinear strain-displacement relation and equilibrium being formulated on the deformed structure. For these problems strains are not generally proportional to displacements. The nonlinearity must be considered in the formulation of the stiffness matrix.

## 2.2 THE TANGENT STIFFNESS MATRIX

The tangent stiffness matrix used in this study was derived by Holzer and is presented in detail in Ref. 25. The undeformed state and the deformed state of a typical truss element are shown in Fig. 1. During the deformation the element may translate and rotate significantly with only small strains being produced. Expressing the displacements of the element as the sum of rigid body displacements and deformations is desirable. The initial, undeformed state is labeled I.S., the rigid body state is labeled R.B.S. and the deformed state D.S. The tangent stiffness matrix of an element  $i$  is given by

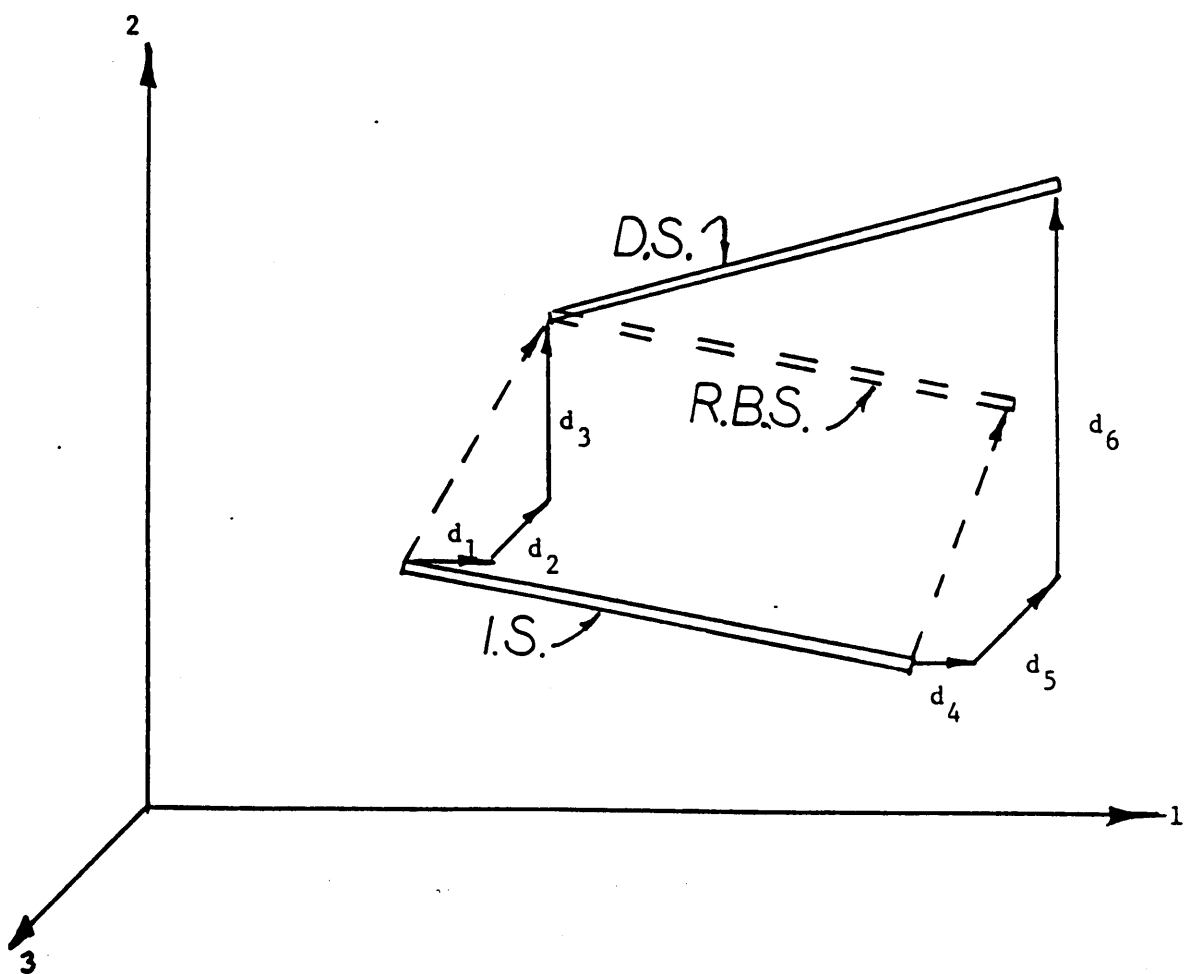


Figure 1: Member end displacements for a typical truss element.

$$K^i = \left[ \frac{\partial^2 U}{\partial d_j \partial d_k} \right] \quad (1)$$

where  $U$  is the strain energy of the element. The resulting matrix is the sum of the familiar linear stiffness matrix for a space truss and a nonlinear matrix. They combine to form the tangent stiffness matrix for an element given by

$$K^i = \begin{bmatrix} \bar{K}^i & -\bar{K}^i \\ -\bar{K}^i & \bar{K}^i \end{bmatrix} \quad (2)$$

where

$$\bar{K}^i = \gamma_i \begin{bmatrix} \frac{L_i}{L_{0i}} - (1 - C_1^2) & C_1 C_2 & C_1 C_3 \\ C_1 C_2 & \frac{L_i}{L_{0i}} - (1 - C_2^2) & C_2 C_3 \\ C_1 C_3 & C_2 C_3 & \frac{L_i}{L_{0i}} - (1 - C_3^2) \end{bmatrix} \quad (3)$$

sym.

and

$$\gamma_i = \frac{E_i A_i}{L_i} \quad (4)$$

For each member ' $i$ ',  $E_i$  is Young's Modulus of the material,  $A_i$  is the cross-sectional area,  $L_i$  is the deformed length and  $L_{0i}$  is the undefor med length.  $C_1$ ,  $C_2$ , and  $C_3$  are the direction cosines in the global 1, 2, and 3 directions, respectively.

### 2.3 DOME MODELS

Two structural models are used for analysis. One dome is a large lamella dome used in a study by Richter (46). A diagram appears in Fig. 2. The dome has a 100 foot base, a 14 foot height at the center and lies on the surface of a 200 foot diameter sphere. All of the members are tubular with an outside diameter of 6.00 in., a cross sectional area of  $3.18 \text{ in.}^2$ , and a cross sectional inertia of  $15.64 \text{ in.}^4$ . The material is T60-6011 aluminum (49) with a yield strength of 35 ksi. and a modulus of elasticity of 10,300 ksi. The lamella dome has three rings and ten radial sections. This structure was chosen for several reasons:

1. Data for the static analysis is readily available.
2. The geometry of the lamella dome is relatively easy to define.
3. There is a natural truncation ring at the base of the dome.

Two different boundary conditions are used for this dome, one for the static analysis and one for the dynamic analysis. For the static analysis a complete dome with a tension ring provides the most realistic model. With the tension ring the dome has 150 members, 61 joints, and 149 degrees of freedom. It is constrained in the vertical direction at every base joint, in both horizontal directions at the top of

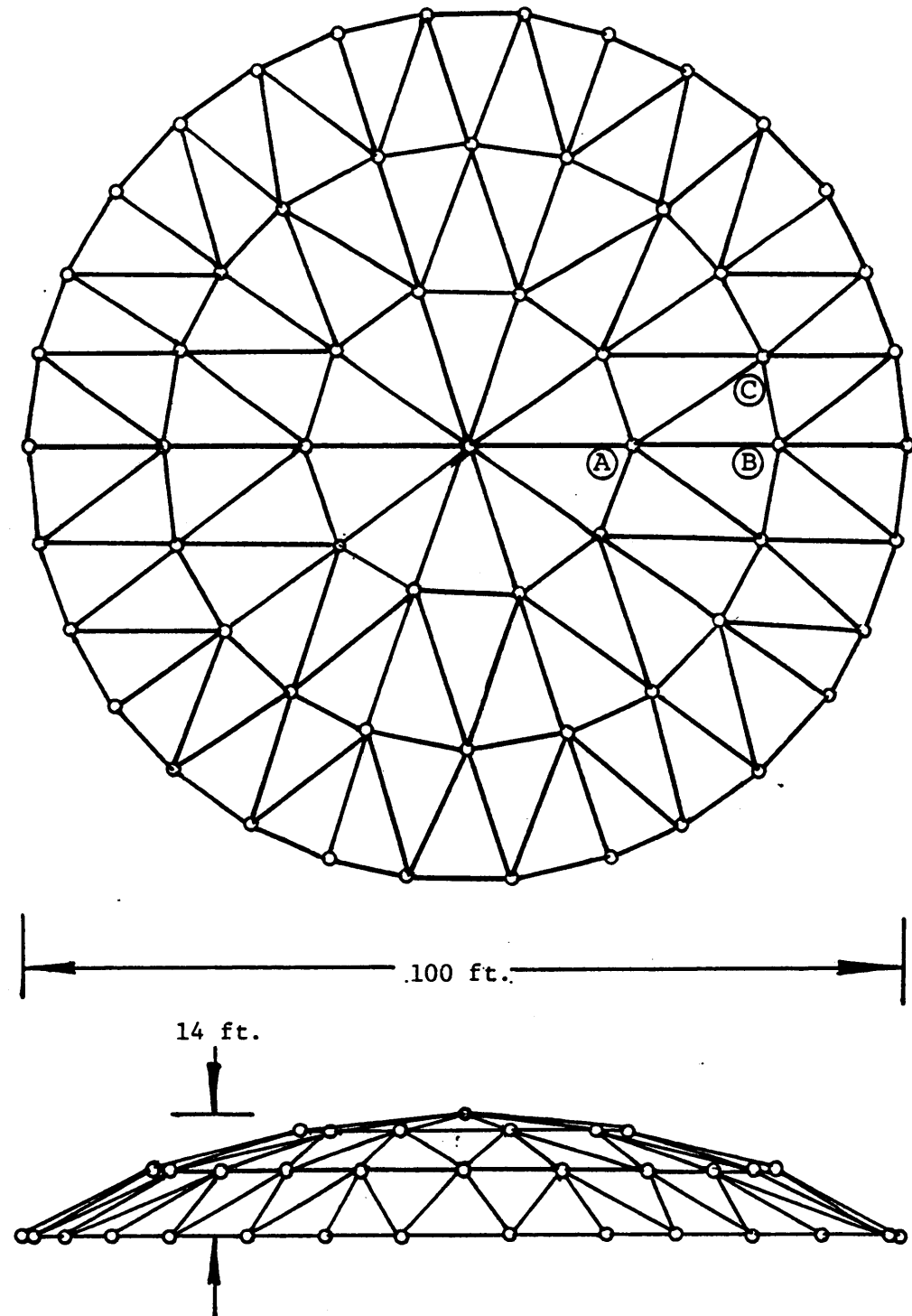


Figure 2: Large lamella dome.

the dome (to avoid translation of the dome) and in two other horizontal directions (to avoid rotation of the dome). For the dynamic analysis base joints are pinned. This model has 120 members, 61 joints, and 93 degrees of freedom. Since each base joint is constrained in all three directions the tension ring is rendered useless and the members are not included.

For the second model a smaller lamella dome was desirable because:

1. A comparison between similar domes of different sizes could be made.
2. Fewer degrees of freedom will require far less computer time; therefore, more extensive testing may be performed.

The dome chosen was a truncation of the larger dome at its second ring (See Fig. 3). All element properties and dimensions are the same as in the larger dome.

As before, two different boundary conditions for this dome are considered. For the static analysis the dome with the tension ring has 70 members, 31 joints, and 69 degrees of freedom. It is constrained in the same manner as the larger dome. The fixed base dynamic model has 50 members,

15

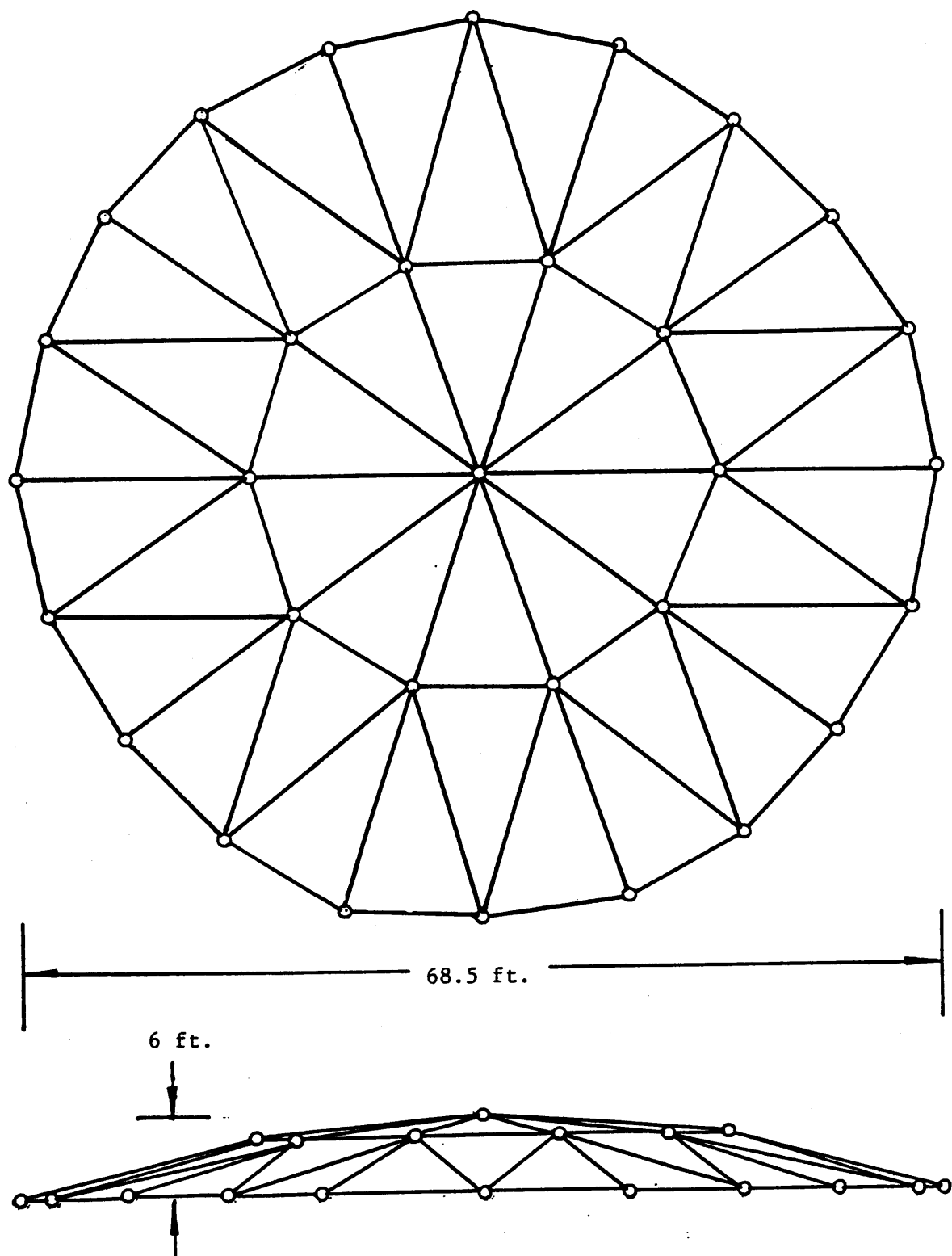


Figure 3: Small lamella dome

31 joints, and 33 degrees of freedom. This 33 degree-of-freedom dome requires much less computer time per run and is used in a majority of the dynamic testing.

A geodesic geometry was considered for comparison with the small lamella dome. However, a small geodesic with the same number of joints and the same overall dimensions as the lamella could not be defined without severely modifying the geodesic geometry to form a base ring. The geodesic geometry has no natural truncation ring for a shallow dome. Also, a limit on the expense of the dynamic analyses was desired, therefore, the geodesic dome was not included.

## Chapter III

### STATIC ANALYSIS

In this chapter a description of the static analysis process is given. The nonlinear solution technique used is the Newton-Raphson method. This description is followed by discussions on convergence criteria and stability of domed structures.

#### 3.1 INTRODUCTION

A description of the static analysis process is included in this study. The reasons that it is included are:

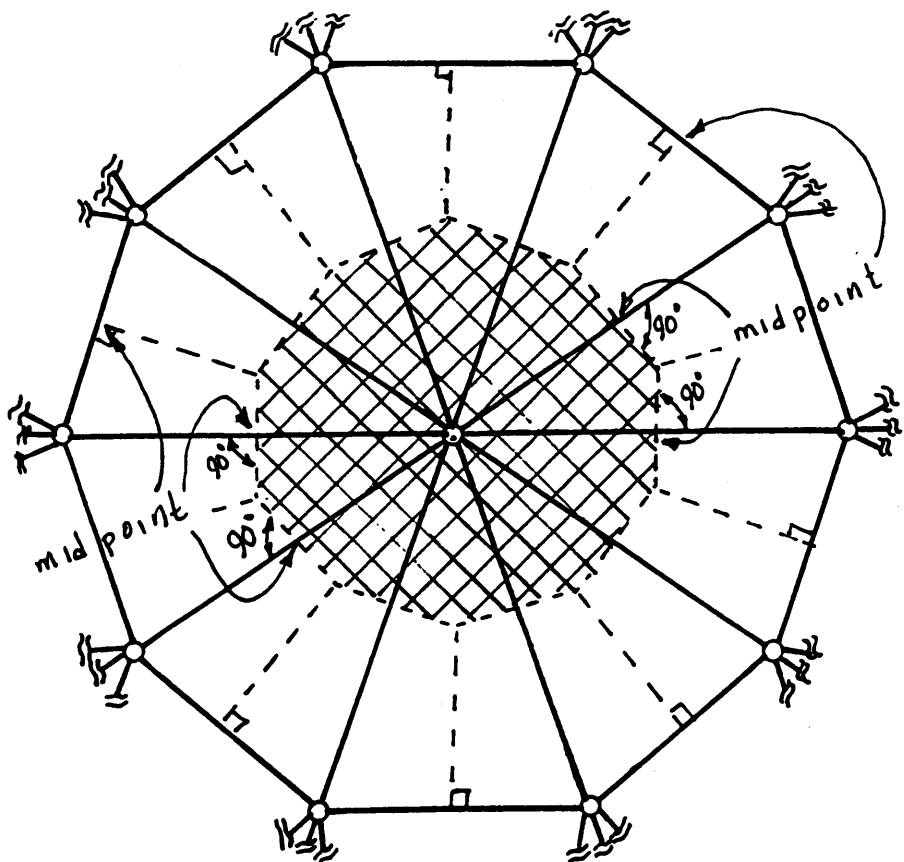
1. Static analyses are the most common analyses for space structures.
2. The dynamic analysis is actually reduced to an equivalent static analysis at every time step by the Newmark-Beta method.
3. A static analysis should always precede a dynamic analysis when designing a structure.

The static procedure was used in this study to determine the nodal displacements and the element stresses caused by several distributed live loads. The live loads used are 10, 20, 30, and 40 lb./ft.<sup>2</sup>. These values represent the maximum snow loads for most regions of the United States according

to Ref. 17. Several loads are used in order to show a comparison between loads, displacements and stresses.

The distributed load must be transformed into a series of concentrated nodal forces in order to include it in the analysis. Each force is equal to the snow load times the tributary area around the node. An example of the tributary area for the top node of both domes is given in Fig. 4. This area is the projected area on the horizontal plane and is equal to 250.8 square feet. The tributary area for each node in the first ring (node type A of Fig. 2) is 154.2 square feet. The tributary area for each node of the second ring is 145.8 square feet for node type B of Fig. 2, and 149.1 square feet for node type C. The same areas apply to the small dome of Fig. 3. A load vector may be formulated by multiplying the distributed load times these areas.

Transforming the distributed load into a load vector is a realistic assumption for many domes since suspending a load carrying sheet from the joints of a dome is common. For these domes the snow load is truly applied to the nodes. For many other domes, however, rigid panels are attached directly to the members. In these domes bending strains develop that cannot be neglected. A paper by Renton (45) addresses the modeling of space trusses for beam-like behavior and McConnel and Klimke (33) discuss the analysis of pinned-



PROJECTION ON THE HORIZONTAL PLANE FOR TOP NODE.

- TRIBUTARY AREA. (250.8 sq. ft.)

Figure 4: The tributary area for the top node of the domes.

end space frames. In this study, however, the bending effects are not considered.

### 3.2 NEWTON-RAPHSON METHOD

The basic equation to be solved in nonlinear analysis is

$$Q - \lambda + \Delta\lambda F = 0 \quad (5)$$

$Q$  is the external nodal load vector which can also be written as  $(\lambda + \Delta\lambda)\bar{Q}$  where  $\lambda$  is a scalar and  $\bar{Q}$  is a constant vector, and  $\lambda + \Delta\lambda_F$  is the nodal force vector that results from element stresses. When Eq. (5) is satisfied the system is in equilibrium. A nonlinear solution technique is required since  $\lambda + \Delta\lambda_F$  is not a linear function of the nodal displacement vector  $\lambda + \Delta\lambda_q$ . This description of the nonlinear solution technique is given for the static analysis. The reader should understand that the technique is the same for dynamic analyses where  $t$  may replace  $\lambda$ .

One of the most popular techniques for the solution of nonlinear equations is the Newton-Raphson method. By applying this method Eq. (5) becomes

$$K^{(i)} \Delta q^{(i+1)} = Q - F^{(i)} = R^{(i)} \quad (6)$$

for the  $i$ 'th iteration where  $K^{(i)}$  is the tangent stiffness matrix at  $q^{(i)}$ . A complete derivation appears in Ref. 3.

Eq. (6) is solved repeatedly until a new equilibrium state is obtained with a sufficient degree of accuracy (See section 3.3).

The Newton-Raphson method requires a known equilibrium position ( $q^0, Q^0$ ) to start the iterative process. Refer to Fig. 5 for a graphical representation of a one degree-of-freedom system. The load is incremented from  $Q^0$  to  $Q$  where a new equilibrium position is sought. The tangent stiffness matrix  $K^{(0)}$  at  $q^{(0)}$  is determined and Eq. (6) is solved for  $i=0$  and  $R^{(0)} = Q - F^{(0)}$ . A new equilibrium position

$$q^{(i+1)} = q^{(i)} + \Delta q^{(i+1)} \quad (7)$$

can be found along with the nodal point forces  $F^{(i+1)}$  corresponding to  $q^{(i+1)}$ . Residual forces

$$R^{(i+1)} = (\lambda + \Delta \lambda) \bar{Q} - F^{(i+1)} \quad (8)$$

are determined and a convergence check is performed. If convergence is not reached then the tangent stiffness matrix  $K^{(i)}$  is computed and Eq. (6) is solved. This process is repeated until convergence is reached.

A modified method can also be used. The tangent stiffness matrix  $K^{(0)}$  is found for the first iteration only and Eq. (6) is solved using  $K^{(0)}$  for  $K^{(i)}$  for every iteration. A graphical representation for a one degree-of-freedom sys-

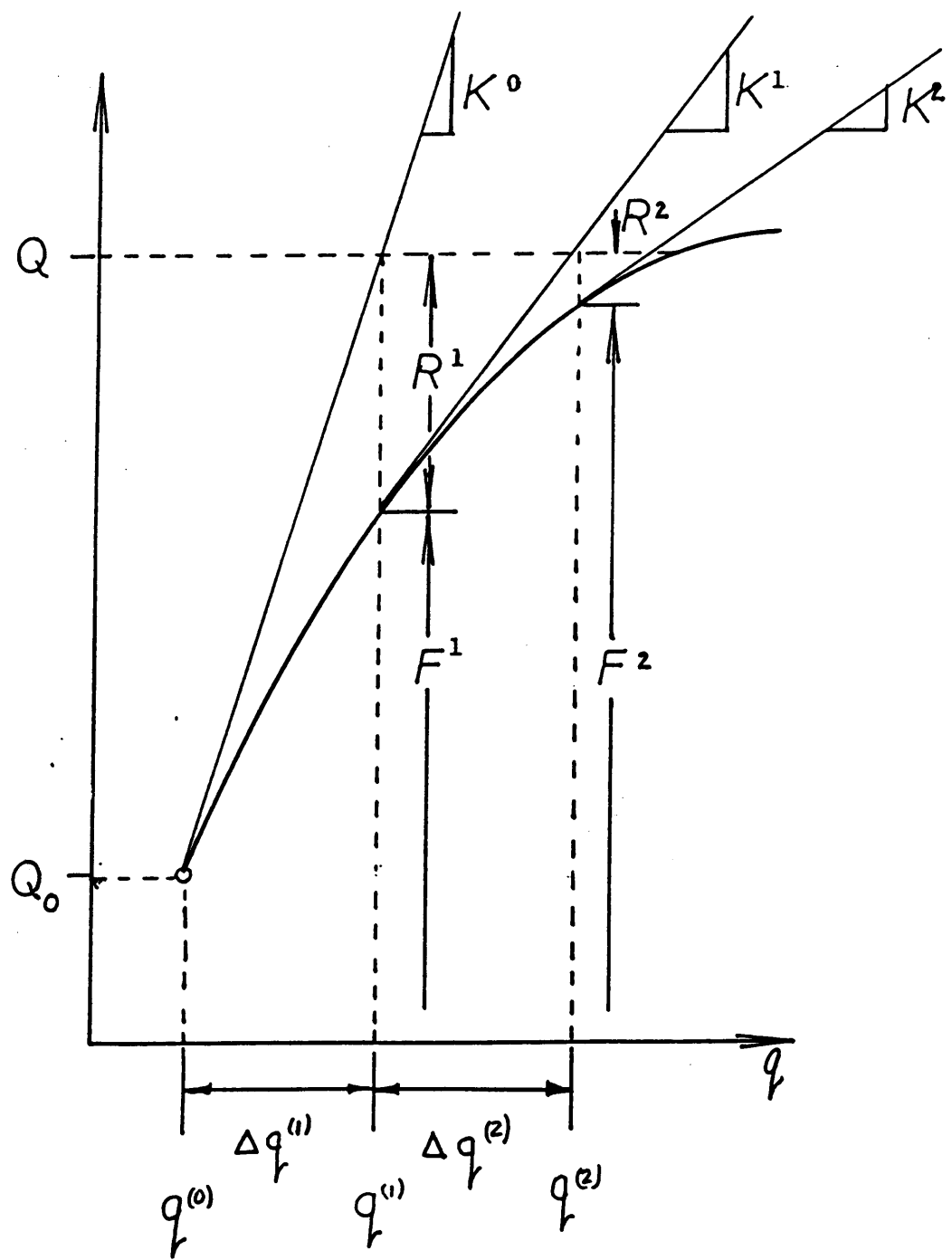


Figure 5: The Newton-Raphson method for a one degree-of-freedom system.

tem appears in Fig. 6. Using a constant tangent stiffness matrix eliminates the need for the costly processes of computing and factorizing the stiffness matrix for every iteration.

### 3.3 CONVERGENCE CRITERIA

Mathematically, the Newton-Raphson procedure will converge to an exact solution; however, it will not do so in a finite number of iterations. A condition referred to as a convergence criterion must be defined so that the iterative process may be stopped at an appropriate vector  $\mathbf{q}^{(i+1)}$  in Eq. (7). The convergence criterion may be a check on the magnitude of  $\Delta\mathbf{q}^{(i+1)}$  or on the magnitude of the unbalanced force vector  $\mathbf{R}^{(i+1)}$ . It must assure that the desired accuracy of the solution is found without excessive computational effort. Once the condition is satisfied and convergence is achieved the Newton-Raphson process is ended and the analysis proceeds on to the next load or time step.

Several methods exist to check convergence. The simplest is convergence of the norm of the change in the displacement vector

$$\|\Delta\mathbf{q}^{(i+1)}\| < \epsilon \quad (9)$$

where the norm may represent either the Euclidean norm

$$\|\Delta\mathbf{q}^{(i+1)}\| = (\sum_j \Delta q_j^{(i+1)})^{1/2} \quad (10)$$

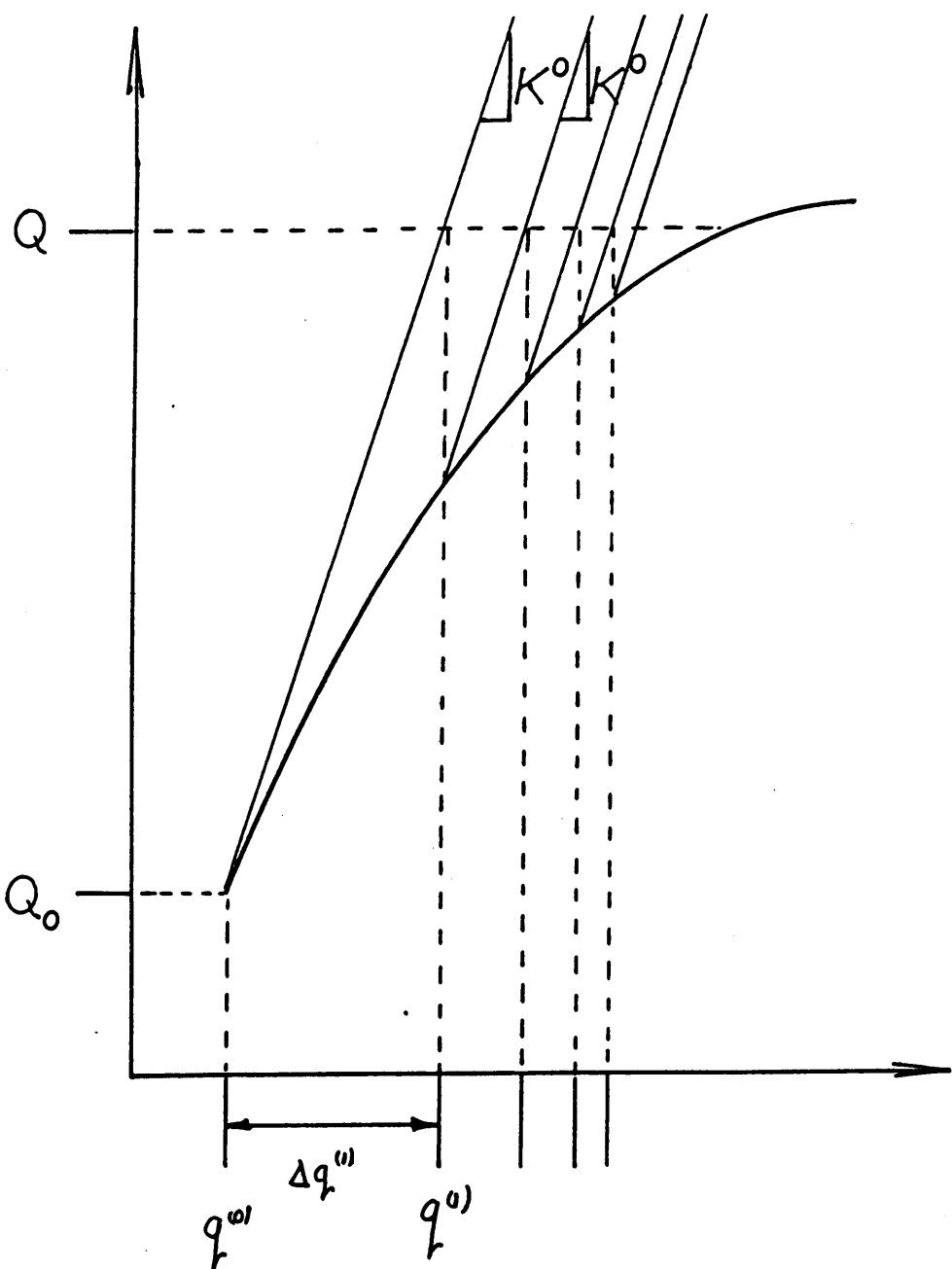


**Figure 6:** The Modified Newton-Raphson method for a one degree-of-freedom system.

or the largest absolute value of the components of  $\Delta q^{(i+1)}$ . It is apparent that the norm is not a dimensionless quantity, therefore, the value for  $e$  must be determined by considering the dimensions of the actual system. This creates a problem in that  $e$  may need to be changed for analyses of various systems. To avoid this problem the nondimensional criterion

$$\|\Delta q^{(i+1)}\| / \|q^{(i+1)}\| < e \quad (11)$$

may be used. Again,  $\|q^{(i+1)}\|$  is the norm of the total displacement vector and may be either the Euclidean norm or the largest single component of the vector. The criterion used throughout most of this study was that of Eq. (11). Bathe (6) suggests using  $e=0.001$  for this criterion.

A check on the unbalanced force vector is similar to the methods presented above. The simpler check is on the unbalanced force vector

$$\|R^{(i+1)}\| < e_R \quad (12)$$

where  $\|R^{(i+1)}\|$  may be either

$$\|R^{(i+1)}\| = (\sum_j R_j^{(i+1)2})^{1/2} \quad (13)$$

or the largest absolute value of the vector components. Here, too,  $e_R$  may need to be changed for different systems.

In order to nondimensionalize this quantity, the unbalanced force vector must be divided by the restoring force vector to create the ratio

$$\| R^{(i+1)} \| / \| F^{(i+1)} \| < e_R. \quad (14)$$

When this ratio is small enough then the  $R^{(i+1)}$  vector is insignificant and convergence is reached. This would guarantee that  $F^{(i+1)}$  is close enough to  $Q$  to assure convergence. The value of  $e_R$  could remain unchanged for different systems.

### 3.4 DISCUSSION OF STABILITY

Reticulated domes are very strong for their light weight and are able to resist great static loads. For example, the large lamella dome used in this study was able to resist a static load of 24 times its own self-weight. The geometries and relative lightness of these domes, though, make them susceptible to instabilities. A reticulated dome may become unstable long before yield stresses in the material are reached. Special consideration of instabilities may be required in order to effectively design a reticulated dome.

For the space truss the possibilities of member instabilities and global instabilities exist. For a truss member the internal force increases linearly with axial deformation

in compression until it is near the buckling load. In the vicinity of the buckling load a real, imperfect member experiences transverse deflections that increase significantly for small increases in loading provided the material remains elastic. The truss elements used in this study, however, are modeled as perfect elements that do not allow transverse deflections. In order to include a more realistic behavior, the compressive loads are assumed to increase linearly with axial deformation until the buckling load is reached, after which the compressive force is held constant at the buckling load. The buckling of a member may or may not result in a global instability that is defined below and is usually less catastrophic. One reason for this may be that the buckling of a member could redistribute forces in the structure and adjacent members may compensate for the loss in stiffness.

Global instabilities result from a decrease or loss in stiffness of the structure and exist in two forms: limit point instabilities and bifurcation instabilities. Either of these can be determined mathematically using the tangent stiffness matrix. For the nonlinear problem the tangent stiffness matrix is updated at least once every load step while for some analyses it is updated more often. Instabilities cause the stiffness matrix to become singular. For the bifurcation instability, the Newton-Raphson procedure

may be used to trace beyond the point and over the unstable post-bifurcation curve. It cannot be used, however, to trace an equilibrium path beyond a limit point. The inability to proceed past a limit point is an inherent weakness of the Newton-Raphson method. To analyze the dome past a limit point other methods such as the Riks-Wempner method (26) are required.

A practical description of both types of instabilities is presented by Supple (51). He states that under increasing deformation the dome may gradually lose its stiffness until a complete loss of stiffness is realized. At this time a dynamic jump occurs to a highly displaced configuration that is usually symmetric. This may be a limit point instability. A graphical representation for a one degree-of-freedom system is shown in Fig. 7. The complete inversion of a domed structure is an example of the equilibrium state after a limit point instability. The dome may also exhibit a sudden loss of stiffness and displace into a configuration that is different from its initial configuration. This is the bifurcation instability. The suddenness of the loss in stiffness is what differentiates the bifurcation from the limit point instability. The bifurcation is shown for a one degree-of-freedom system in Fig. 7. The equilibrium configuration reached after a bifurcation instability does not

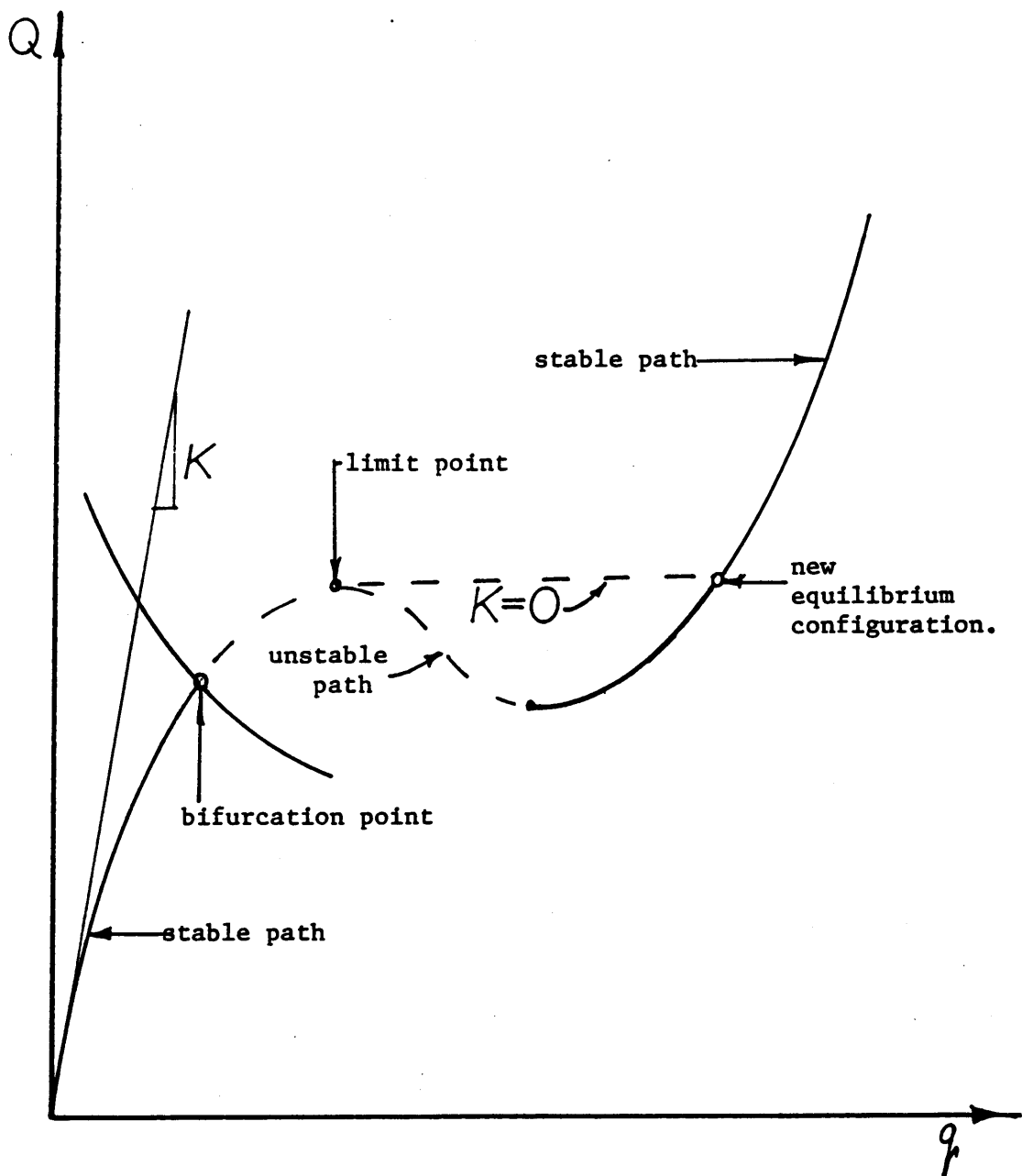


Figure 7: Equilibrium path for a one degree-of-freedom system.

have to be similar to the equilibrium configuration after a limit point instability.

## Chapter IV

### DYNAMIC ANALYSIS

In this chapter the equations associated with the dynamic analysis are presented. The dynamic finite element equations are given first followed by the method used to include earthquake excitations. The direct integration scheme chosen for this study is the Newmark-Beta method. The method's application to linear and nonlinear problems is given along with the damping matrix formulation and a discussion on time steps.

#### 4.1 INTRODUCTION

The equations of motion for a multi-degree-of-freedom system can be expressed

$$M\ddot{q} + C\dot{q} + Kq = Q \quad (15)$$

where

M-the mass matrix

C-the damping matrix

K-the stiffness matrix

$\ddot{q}$ -the nodal acceleration vector

$\dot{q}$ -the nodal velocity vector

$q$ -the nodal displacement vector

$Q$ -the dynamic nodal load vector

The type of analysis chosen for this study to solve Eq. (15) is the direct integration method because it is suitable for the nonlinear analysis that is presented in section 4.4.2.

Direct integration is an incremental procedure by which the displacements, velocities and accelerations are solved at successive time steps  $\Delta t$  using the displacements, velocities and accelerations of previous time steps. At each time step there are  $3n$  unknowns that must be computed. They are  $q$ ,  $\dot{q}$  and  $\ddot{q}$ . The direct integration method used in this study reduces these to  $n$  unknowns by making an assumption about the change in acceleration over the time step. The result is an effective static formulation that can be easily solved at each step.

#### 4.2 MODELING EARTHQUAKE EXCITATIONS

The base excitation of the structure may be included in the analysis as known displacements. The finite element equations may be written

$$\begin{bmatrix} M_{aa} & M_{ab} \\ M_{ba} & M_{bb} \end{bmatrix} \begin{Bmatrix} \ddot{u}_a \\ \ddot{u}_b \end{Bmatrix} + \begin{bmatrix} K_{aa} & K_{ab} \\ K_{ba} & K_{bb} \end{bmatrix} \begin{Bmatrix} u_a \\ u_b \end{Bmatrix} = \begin{Bmatrix} Q_a \\ Q_b \end{Bmatrix} \quad (16)$$

if  $u_a$  are the unknown degrees of freedom,  $u_b$  are known base excitations and  $Q_a$  are known nodal forces. The first set of equations is

$$M_{aa}\ddot{u}_a + M_{ab}\ddot{u}_b + K_{aa}u_a + K_{ab}u_b = Q_a \quad (17)$$

Both  $u_a$  and  $u_b$  are displacements in a fixed global reference frame. Only the displacements in the relative reference frame, however, result in strains in the system. Therefore, substituting

$$u_a = q + \eta \quad (18)$$

is convenient if  $\eta$  is a vector having the same magnitude as  $u_a$  and entries for the horizontal degrees-of-freedom equal to the base displacements. The vector  $q$  is composed of nodal displacements in the relative reference frame. Eq..(17) is rewritten

$$M_{aa}\ddot{q} + K_{aa}q = Q_a - M_{aa}\ddot{\eta} - M_{ab}\ddot{u}_b - (K_{aa}\eta + K_{ab}u_b) \quad (19)$$

A computer program written by the author was used to prove that

$$K_{aa}\eta + K_{ab}u_b = 0 \quad (20)$$

for the domed structures used. If the mass is also assumed to be lumped then

$$M_{ab} = 0 \quad (21)$$

and (19) reduces to

$$M\ddot{q} + Kq = Q - M\ddot{\eta} \quad (22)$$

The subscripts 'a' may be dropped since it is understood that q applies to unknown degrees of freedom. One can see that the effect of the base excitation can be modeled as a nodal force vector of the mass times the base acceleration. This equation is commonly used in the literature.

The self-weight of the structure is also included in this study to provide more realistic results. Self-weight is defined as the product of mass and the acceleration due to gravity. To account for this an acceleration of 32.21 ft./sec.<sup>2</sup> is added to each vertical degree of freedom in the  $\ddot{\eta}$  vector. This results in a constant downward force at each node which is equivalent to the effect of gravity.

#### 4.3 DAMPING MATRIX

The damping matrix, C, is unlike the mass and stiffness matrices in that it is not constructed from element damping matrices. The damping matrix is only intended to model the energy dissipative properties of the system. At best, it is an approximation, however, it should be included to realistically model the behavior of a structure.

For Rayleigh damping the damping matrix is approximated by a proportion of the mass and the stiffness matrices. It can be represented as

$$C = \alpha M + \beta K. \quad (23)$$

Values for  $\alpha$  and  $\beta$  are determined by solving the two simultaneous equations

$$\alpha + \beta w_i^2 = 2w_i \xi_i \quad i = 1, 2 \quad (24)$$

where  $w_i$  are two frequencies of vibration of the structures and  $\xi_i$  are two damping ratios either determined experimentally or assumed. For structures with many frequencies Bathe (5) suggests using average values for  $w_i$  and  $\xi_i$ . Engineering judgement may be used to assume these values.

To accurately model damping all of the frequencies of each structure are considered. Lists of the frequencies appear in Appendix A and Appendix B. A computer program written by Dib (14) was used to find these frequencies. Since the frequencies of both structures seemed to be divided into two groups the average frequency of each group was taken for  $w_i$ . A damping ratio of 1% was assumed for the lower  $w_i$  and a ratio of 3% was assumed for the higher  $w_i$ . These  $\xi$  values were not experimentally determined but were chosen in order to represent light damping characteristics. For the small lamella dome the average values for  $w_1$  and  $w_2$  are 1.725 hertz and 21.376 hertz, respectively. They yield an  $\alpha$  value of 0.0259 and a  $\beta$  value of 0.00285. For the large lamella dome  $w_1$  and  $w_2$  are 1.608 hertz and 19.198 hertz which yield an  $\alpha$  of 0.0241 and a  $\beta$  of 0.00306.

#### 4.4 THE NEWMARK-BETA METHOD

##### 4.4.1 Linear Analysis

Given the conditions of the nodes at a time  $t$  an expression for the accelerations and velocities at a time  $t+\Delta t$  can be derived with the Newmark-Beta method found in Ref. 34. The resulting equations of this method are

$$\ddot{t}_{q+\Delta t} = (1/\beta \Delta t)^2 (t_{q+\Delta t} - t_d) \quad (25)$$

and

$$\dot{t}_{q+\Delta t} = t_v + (1/2\beta \Delta t) (t_{q+\Delta t} - t_d) \quad (26)$$

where

$$t_d = t_q + \dot{t}_q \Delta t + 1/4 \ddot{t}_{q \Delta t}^2 \quad (27)$$

and

$$t_v = \dot{t}_q + 1/2 \ddot{t}_{q \Delta t} \quad (28)$$

Once Eq. (25) and Eq. (26) are derived, linear analysis by Newmark's method is straightforward. Substituting them into Eq. (15) yields

$$(1/\beta \Delta t)^2 M (t_{q+\Delta t} - t_d) + C (t_v + (1/2\beta \Delta t) (t_{q+\Delta t} - t_d)) \quad (29)$$

$$+ K t_{q+\Delta t} = t_{Q+\Delta t}$$

At any time  $t+\Delta t$ ,  $\hat{t}^{+\Delta t} q$  are the only unknowns in these equations. By rearranging the equations the following form is realized:

$$\hat{K} \hat{t}^{+\Delta t} q = \hat{t}^{+\Delta t} Q \quad (30)$$

where

$$\hat{K} = (1/\beta \Delta t^2) M + (1/2\beta \Delta t) C + K \quad (31)$$

and

$$\hat{t}^{+\Delta t} Q = \hat{t}^{+\Delta t} Q + (1/\beta \Delta t^2) M \hat{t}_d + C((1/2\beta \Delta t) \hat{t}_d - t_v) \quad (32)$$

$\hat{K}$  is referred to as the effective stiffness matrix and includes the apparent stiffness effects of the mass (inertia effects) and the damping.

#### 4.4.2 Nonlinear Analysis

In this section the reduction methods presented in the preceding section are combined with the Newton-Raphson technique presented in Chapter 3. The Newmark-Beta method is used to reduce the dynamic problem, then the Newton-Raphson technique is used to iterate to the solution. The same criterion for convergence as in the static analysis applies to the dynamic analysis.

If 'k' is the counter of the iteration then the displacement vector

$$\mathbf{t}^{+\Delta t} \mathbf{q}^{(k)} = \mathbf{t}^{+\Delta t} \mathbf{q}^{(k-1)} + \Delta \mathbf{q}^{(k)} \quad (33)$$

will be found at each 'k' by solving for  $\Delta \mathbf{q}^{(k)}$  until convergence is reached. The equations of equilibrium for the nonlinear analysis are

$$\mathbf{M} \mathbf{t}^{+\Delta t} \ddot{\mathbf{q}}^{(k)} + \mathbf{C} \mathbf{t}^{+\Delta t} \dot{\mathbf{q}}^{(k)} + \mathbf{K} \Delta \mathbf{q}^{(k)} = \mathbf{t}^{+\Delta t} \mathbf{Q} - \mathbf{t}^{+\Delta t} \mathbf{F}^{(k-1)} \quad (34)$$

At this point Newmark's method may be implemented. Accelerations and velocities are found by substituting Eq. (33) into Eq. (25) and Eq. (26). These terms become

$$\mathbf{t}^{+\Delta t} \ddot{\mathbf{q}}^{(k)} = (1/\beta \Delta t^2) (\mathbf{t}^{+\Delta t} \mathbf{q}^{(k-1)} + \Delta \mathbf{q}^{(k)} - \mathbf{t}_d) \quad (35)$$

and

$$\mathbf{t}^{+\Delta t} \dot{\mathbf{q}}^{(k)} = \mathbf{t}_v + (1/2\beta \Delta t) (\mathbf{t}^{+\Delta t} \mathbf{q}^{(k-1)} + \Delta \mathbf{q}^{(k)} - \mathbf{t}_d) \quad (36)$$

respectively. By placing these into Eq. (34) and rearranging, the following formulation is reached:

$$\hat{\mathbf{K}} \Delta \mathbf{q}^{(k)} = \hat{\mathbf{Q}}_{\text{eff}} \quad (37)$$

where

$$\begin{aligned} \hat{\mathbf{Q}}_{\text{eff}} &= \mathbf{t}^{+\Delta t} \mathbf{Q} - \mathbf{t}^{+\Delta t} \mathbf{F}^{(k-1)} - [(1/\beta \Delta t^2) \mathbf{M} \\ &\quad + (1/2\beta \Delta t) \mathbf{C}] \mathbf{t}^{+\Delta t} \ddot{\mathbf{q}}^{(k-1)} - \mathbf{C} \mathbf{t}_v \end{aligned} \quad (38)$$

$$t + \Delta t_q^{(k-1)} = (t + \Delta t_q^{(k-1)} - t_d) \quad (39)$$

and

$$\hat{K} = (1/\beta \Delta t^2)M + (1/2\beta \Delta t)C + K. \quad (40)$$

The Newmark method becomes unconditionally stable when the constant-average-acceleration method, or  $\beta=1/4$ , is used according to Ref. 23.

#### 4.5 DISCUSSION OF TIME STEPS

Choice of the correct time step is critical in dynamic analysis. The time step must be small enough to insure an accurate solution but not so small that excessive computer time is needed. Since the Newmark method for  $\beta=1/4$  is unconditionally stable the choice of the time step will be with regard to the accuracy of the solution. Bathe (4) suggests using a time step  $\Delta t = T_n/10$  if  $T_n$  is the smallest period of oscillation of the structure to account for the response of all modes. For many structures, however, he states that the primary response is found in the lower modes so that the higher frequencies and mode shapes may be neglected and the time steps be lengthened. In these instances the time steps may be increased to  $T_p/10$  where  $T_p$  is the period of oscillation of the highest frequency considered. Using  $T_p$  instead of  $T_n$  may increase the time step dramatically and still maintain accurate results.

As can be seen in Appendix A and Appendix B the frequencies of both the small dome and the large dome are divided into two groups. Only the mode shapes associated with the lower group of frequencies were assumed to be needed to effectively model the dynamic response. For the small structure 1.952 cycles per second is chosen as the critical frequency because it is the highest of that group. For the large structure 1.842 cycles per second is chosen. The corresponding periods of oscillation,  $T_p$ , are 0.512 seconds and 0.543 seconds, respectively. In order to obtain an accurate solution the time step should be at the most  $T_p/10$  or about 0.053 seconds. Also, Wilson, et al. (54) states that for earthquake loading there is little justification to use time steps less than 0.05 sec.

The available earthquake data from the El Centro earthquake (21) is digitized in increments of 0.020 sec. At a time step of 0.020 sec.  $\Delta t/T_p$  would have a value of 0.0377. For Newmark's method this would result in less than 1% period elongation which is acceptable for many engineering situations according to Ref. 23. Also, if the time step used is reduced to 0.020 seconds the earthquake data would not need to be redigitized which is a complicated process. Therefore, for the purpose of convenience and accuracy the time step used in this study is 0.020 seconds.

## Chapter V

### RESULTS

The WATFIV program that appears in Appendix C was written by the author for use in this study. It is a finite element program to model space truss behavior under static load or dynamic base excitation. Nodal displacements and axial forces in each member can be determined at each load or time step in addition to nodal velocities and accelerations. The static analysis capabilities are strictly nonlinear while the dynamic analysis may be either linear or nonlinear. Also, Rayleigh damping may be included as well as a choice between lumped or consistent mass matrices. The nonlinear solution technique may be either the Newton-Raphson or the Modified Newton-Raphson method.

In this chapter results of the program are compared to results of other researchers to check the program's accuracy. Following this, the displacements and stresses caused by the static loads on both the small and large lamella domes are presented along with the displacements and maximum stresses caused by the live loads and the earthquake excitations. The digitized acceleration data of the El Centro earthquake of May 18, 1940 was chosen for use in this study because it was the most severe data available. A comparison

is then made of the axial stresses of all members for both the static and dynamic analyses. The percentage increases in stress due to the earthquake are then given.

### 5.1 THE FINITE ELEMENT PROGRAM

#### 5.1.1 Comparison with Previous Results

Few sources were found that provided results for a dynamically loaded, nonlinear space truss with which to check the program. None were found that modeled base excitations. The simplest comparison found is offered by Nickell (36) who analyzes the one degree-of-freedom plane truss shown in Fig. 8. In this study, the spring is replaced by a long truss element that exhibits the same stiffness characteristics. The first test performed was a static analysis. A graph of the load  $P$  and the vertical downward displacement of the joint is shown in Fig. 9. A dynamic test follows where  $P$  increases linearly from 0 to five lbs. in 0.1 sec. and is held constant thereafter. Both Nickell and the author use a time step of  $\Delta t=0.1$  sec. Results are shown in Fig. 10 and for both cases the author's results are nearly identical to those of Nickell.

A larger two dimensional truss system shown in Fig. 11 is presented by Noor and Peters (38). The horizontal members have cross-sectional areas of  $1.6 \times 10^{-4} \text{ m}^2$  while the diagonal

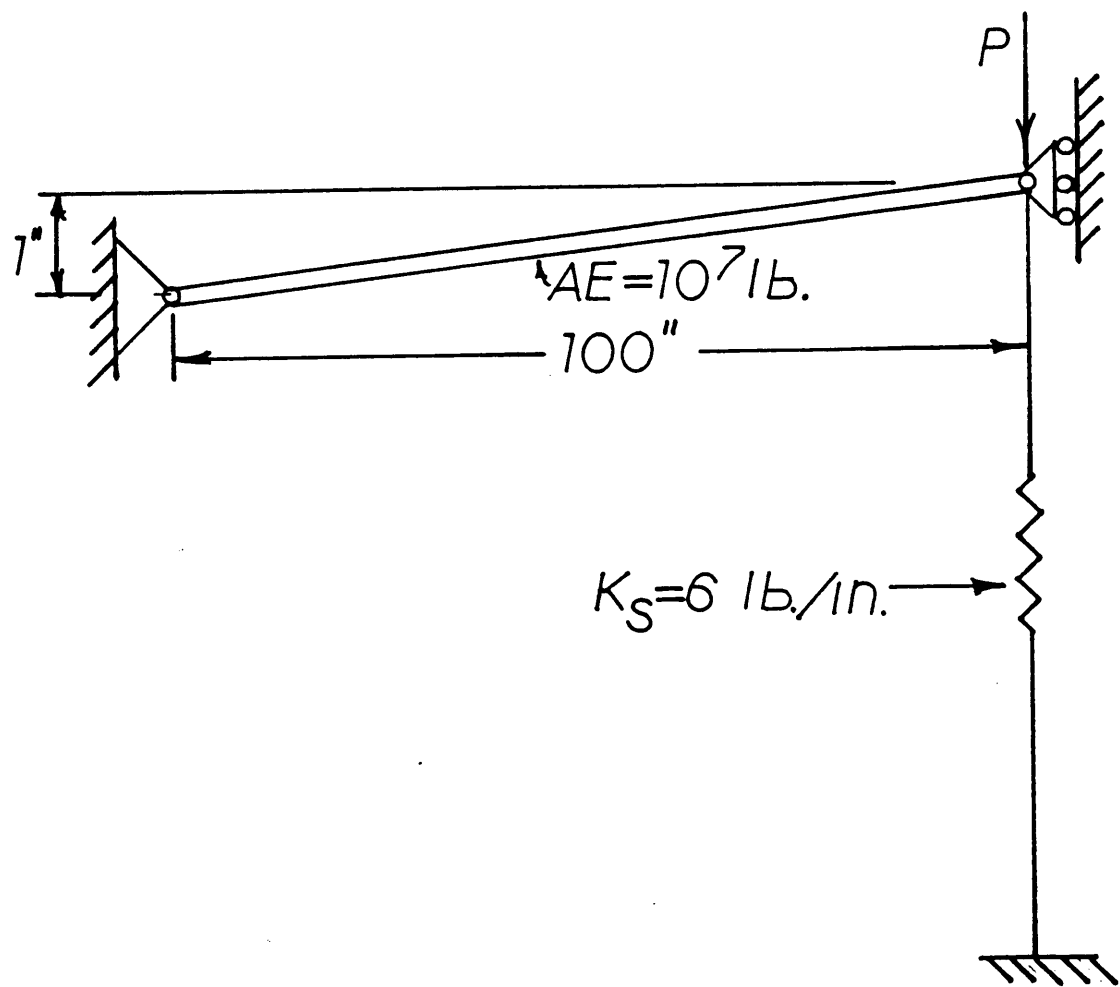


Figure 8: One degree-of-freedom plane truss presented by Nickell.

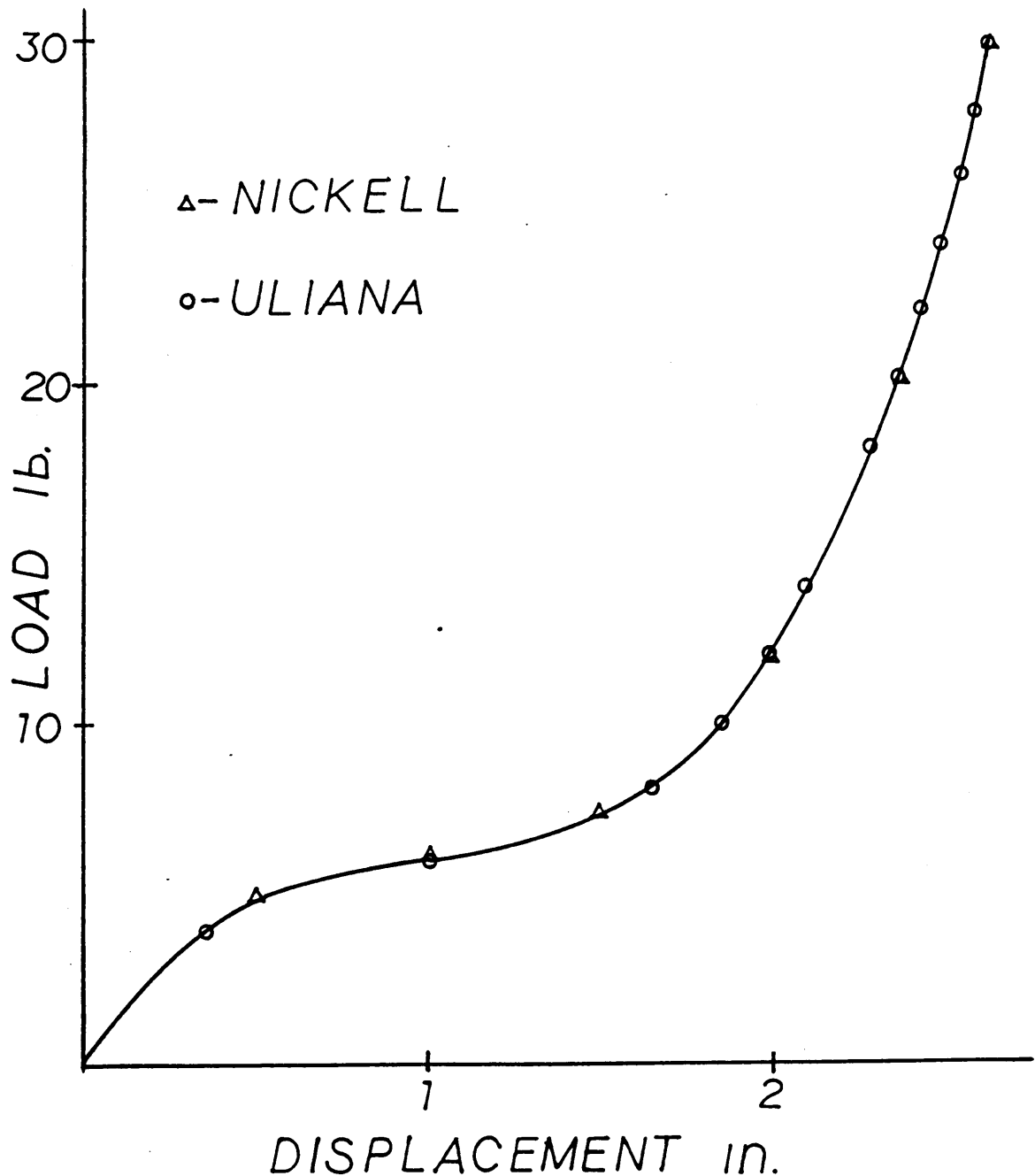


Figure 9: Displacement vs. load graph for the static analysis of the one degree-of-freedom truss presented by Nickell.

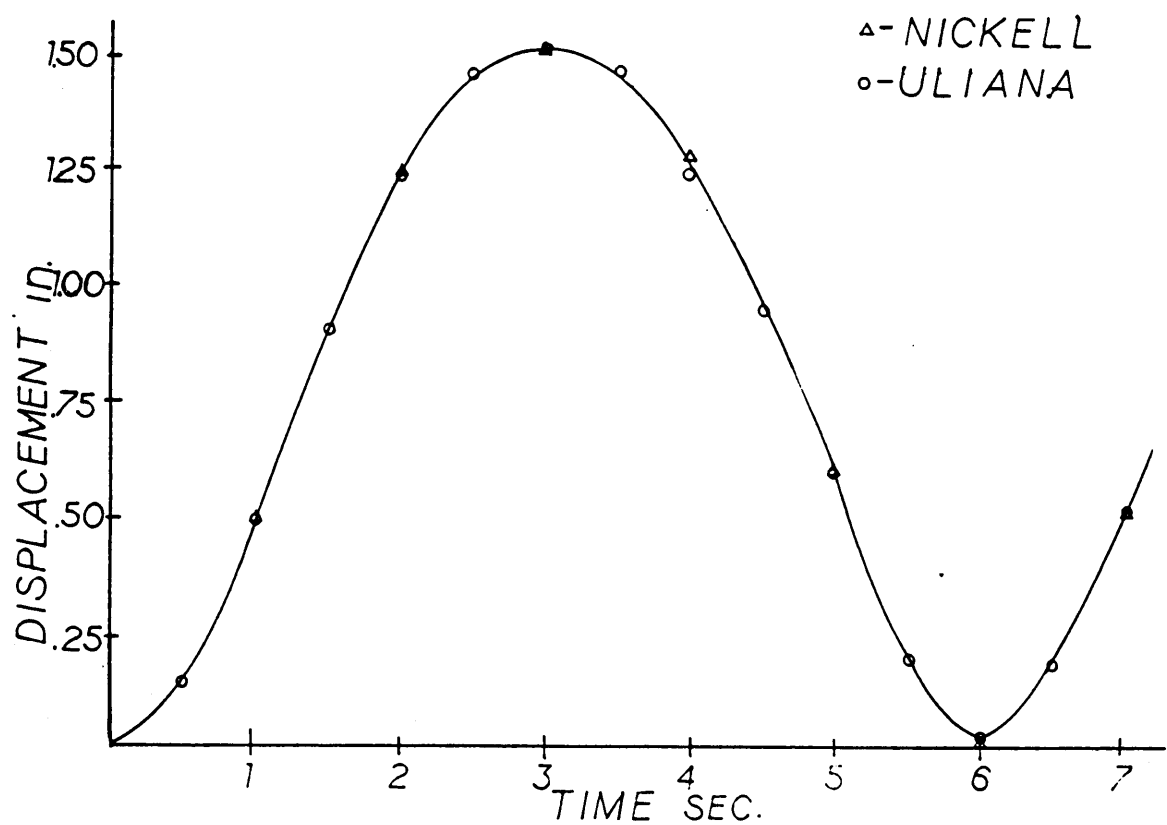
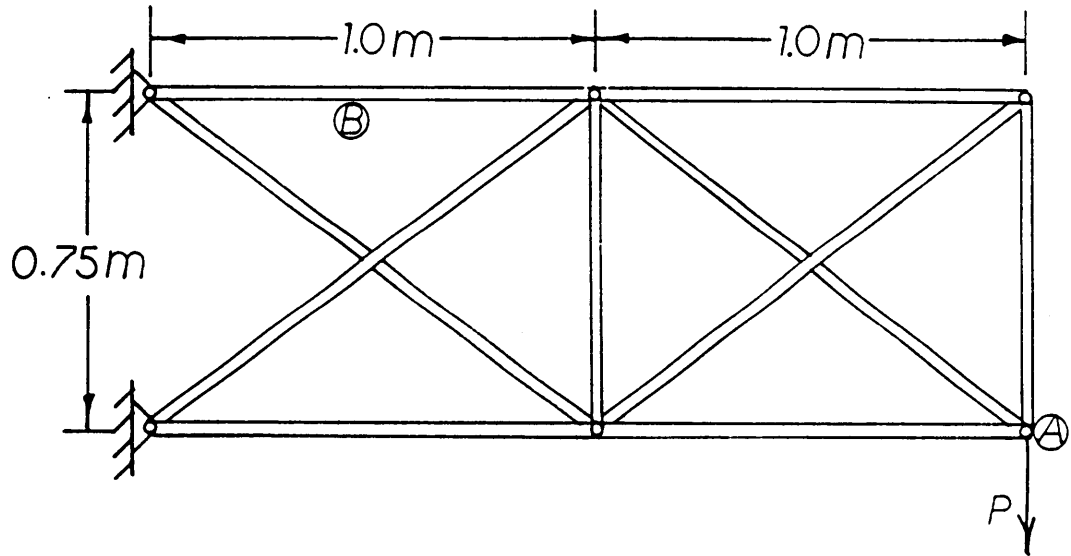


Figure 10: Displacement vs. time graph for the dynamic analysis of the one degree-of-freedom truss presented by Nickell.



**Figure 11:** Ten member plane truss presented by Noor and Peters

and vertical members have  $1.3 \times 10^{-4} \text{ m}^2$  cross-sectional areas. The Young's modulus of the material is  $7.17 \times 10^2 \text{ N/m}^2$  and the density is  $2768 \text{ kg/m}^3$ . These values are the same as those of aluminum. The load P is an instantaneously applied load of  $4.5 \times 10^4$  Newtons acting downward. The critical time step for stability of the mixed method presented by Noor and Peters is  $\Delta t = 2.63 \times 10^{-4}$  sec. The time step used is  $0.625 \times 10^{-4}$  sec. Results for both linear and nonlinear analyses are available.

The displacement of joint A with respect to time for both linear and nonlinear analyses is presented in Fig. 12. For both cases the author's results match very closely with those of Noor and Peters. Data for the axial force in member B with respect to time is also available for linear and nonlinear analyses. Results are shown in Fig. 13 for the linear analysis and Fig. 14 for the nonlinear analysis. The author's results for the linear problem are nearly identical to those of Noor and Peters. Results for the nonlinear problem, however, differ slightly. A probable cause is that the stress-strain curves for the material nonlinearity are different for both cases. Noor chose to represent the curve as a polynomial whereas the author chose a bilinear approximation. A comparison of both appears in Fig. 15. Overall, the results for the two dimensional truss structure show excellent agreement with those of Noor and Peters.

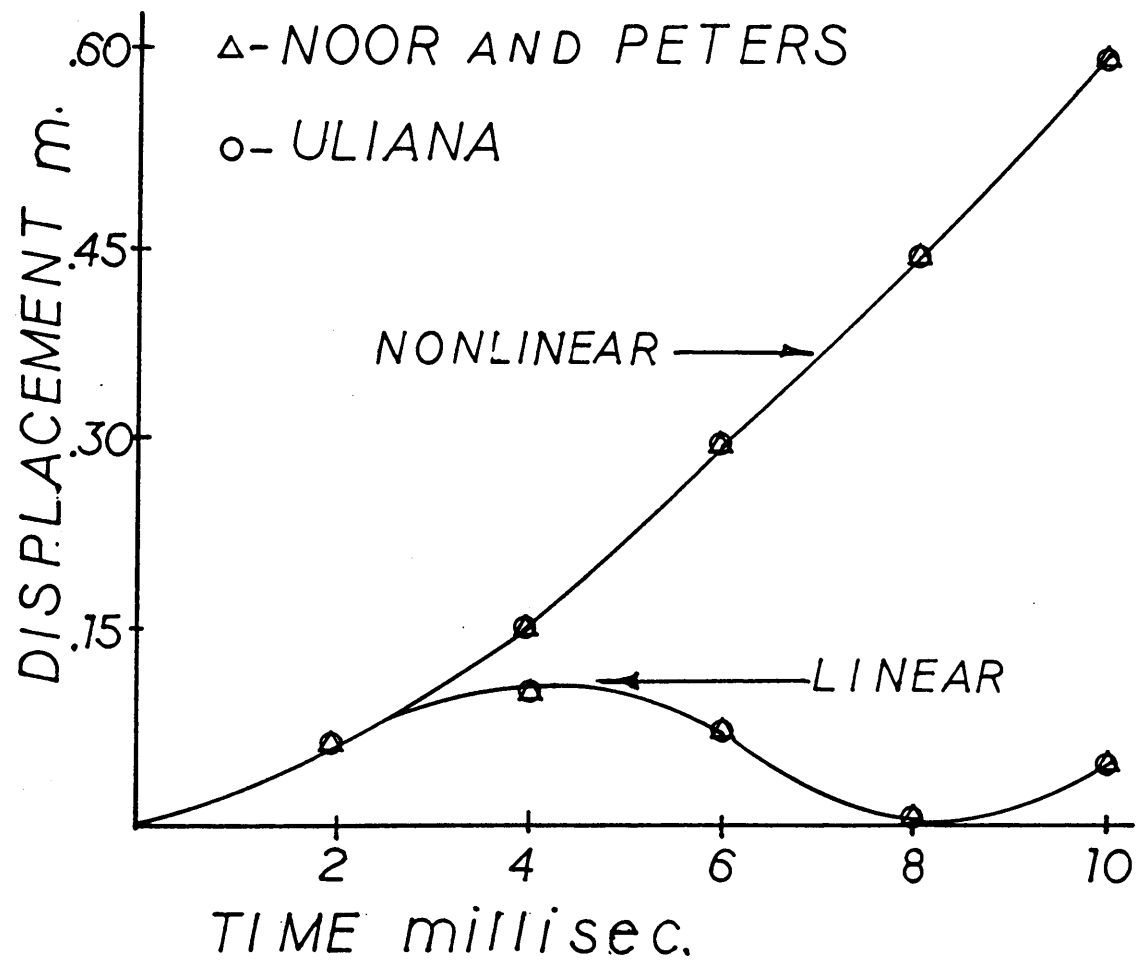


Figure 12: Displacement vs. time graphs of joint A for linear and nonlinear analyses of the ten member truss.

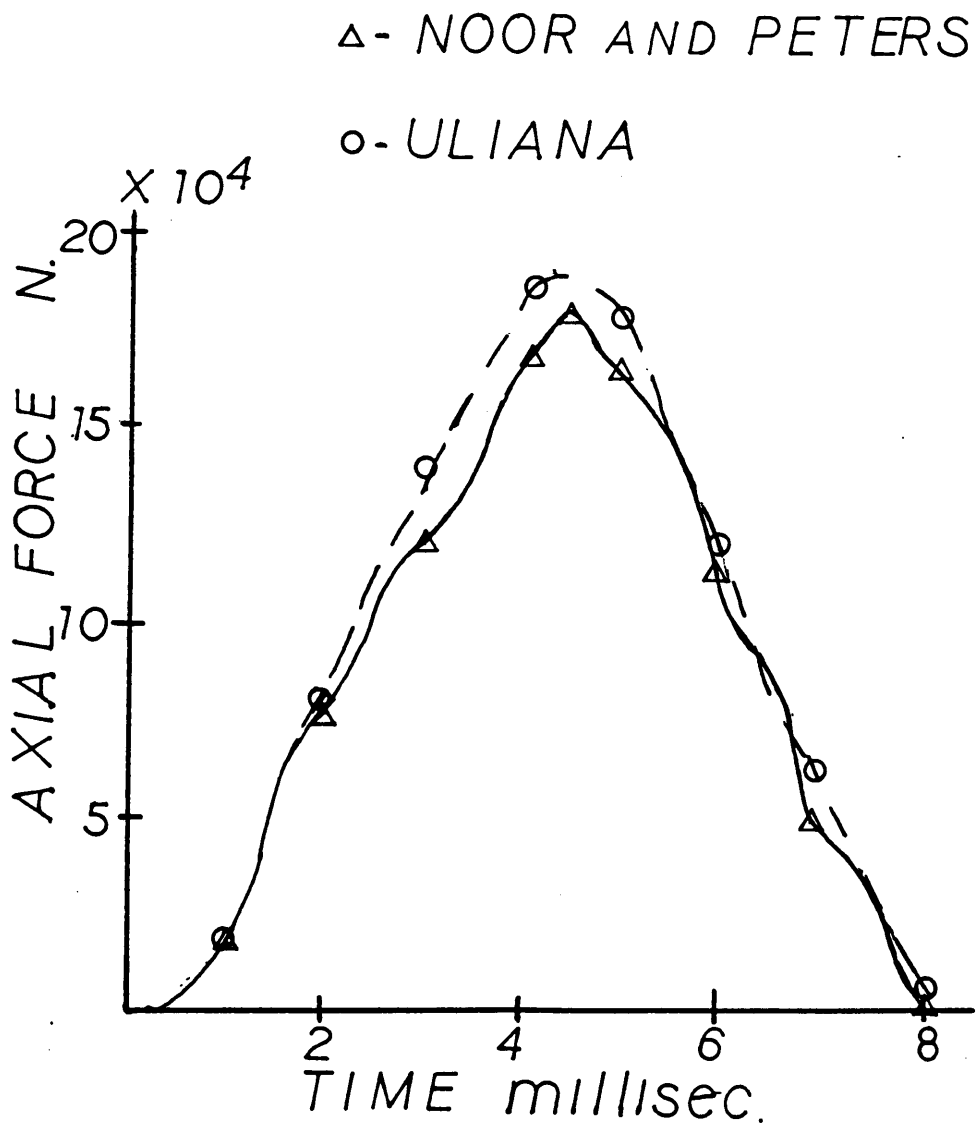


Figure 13: Axial force in member B for the linear analysis of the ten member truss.

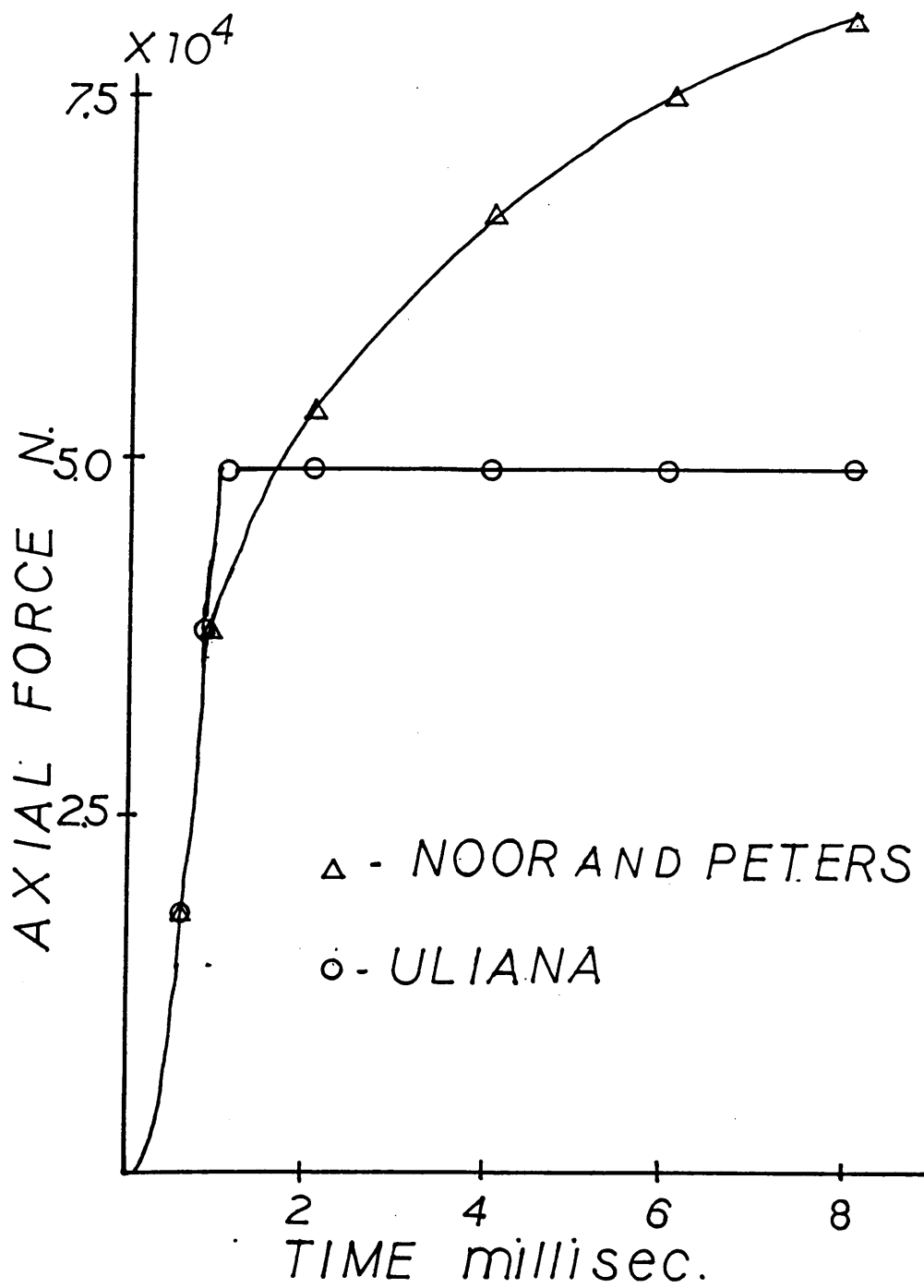


Figure 14: Axial force in member B for nonlinear analysis of the ten member truss.

$\Delta$  - NOOR AND PETERS

$\circ$  - ULIANA

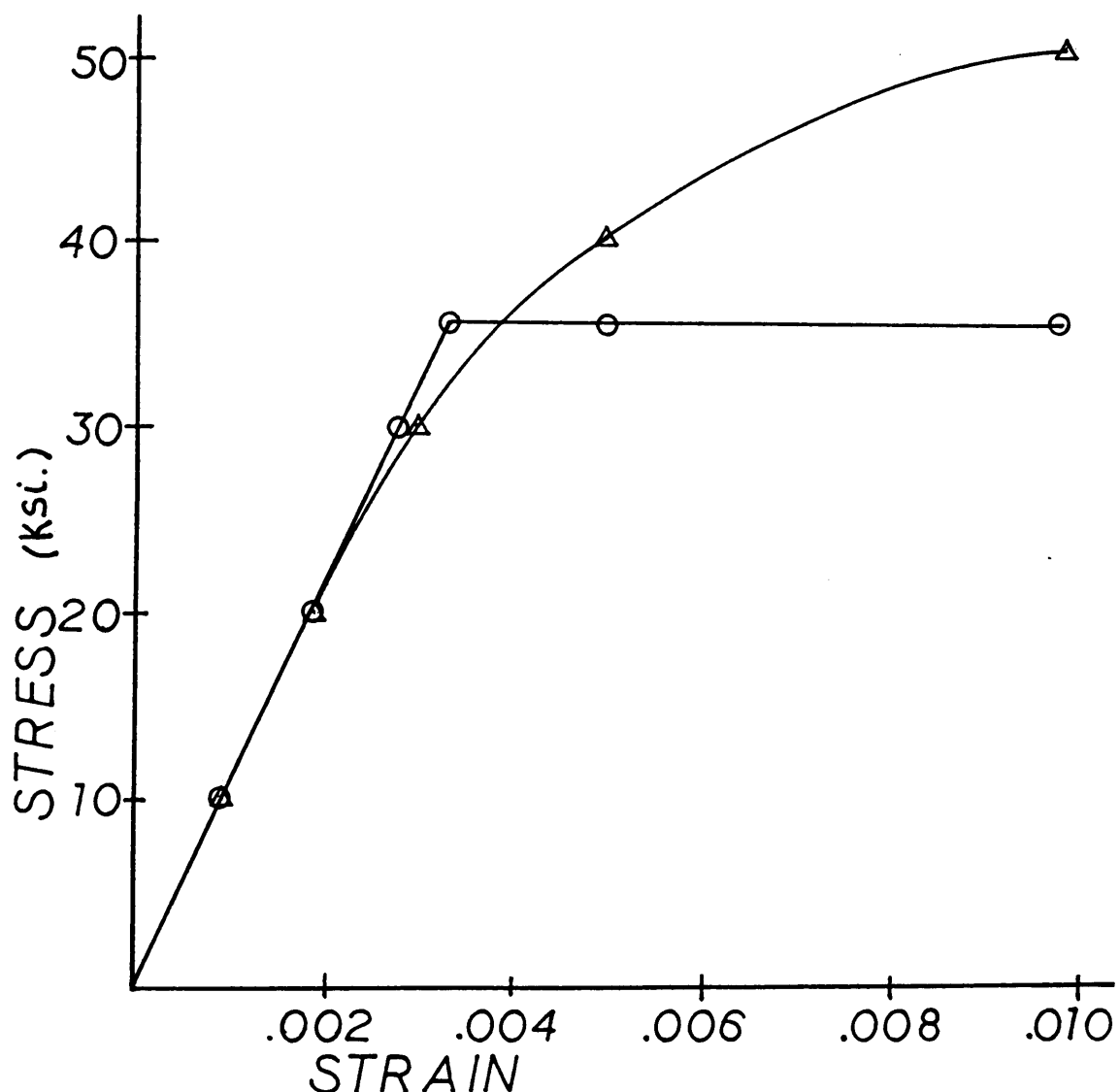


Figure 15: A comparison of the stress-strain relationships.

A large three dimensional truss structure is presented by Noor and Peters (38) and is shown in Fig. 16. The longitudinal members have cross-sectional areas of  $0.8 \times 10^{-4} \text{ m}^2$ , the diagonals have  $0.4 \times 10^{-4} \text{ m}^2$  cross-sections and the battens have  $0.6 \times 10^{-4} \text{ m}^2$  cross-sections. The material properties are the same as those of the previous problem. The time step used by Noor is  $\Delta t = 0.45 \times 10^{-3}$  sec. and the load is 5000 Newtons instantaneously applied to the four center nodes indicated in the diagram. Again, the results for the linear and nonlinear analyses are available.

The displacement of joint A in the direction of the load for the linear analysis is presented in Fig. 17. The axial force in member B as a function of time is graphed in Fig. 18. Both analyses yield nearly identical results. A comparison of the displacements for the nonlinear analysis is shown in Fig. 19 while a comparison of the axial force in member B is shown in Fig. 20. The results show some deviation of the displacements possibly due to the fact that the material nonlinearities are different. The graphs exhibit good agreement in the linear range of the material; however, when the bilinear assumption of the author applies the displacements deviate slightly.

For all tests the results of the author are in close agreement with those of other researchers. The only appre-

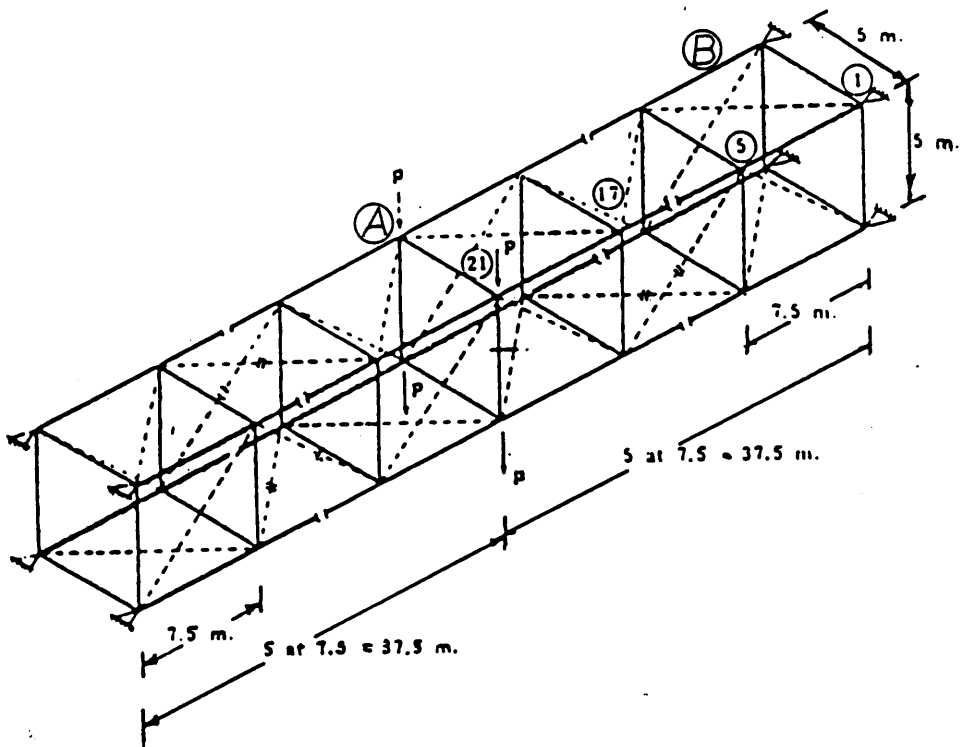


Figure 16: Large ten-bay truss presented by Noor and Peters.

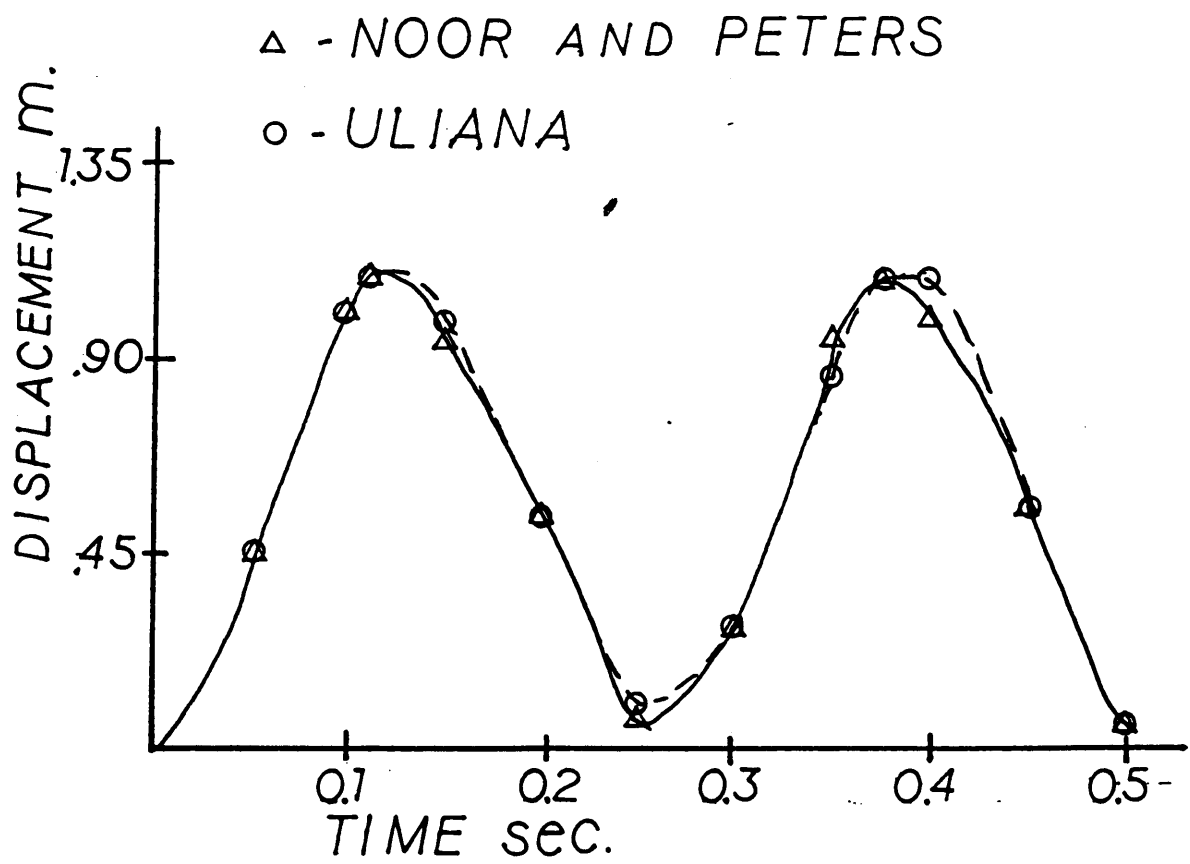


Figure 17: The displacement of joint A for the linear analysis of the ten-bay space truss.

△- NOOR AND PETERS

○- ULIANA

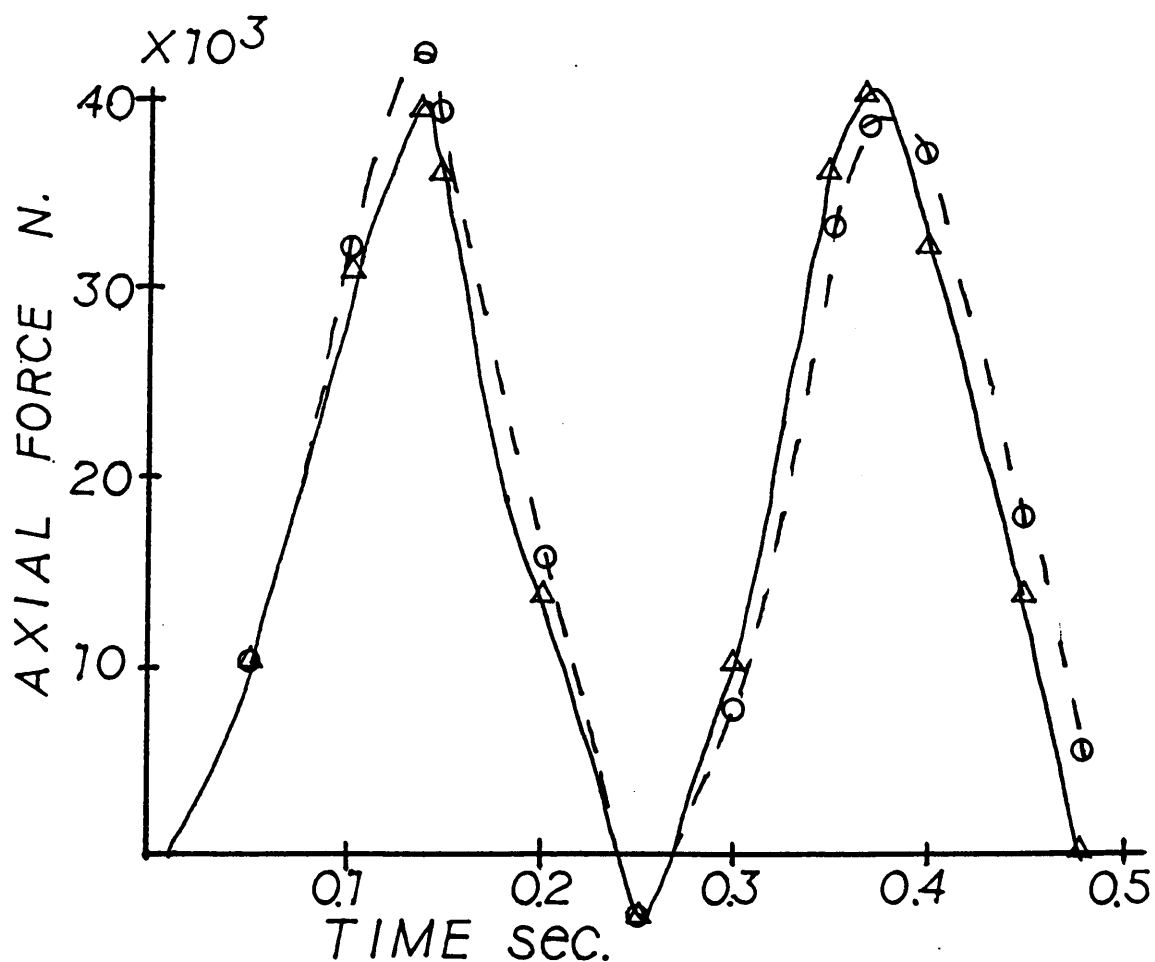


Figure 18: Axial force in member B for linear analysis of the ten-bay space truss.

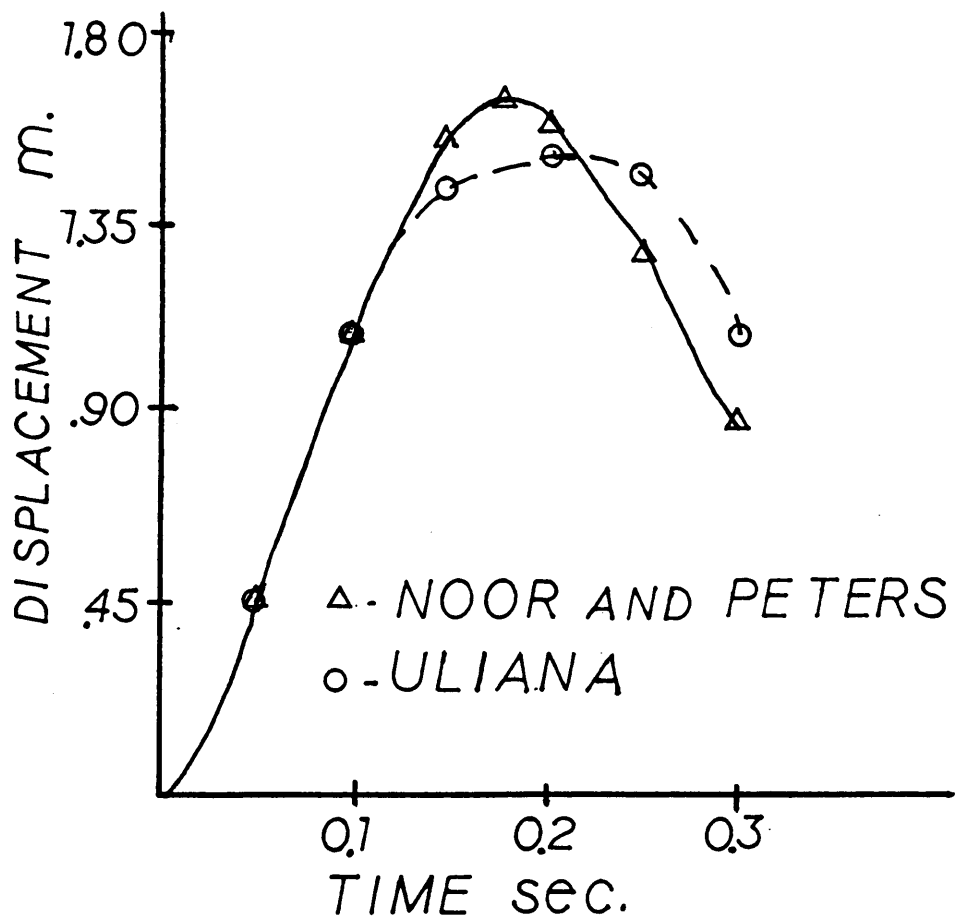


Figure 19: Displacement of joint A for nonlinear analysis of the ten-bay space truss.

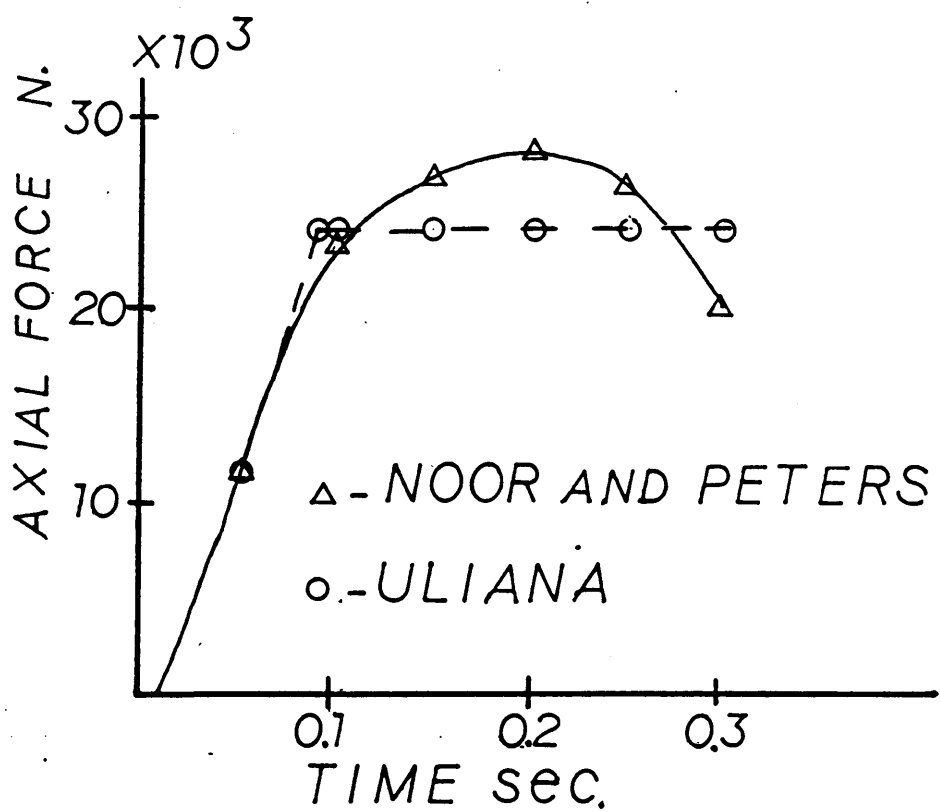


Figure 20: Axial force in member B for nonlinear analysis of the ten-bay space truss.

ciable differences arrise in the nonlinear problems and may be traced back to the bilinear assumption of the material behavior.

### 5.1.2 Checks on Some Assumptions

Before the dome analyses were performed several tests were run on the large dome in order to check some assumptions that were made. The first test was to determine if the use of the Modified Newton-Raphson procedure provides appreciable savings in computational effort. Two short static analyses on the large dome showed that the Newton-Raphson procedure required 405 seconds of CPU time and the Modified procedure needed only 140 seconds. Both analyses gave identical results. Because of the savings and accuracy the Modified method was used for the remainder of the testing.

Next, a check to determine the accuracy of Bathe's suggested convergence criterion (See section 3.4) was performed. A static analysis was run using a very small dimensional criterion  $e=5.0 \times 10^{-5}$  in. The same test was run using the nondimensional  $e=0.001$ . Both produced identical results but the latter used 12% less CPU time. Therefore, the criterion that Bathe suggests is used.

Finally, for the dynamic problem the effect of earthquake motions in different directions was desired. Two dynamic analyses on the small dome were performed with the excitations in two perpendicular directions. The results for both were identical probably due to the high degree of symmetry in these domes. Therefore, the direction of excitation does not affect the results.

## 5.2 SMALL LAMELLA DOME

### 5.2.1 Static Analyses

Static analyses of the small lamella dome that appears in Fig. 21 were performed. The nodal load vector  $\mathbf{Q}$  included the self-weight of the structure along with the live loads. The domes are modeled with an additional skin of aluminum sheet that has a thickness of 0.162 in. in order to closely approximate the weight of a real dome. With this, the dead load is about  $3 \text{ lb./ft.}^2$ . In addition, live loads in increments equivalent to  $10 \text{ lb./ft.}^2$  or less are added until failure of the dome occurs.

For a uniformly distributed live load the small dome is able to withstand  $77 \text{ lb./ft.}^2$  plus the dead load before a singularity in the stiffness matrix is realized. A load-displacement graph for the downward displacement of node A and node B appears in Fig. 22. This graph shows the singu-

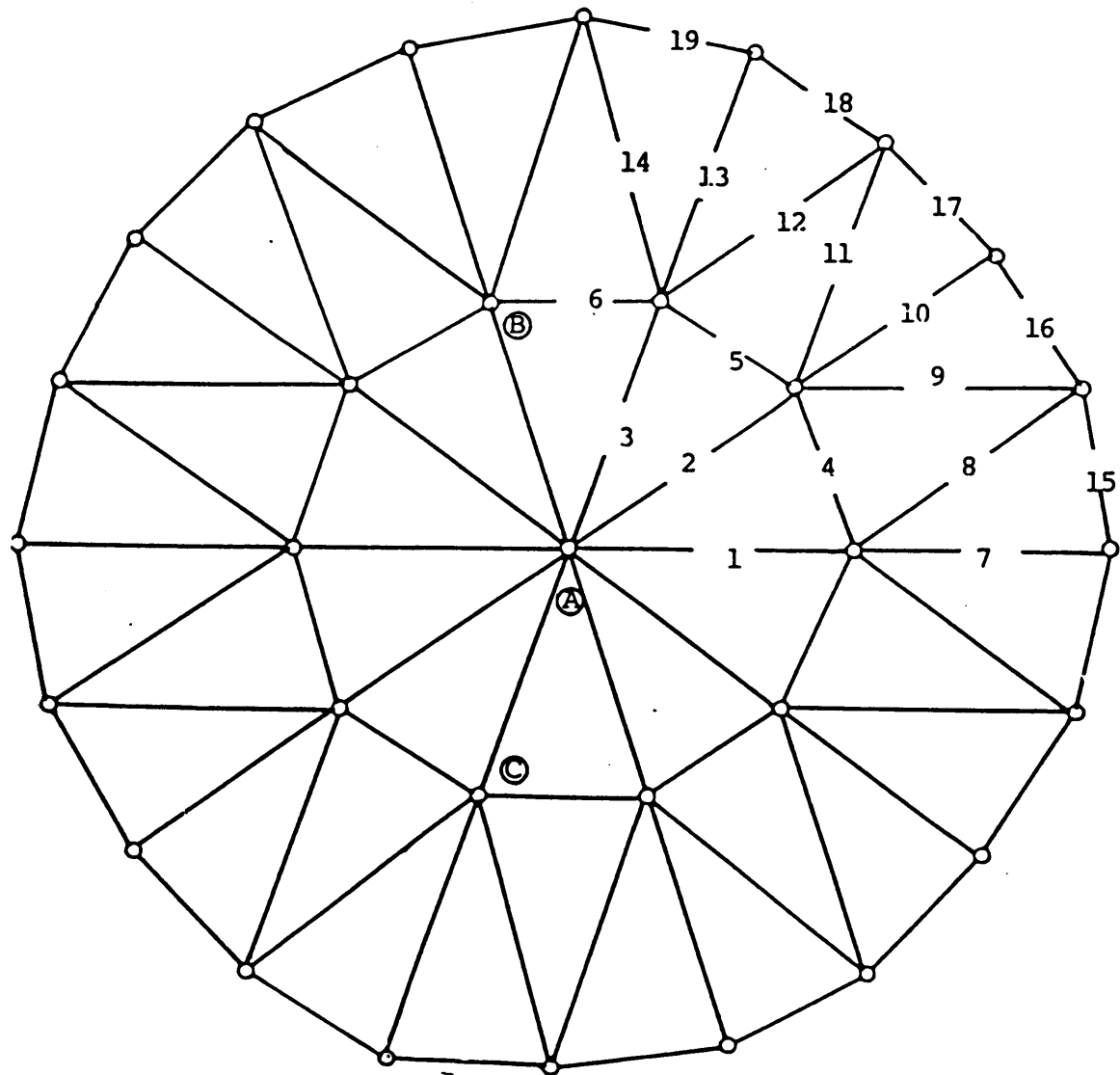


Figure 21: Small lamella dome with numbered members.

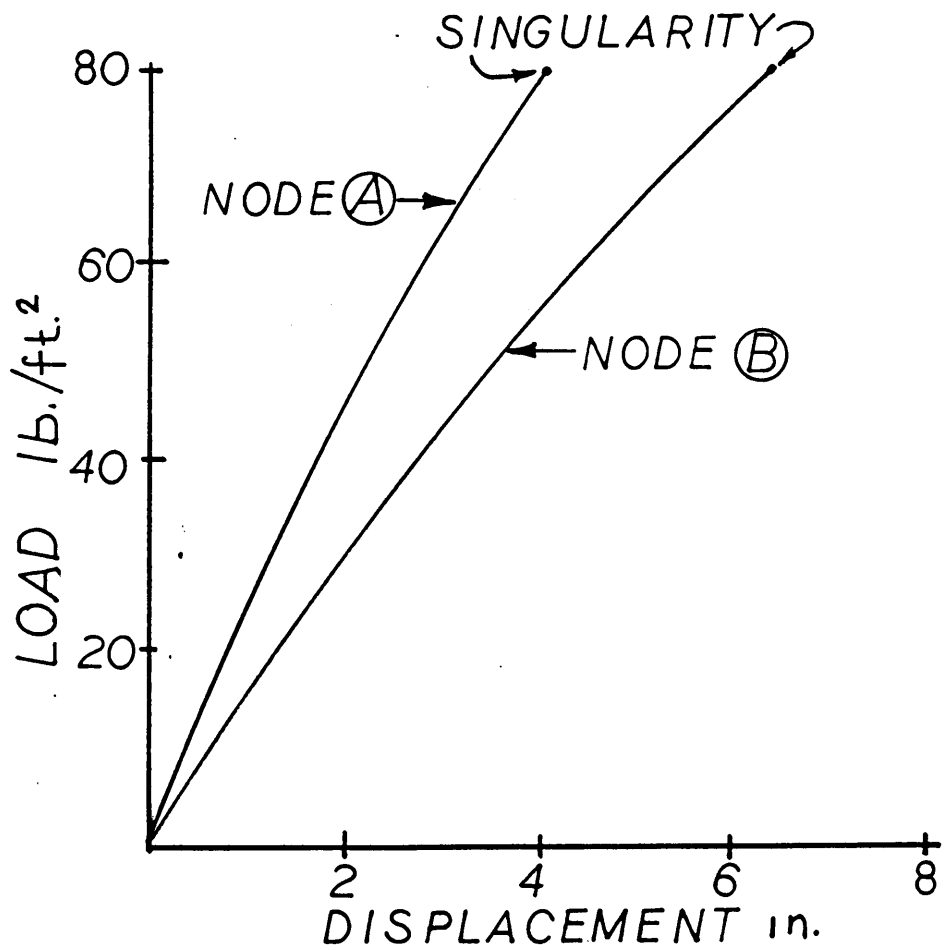


Figure 22: Load vs. displacement curves for uniform load on the small dome.

larity occurs without a significant loss of stiffness. The instability is sudden which would indicate an unstable bifurcation. The analysis is stopped after the bifurcation because it would constitute a failure of the structure.

Stresses at failure in the numbered members are presented in Table 1. Only the stresses in a quarter of the structure are given due to symmetry. Stresses at various other static loads are presented in the next section where they are compared to those of the dynamic analyses. None of the members reached the elastic buckling stress before the global instability. The maximum allowable stresses according to the Aluminum Association (49) and the buckling stresses for the numbered elements of Fig. 21 appear in Table 2.

A nonuniform load condition was also tested where a full live load is placed over half of the structure and one half of this load is placed over the remainder of the structure. The load-displacement curves for nodes A, B and C are given in Fig. 23. Node B is in the fully loaded region and node C is in the partially loaded region. The stiffness matrix of the dome became singular at  $67 \text{ lb./ft.}^2$  plus the dead load. Nineteen members reached the buckling stress before the bifurcation. A complete presentation of the results for the nonuniform loads will not be given because a dynamic analysis is not available.

TABLE 1

Maximum stresses of static analysis for numbered members of the small dome.

ELEMENT NUMBER	MAXIMUM STRESS AT FAILURE (KSI)
1	-5.411
2	-5.448
3	-5.421
4	-17.300
5	-17.302
6	-17.298
7	-8.883
8	-4.629
9	-4.657
10	-8.881
11	-4.653
12	-4.636
13	-8.880
14	-4.643
15	27.698
16	27.706
17	27.706
18	27.701
19	27.701

TABLE 2

Maximum allowable stresses and buckling stresses for numbered members of the small dome.

ELEMENT NUMBER	MAXIMUM ALLOWABLE COMPRESSIVE STRESS (KSI)	BUCKLING STRESS (KSI)
1	-5.10	-9.89
2	-5.10	-9.89
3	-5.10	-9.89
4	-12.34	-25.43
5	-12.34	-25.43
6	-12.34	-25.43
7	-5.10	-9.89
8	-4.26	-8.28
9	-4.26	-8.28
10	-5.10	-9.89
11	-4.26	-8.28
12	-4.26	-8.28
13	-5.10	-9.89
14	-4.26	-8.28
15	-12.34	-25.43
16	-12.34	-25.43
17	-12.34	-25.43
18	-12.34	-25.43
19	-12.34	-25.43

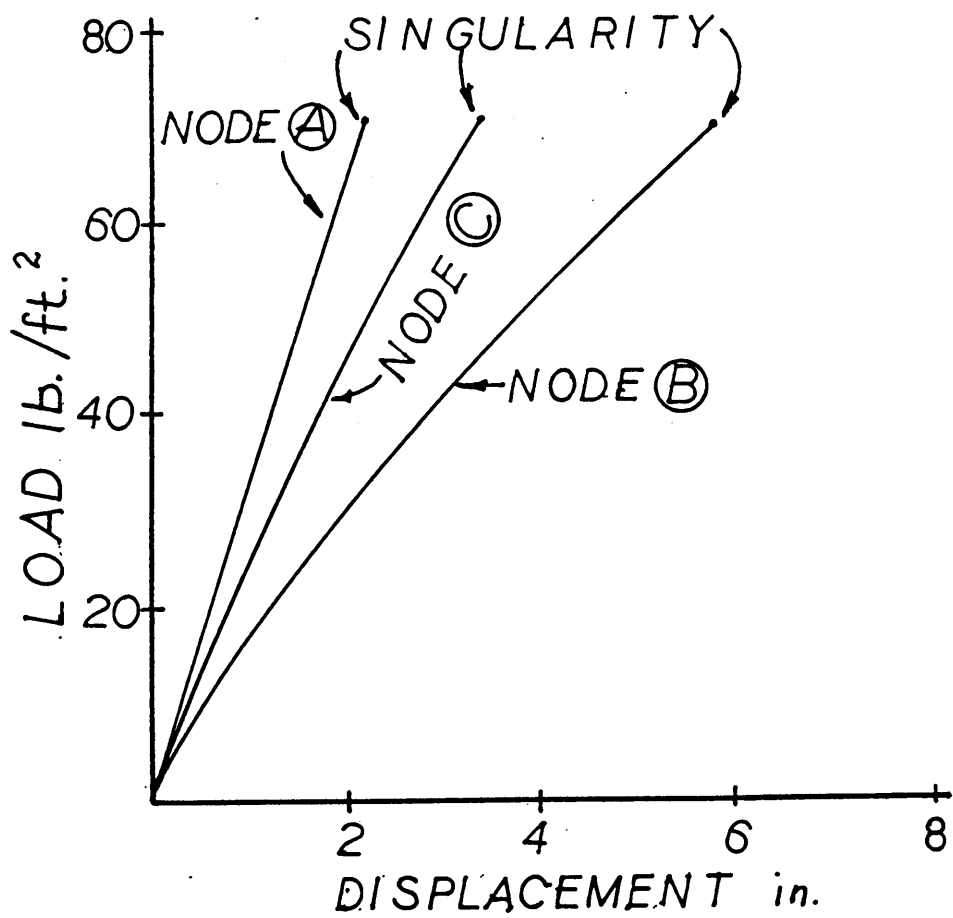


Figure 23: Load vs. displacement curves for nonuniform load on the small dome.

### 5.2.2 Dynamic Analyses

Dynamic analyses of the small dome subjected to the El Centro earthquake of May 18, 1940 (21) were performed for five different load conditions. An accelerogram of the El Centro earthquake appears in Fig. 24. The load conditions are:

1. Dead load only.
2. Dead load plus 10 lb./ft.<sup>2</sup> live load.
3. Dead load plus 20 lb./ft.<sup>2</sup> live load.
4. Dead load plus 30 lb./ft.<sup>2</sup> live load.
5. Dead load plus 40 lb./ft.<sup>2</sup> live load.

Nodal displacements at each time step are calculated in addition to the maximum axial stresses in each member over the entire analysis. The analyses are limited to four seconds of earthquake data because the largest ground accelerations occur within the first four seconds.

In order to include the live load an additional mass is added to each element that is equivalent to the mass of snow on the tributary area about each member. By including an acceleration due to gravity (see section 4.2) an effective nodal load vector is achieved. The initial nodal displacements of the structure due to this gravity load must also be included. If they were not then the load would act as if it were instantaneously applied.

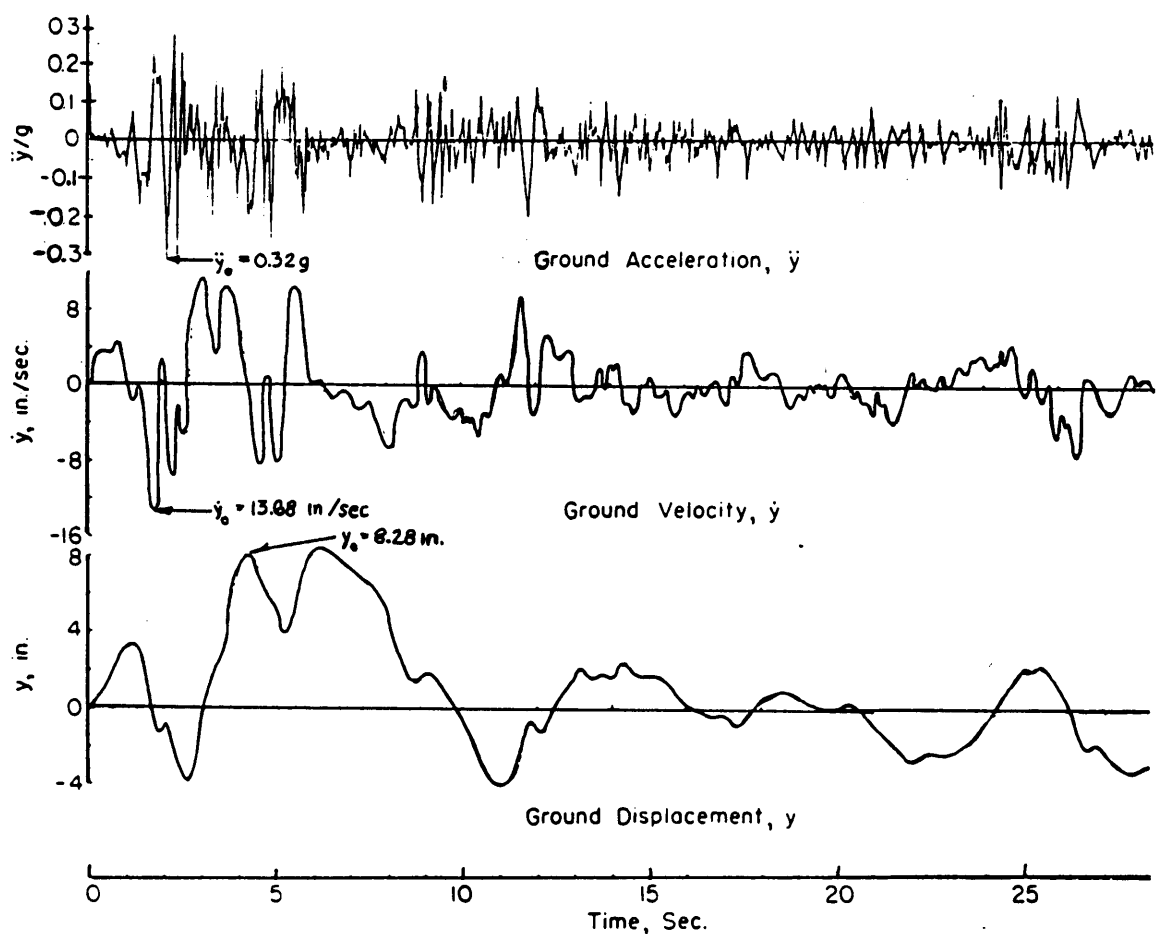


Figure 24: Accelerations, velocities and displacements for the El Centro earthquake of May 18, 1940.

The nodal displacements in the relative reference frame are calculated since they are the displacements that cause deformations. The time-displacement graphs of node A in the direction of the earthquake excitation for all five loads are presented in Figs. 25 through 29. A composite graph of the displacements of the four live loads is also given in Fig. 30. Tables 3 through 7 provide a comparison of the maximum stresses. For all loads the maximum stresses in the numbered elements (see Fig. 21) for the static analysis are compared to those of the dynamic analysis. Stresses in members 15 through 19 are not presented for the dynamic analyses since they are the members of the tension ring which are not included in the fixed base dynamic problem.

### 5.3 LARGE DOME

#### 5.3.1 Static Analyses

The analyses of the large dome are similar to those of the small dome. For a uniformly distributed live load the large dome is able to withstand 72 lb./ft.<sup>2</sup> plus its dead weight before a singularity in the stiffness matrix arises. Load-displacement graphs for the nodes A, B and C of Fig. 31 are given in Fig. 32. As with the small dome, this dome exhibits bifurcation instability. The stresses at failure for the numbered members are presented in Table 8. Stresses

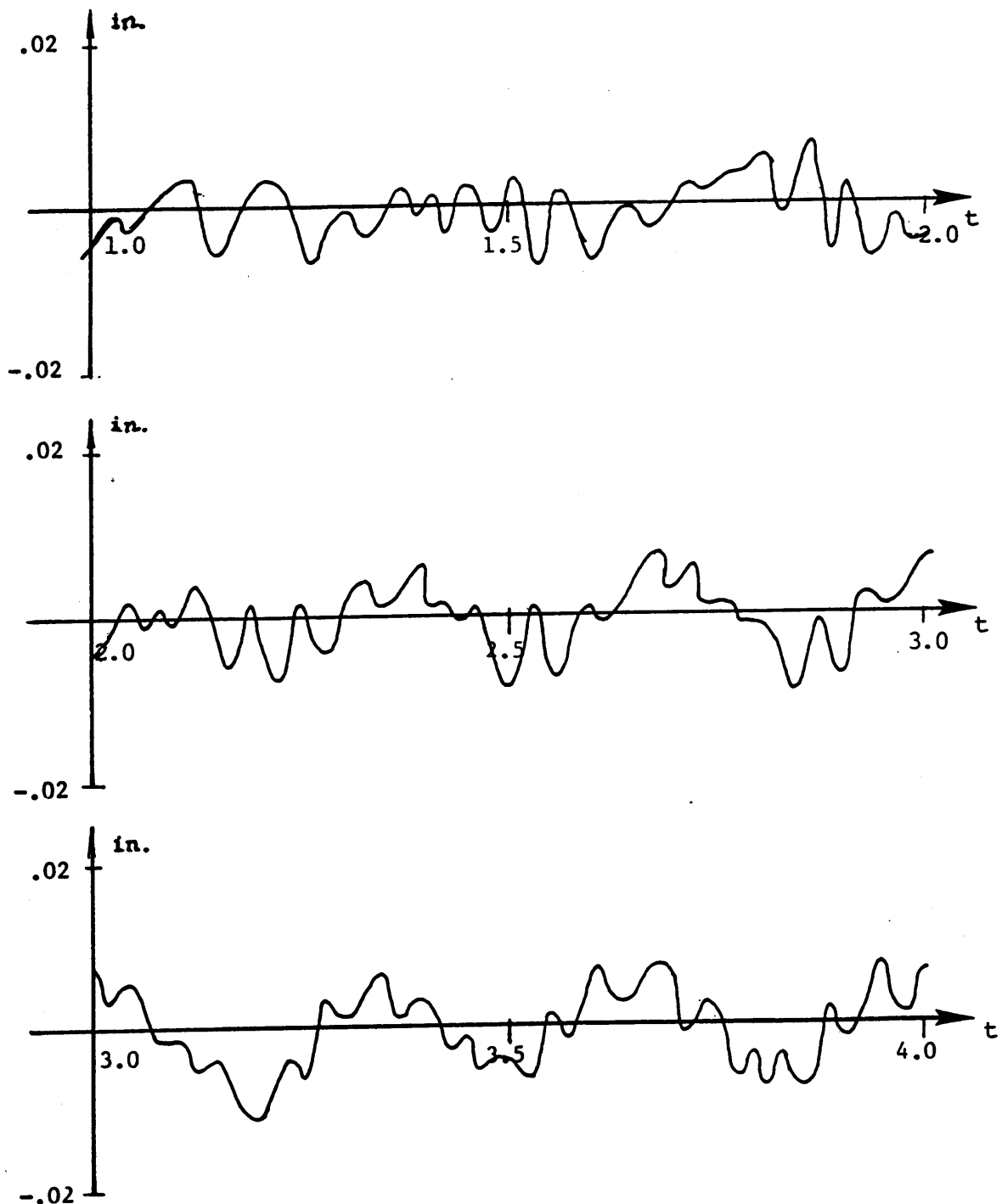


Figure 25: Displacement of joint A for dead load only on the small dome.

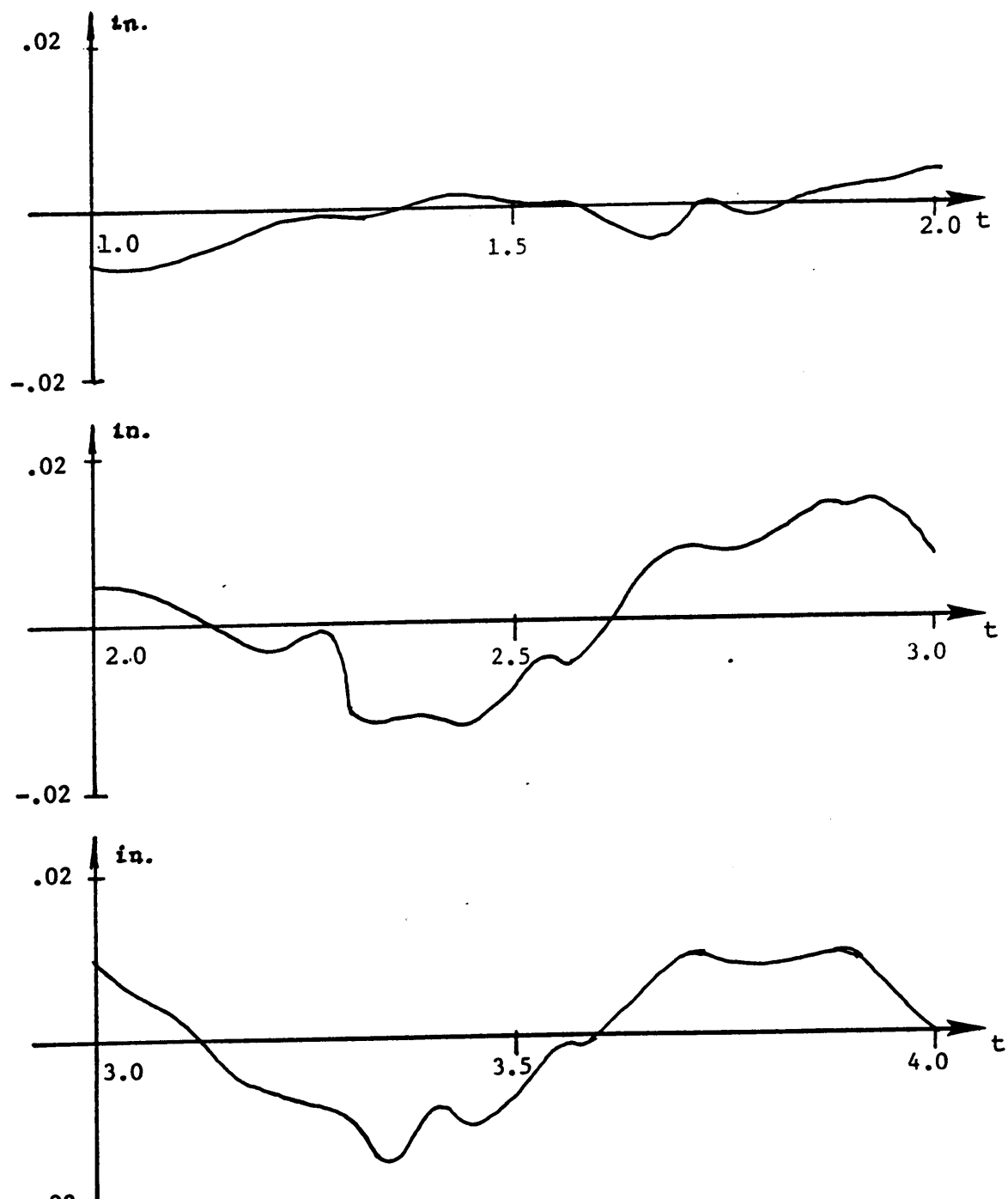


Figure 26: Displacement of joint A for dead load plus 10 lb./ft.<sup>2</sup> on the small dome.

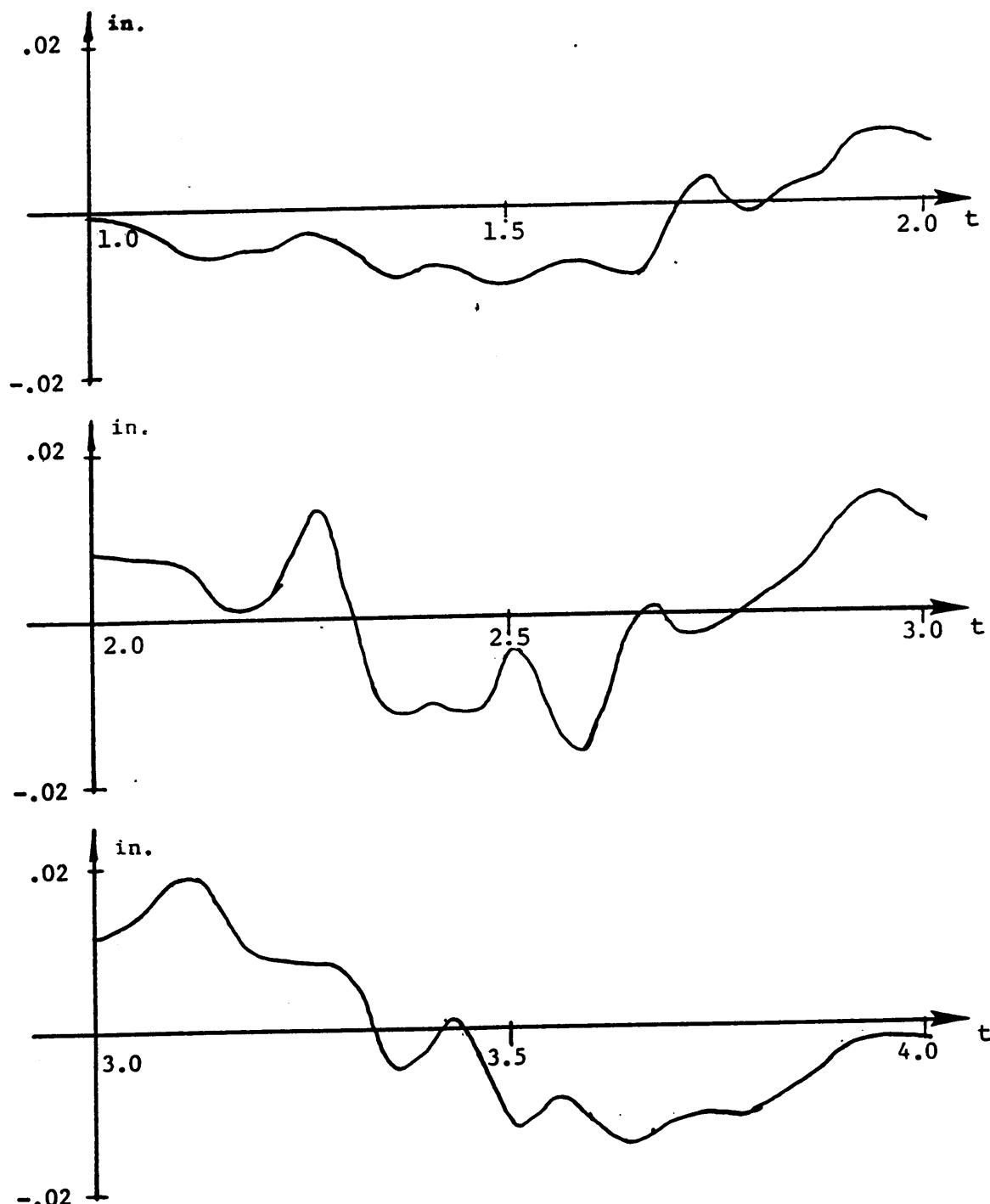


Figure 27: Displacement of joint A for dead load plus 20 lb./ ft.<sup>2</sup> on the small dome.

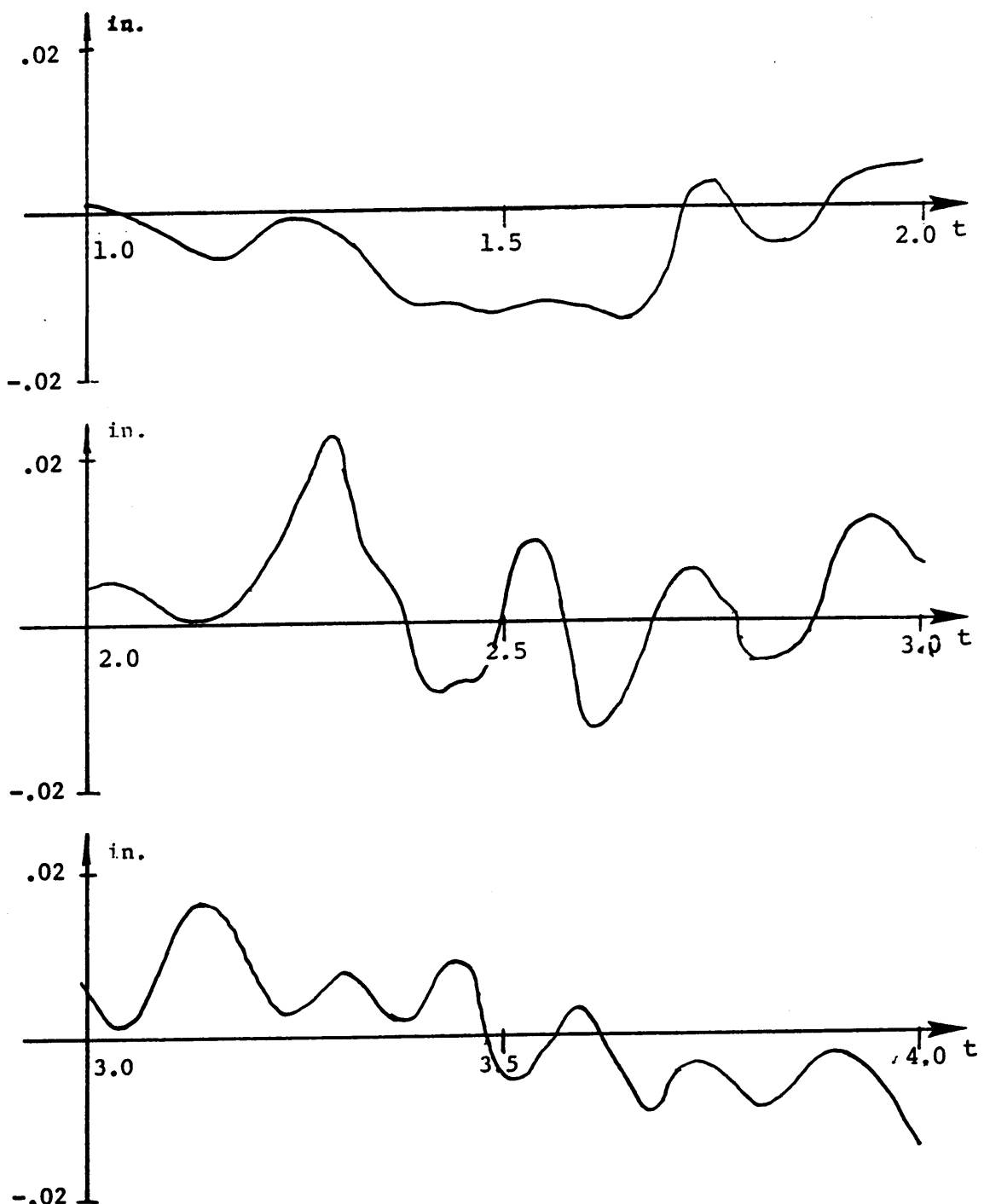


Figure 28: Displacement of joint A for dead load plus 30 lb./ft.<sup>2</sup> on the small dome.

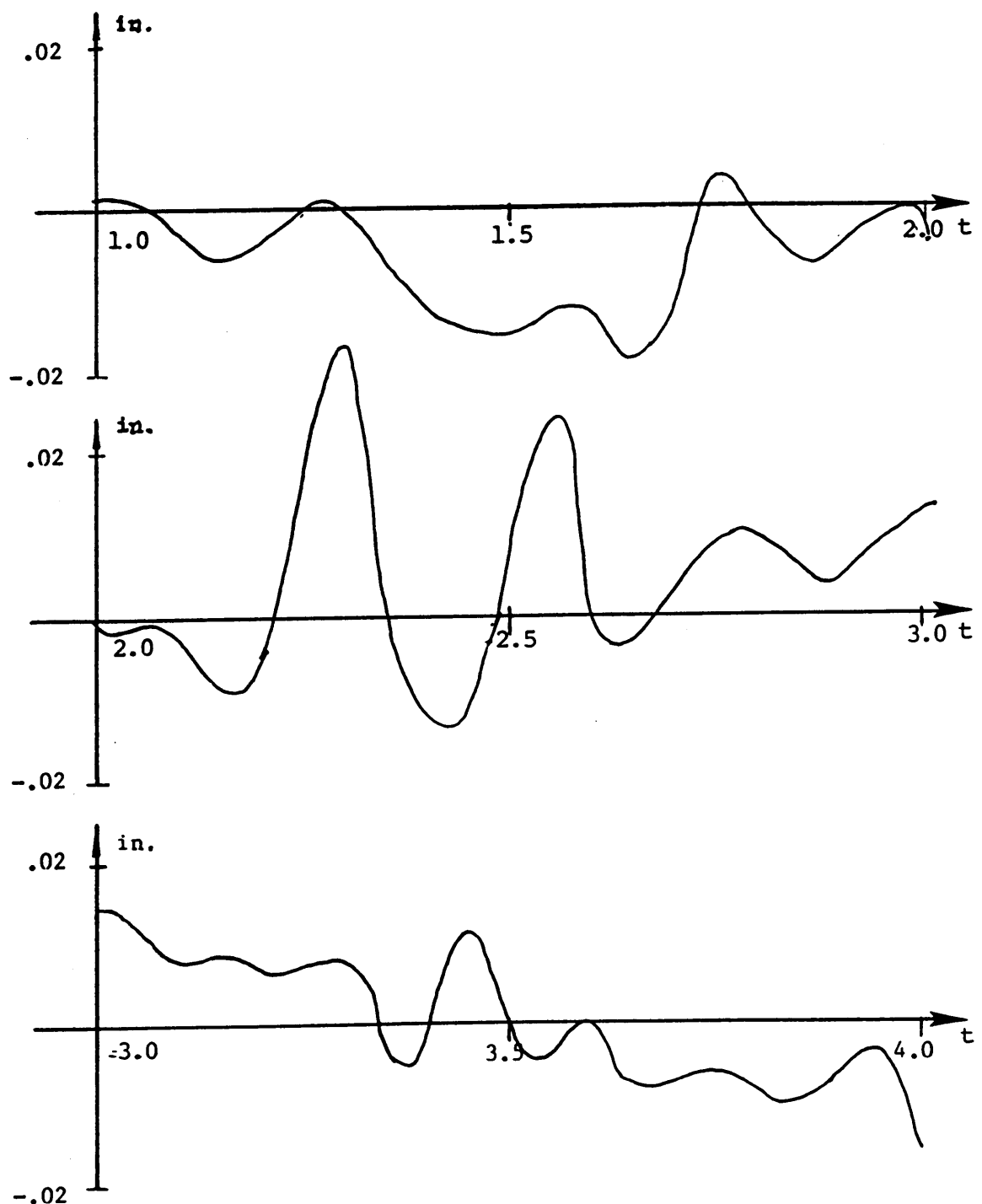


Figure 29: Displacement of joint A for dead load plus 40 lb./ft.<sup>2</sup> on the small dome.

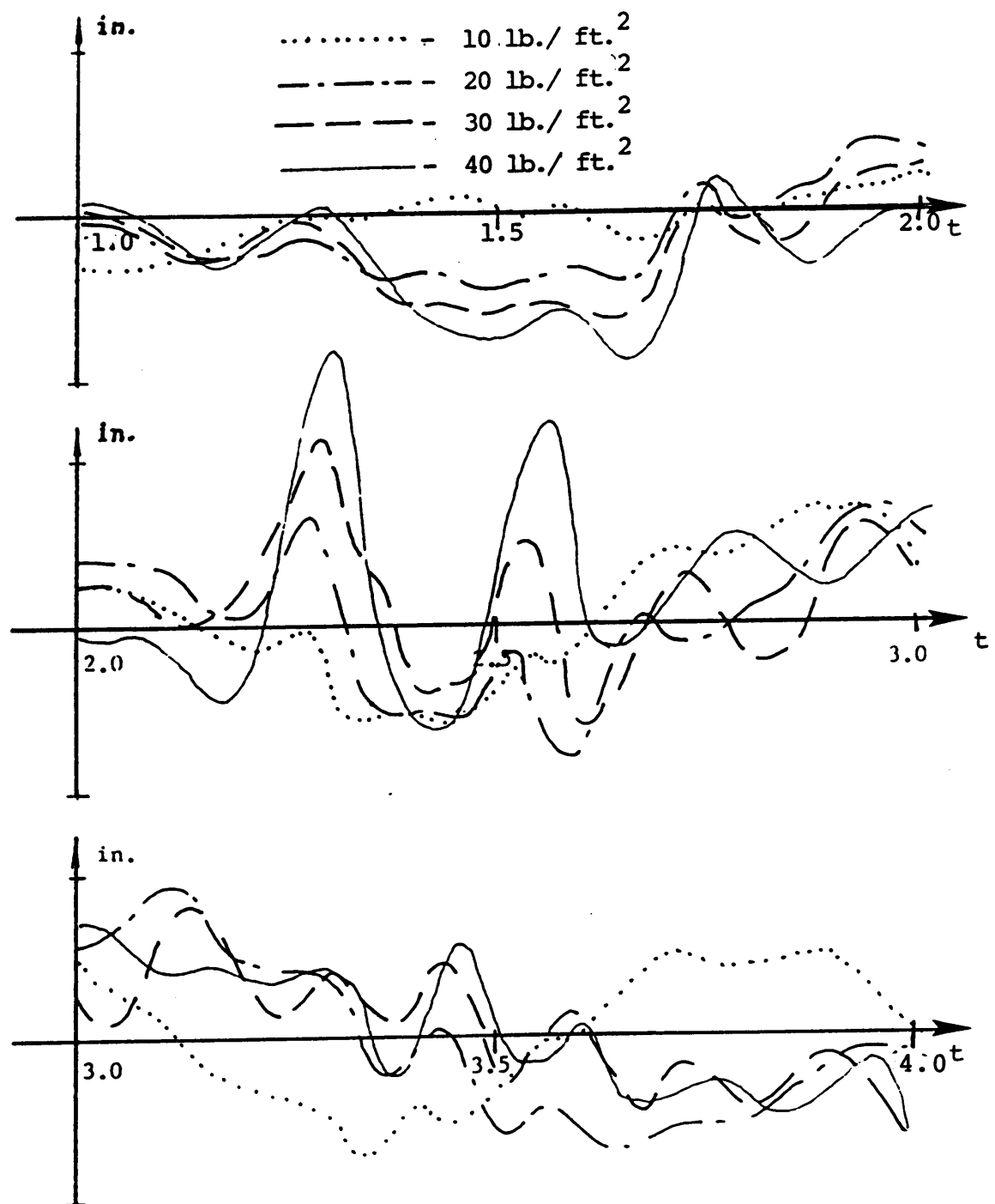


Figure 30: A comparison of the displacements of node A for several live loads on the small dome.

TABLE 3

A comparison of maximum stresses in numbered members of the small dome for dead load only.

ELEMENT NUMBER	MAXIMUM STRESSES (KSI)	
	STATIC	DYNAMIC
1	-0.1724	-0.4997
2	-0.1724	-0.6953
3	-0.1724	-0.7683
4	-0.3775	-1.5300
5	-0.3775	-1.0935
6	-0.3775	-1.3778
7	-0.2248	-0.4164
8	-0.1170	-0.6900
9	-0.1170	-0.6041
10	-0.2248	-0.6106
11	-0.1170	-0.5218
12	-0.1170	-0.7187
13	-0.2248	-0.6977
14	-0.1170	-0.5987
15	0.6954	N.A.
16	0.6954	N.A.
17	0.6954	N.A.
18	0.6954	N.A.
19	0.6954	N.A.

TABLE 4

A comparison of maximum stresses in numbered members of the small dome for dead load plus 10 lb./ft.<sup>2</sup>.

ELEMENT NUMBER	MAXIMUM STRESSES (KSI)	
	STATIC	DYNAMIC
1	-0.9344	-2.0533
2	-0.9349	-2.0505
3	-0.9347	-2.0470
4	-2.0470	-4.2246
5	-2.0470	-4.4516
6	-2.0470	-3.4689
7	-1.2199	-1.4644
8	-0.6346	-1.7334
9	-0.6346	-1.7330
10	-1.2199	-1.4644
11	-0.6346	-1.7340
12	-0.6346	-1.7115
13	-1.2199	-1.3860
14	-0.6346	-1.8266
15	3.7715	N.A.
16	3.7715	N.A.
17	3.7715	N.A.
18	3.7715	N.A.
19	3.7715	N.A.

TABLE 5

A comparison of maximum stresses in numbered members of the small dome for dead load plus 20 lb./ft.<sup>2</sup>.

ELEMENT NUMBER	MAXIMUM STRESSES (KSI)	
	STATIC	DYNAMIC
1	-1.6696	-2.4123
2	-1.6706	-2.4098
3	-1.6701	-2.4983
4	-3.8358	-4.8906
5	-3.8358	-5.1370
6	-3.8358	-5.2127
7	-2.2403	-2.0145
8	-1.1650	-2.3430
9	-1.1657	-2.2771
10	-2.2395	-2.1453
11	-1.1658	-2.4295
12	-1.1657	-2.2287
13	-2.2395	-2.2861
14	-1.1656	-2.3396
15	6.9397	N.A.
16	6.9399	N.A.
17	6.9398	N.A.
18	6.9398	N.A.
19	6.9398	N.A.

TABLE 6

A comparison of maximum stresses in numbered members of the small dome for dead load plus 30 lb./ft.<sup>2</sup>.

ELEMENT NUMBER	MAXIMUM STRESSES (KSI)	
	STATIC	DYNAMIC
1	-2.3857	-3.3636
2	-2.3874	-3.3866
3	-2.3865	-3.4172
4	-5.7541	-6.7501
5	-5.7539	-6.9113
6	-5.7541	-6.9779
7	-3.2925	-2.8283
8	-1.7134	-3.1844
9	-1.7146	-2.9653
10	-3.2912	-2.9316
11	-1.7147	-3.2442
12	-1.7143	-3.0227
13	-3.2913	-3.0731
14	-1.7142	-3.1550
15	10.2090	N.A.
16	10.2090	N.A.
17	10.2090	N.A.
18	10.2090	N.A.
19	10.2090	N.A.

TABLE 7

A comparison of maximum stresses in numbered members of the small dome for dead load plus 40 lb./ft.<sup>2</sup>.

ELEMENT NUMBER	MAXIMUM STRESSES (KSI)	
	STATIC	DYNAMIC
1	-3.1233	-4.3309
2	-3.1233	-4.2975
3	-3.123	-4.5087
4	-7.5331	-9.1166
5	-7.5331	-9.5351
6	-7.5331	-9.7253
7	-4.3104	-3.6836
8	-2.2447	-4.6477
9	-2.2447	-3.9668
10	-4.3104	-4.0932
11	-2.2447	-4.7786
12	-2.2447	-4.0695
13	-4.3104	-4.3567
14	-2.2447	-4.4925
15	13.3654	N.A.
16	13.3654	N.A.
17	13.3654	N.A.
18	13.3654	N.A.
19	13.3654	N.A.

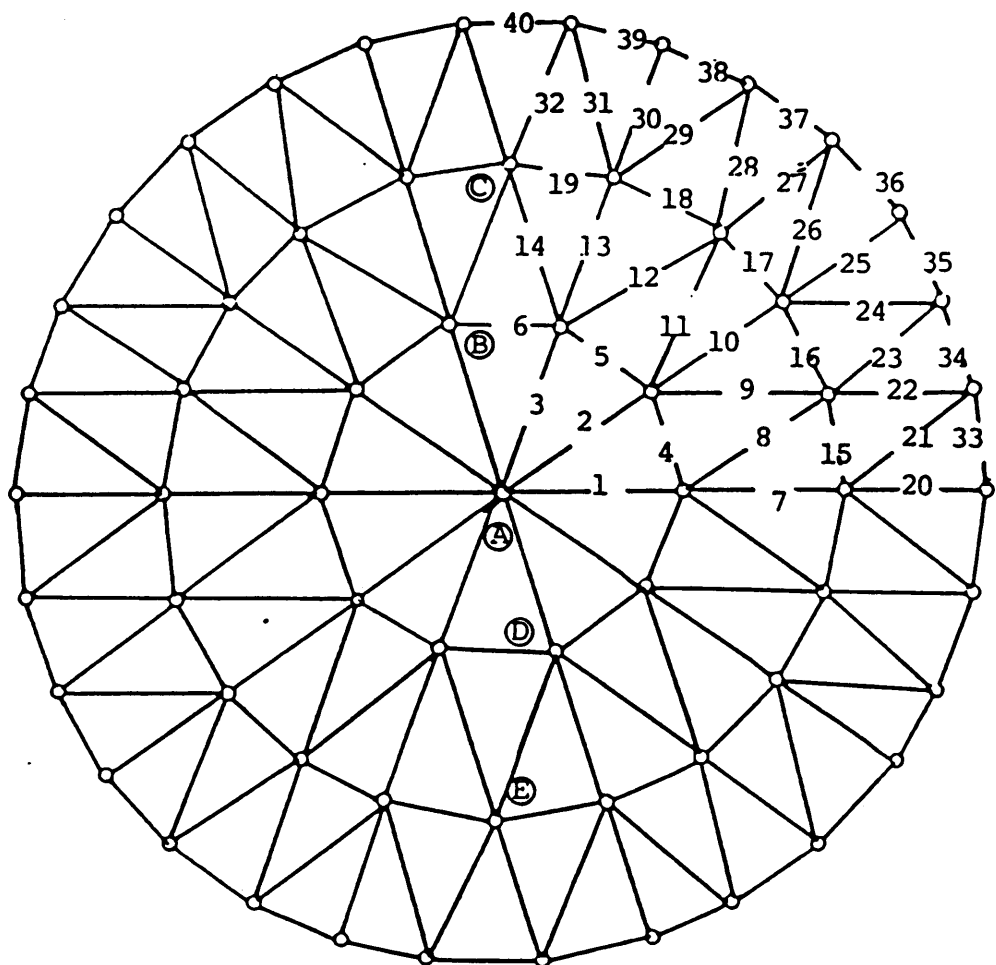


Figure 31: Large lamella dome with numbered members.

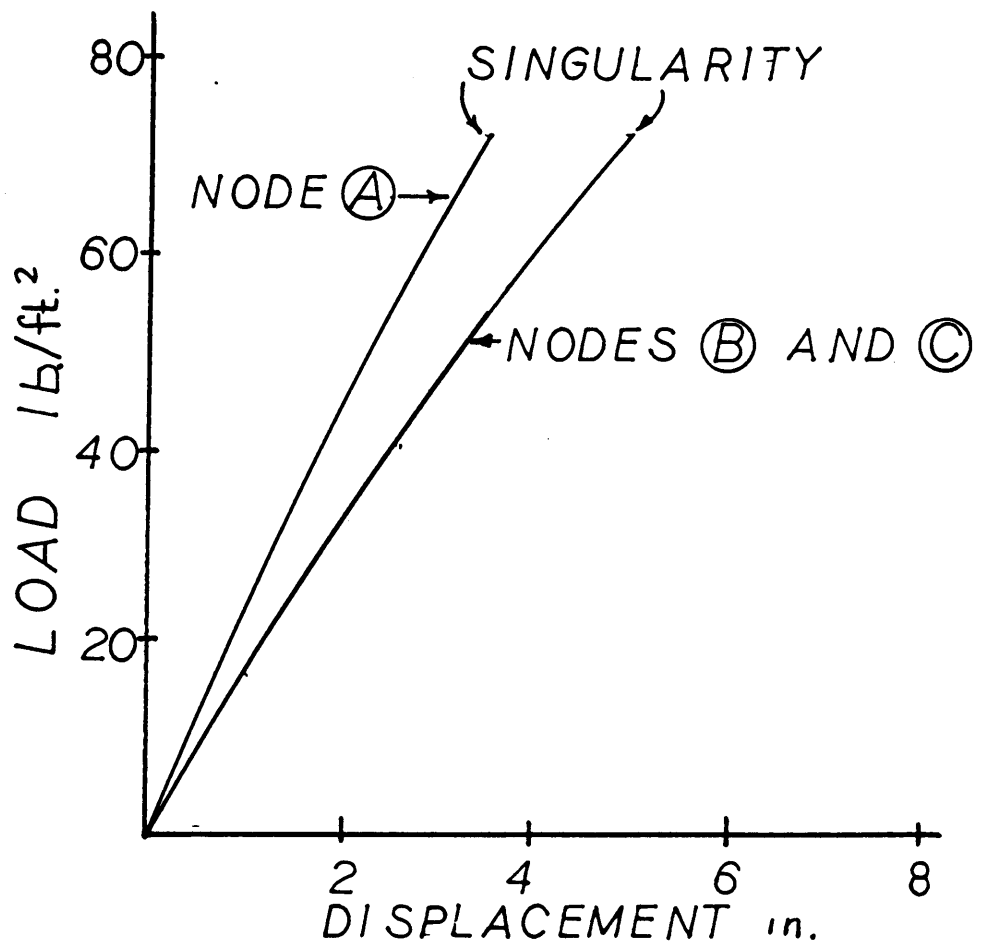


Figure 32: Load vs. displacement curves for uniform load on the large dome.

TABLE 8

**Maximum stresses of static analysis for numbered members of the large dome.**

ELEMENT NUMBER	MAXIMUM STRESS AT FAILURE(KSI)	ELEMENT NUMBER	MAXIMUM STRESS AT FAILURE(KSI)
1	-5.331	21	-2.232
2	-5.331	22	-5.513
3	-5.333	23	-5.513
4	-11.860	24	-2.232
5	-11.860	25	-7.447
6	-11.860	26	-2.232
7	-7.370	27	-5.513
8	-3.484	28	-5.513
9	-3.484	29	-2.232
10	-7.370	30	-7.439
11	-3.484	31	-2.232
12	-3.484	32	-5.511
13	-7.370	33	32.355
14	-3.434	34	32.603
15	-9.654	35	32.357
16	-9.657	36	32.356
17	-9.655	37	32.602
18	-9.655	38	32.357
19	-9.655	39	32.357
20	-7.447	40	32.603

for other loads are given in the next section where they are compared to the dynamic results. The maximum allowable stresses and the buckling stresses for the numbered elements of Fig. 31 are given in Table 9. Again, none of the members reached the buckling stress before the global instability.

For the nonuniform load the stiffness matrix becomes singular at 45 lb./ft.<sup>2</sup> plus the dead load. Fig. 33 shows the load-displacement graph for the downward deflections of nodes A,B,C,D and E. Nodes D and E are in the lesser loaded portion of the dome. In this dome, unlike in the small dome, no members reached their buckling stress prior to global instability.

### 5.3.2 Dynamic Analyses

Due to the cost of analysis of the large dome the loading conditions are reduced to three. They are:

1. Dead load only.
2. Dead load plus 20 lb./ft.<sup>2</sup> live load.
3. Dead load plus 40 lb./ft.<sup>2</sup> live load.

Nodal displacements at each time step are calculated in addition to the maximum stresses in each member.

The time displacement graphs of node A in the direction of the earthquake excitation for all three load conditions are shown in Figs. 34 through 36. A composite graph of the

TABLE 9

Maximum allowable stresses and buckling stresses for numbered members of the large dome.

ELEMENT NUMBER	MAXIMUM ALLOWABLE COMPRESSIVE STRESS (KSI)	BUCKLING STRESS (KSI)
1	-5.10	-9.89
2	-5.10	-9.89
3	-5.10	-9.89
4	-12.34	-25.43
5	-12.34	-25.43
6	-12.34	-25.43
7	-5.10	-9.89
8	-4.26	-8.28
9	-4.26	-8.28
10	-5.10	-9.89
11	-4.26	-8.28
12	-4.26	-8.28
13	-5.10	-9.89
14	-4.26	-8.28
15	-12.34	-25.43
16	-12.34	-25.43
17	-12.34	-25.43
18	-12.34	-25.43
19	-12.34	-25.43

TABLE 9 (cont'd)

ELEMENT NUMBER	MAXIMUM ALLOWABLE COMPRESSIVE STRESS	BUCKLING STRESS
20	-5.10	-9.89
21	-4.65	-9.03
22	-4.65	-9.03
23	-4.65	-9.03
24	-4.65	-9.03
25	-5.10	-9.89
26	-4.65	-9.03
27	-4.65	-9.03
28	-4.65	-9.03
29	-4.65	-9.03
30	-5.10	-9.89
31	-4.65	-9.03
32	-4.65	-9.03
33	-12.34	-25.43
34	-12.34	-25.43
35	-12.34	-25.43
36	-12.34	-25.43
37	-12.34	-25.43
38	-12.34	-25.43
39	-12.34	-25.43
40	-12.34	-25.43

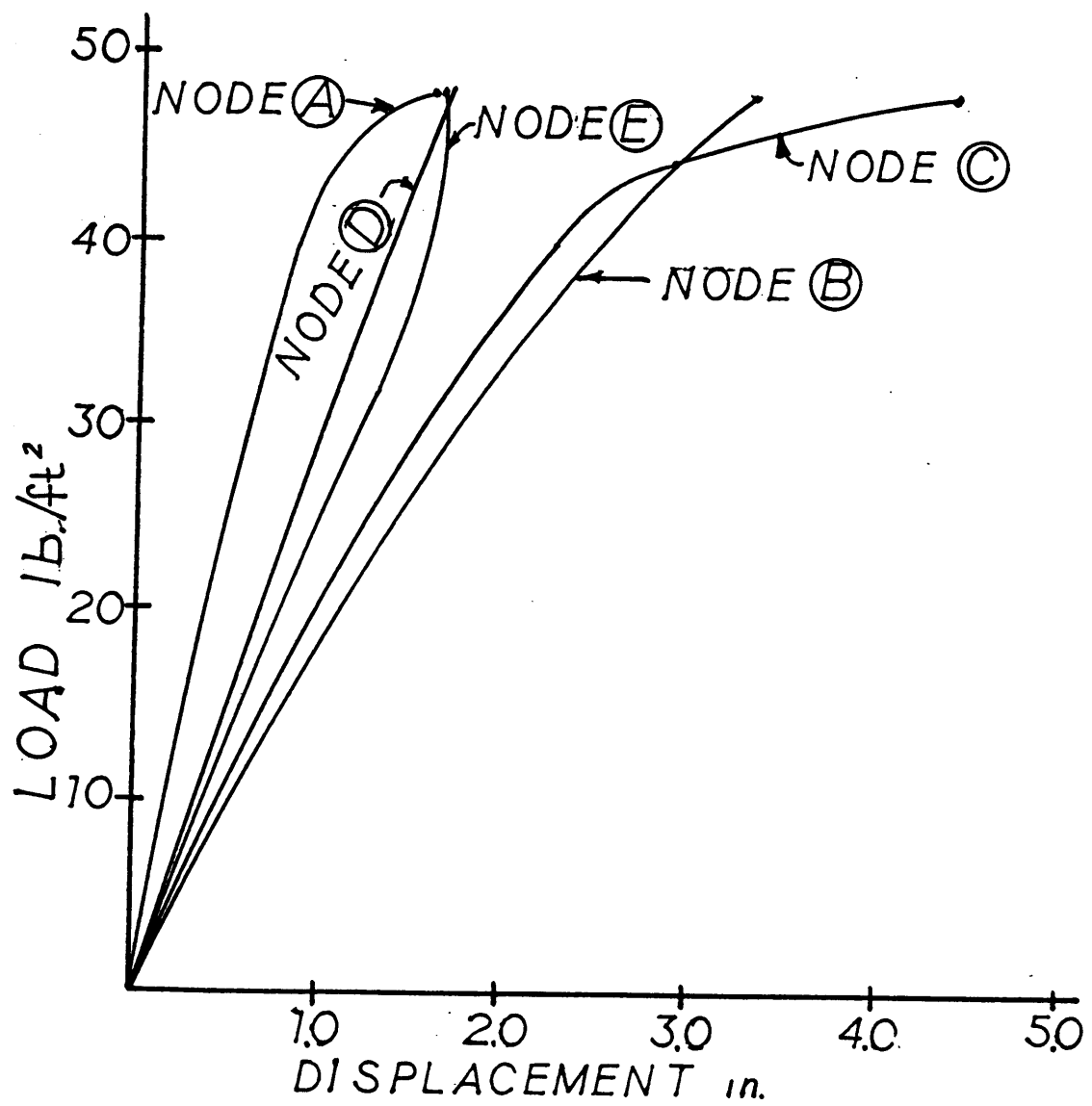


Figure 33: Load-displacement curves for nonuniform load on the large dome.

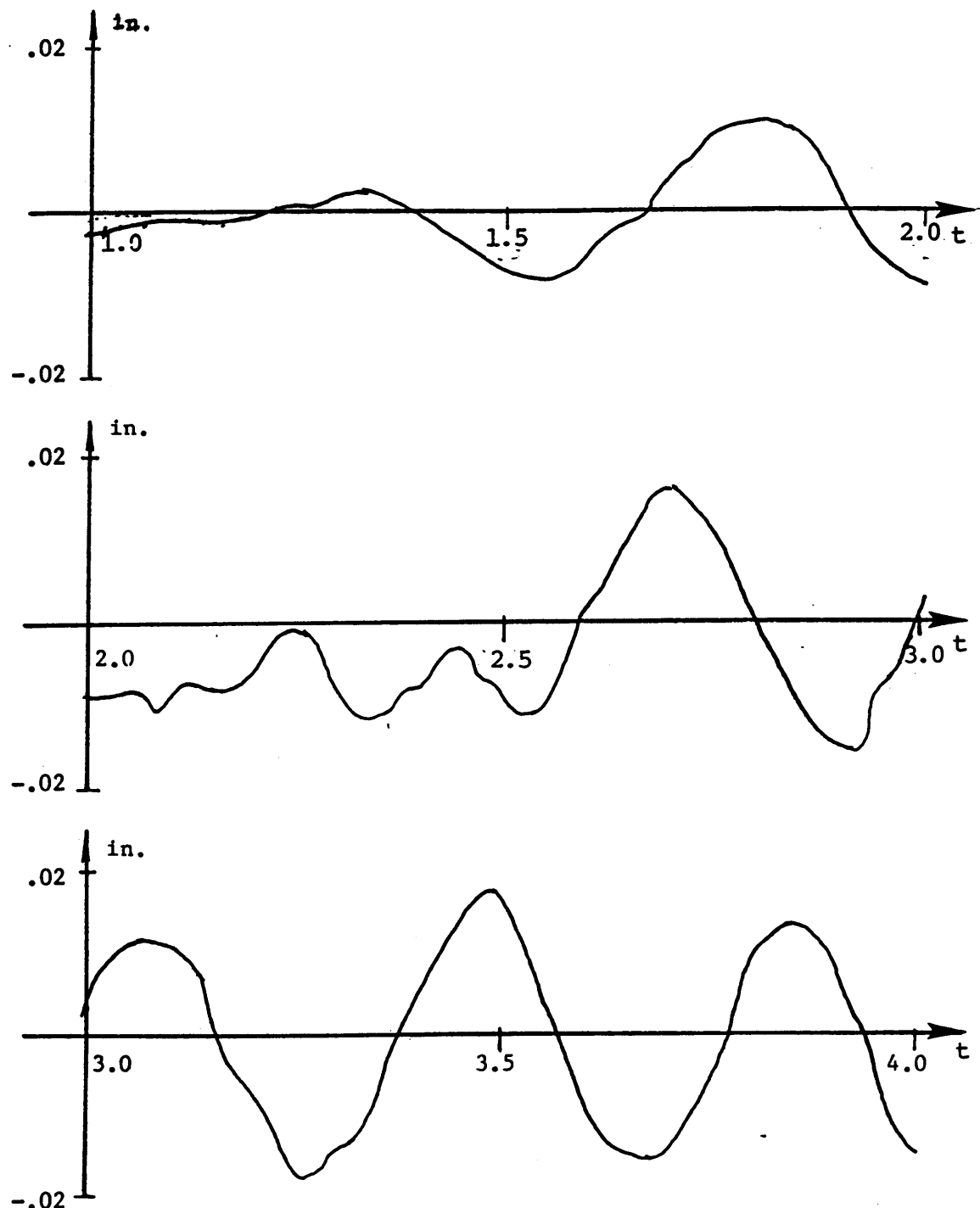


Figure 34: Displacement of joint A for dead load only on the large dome.

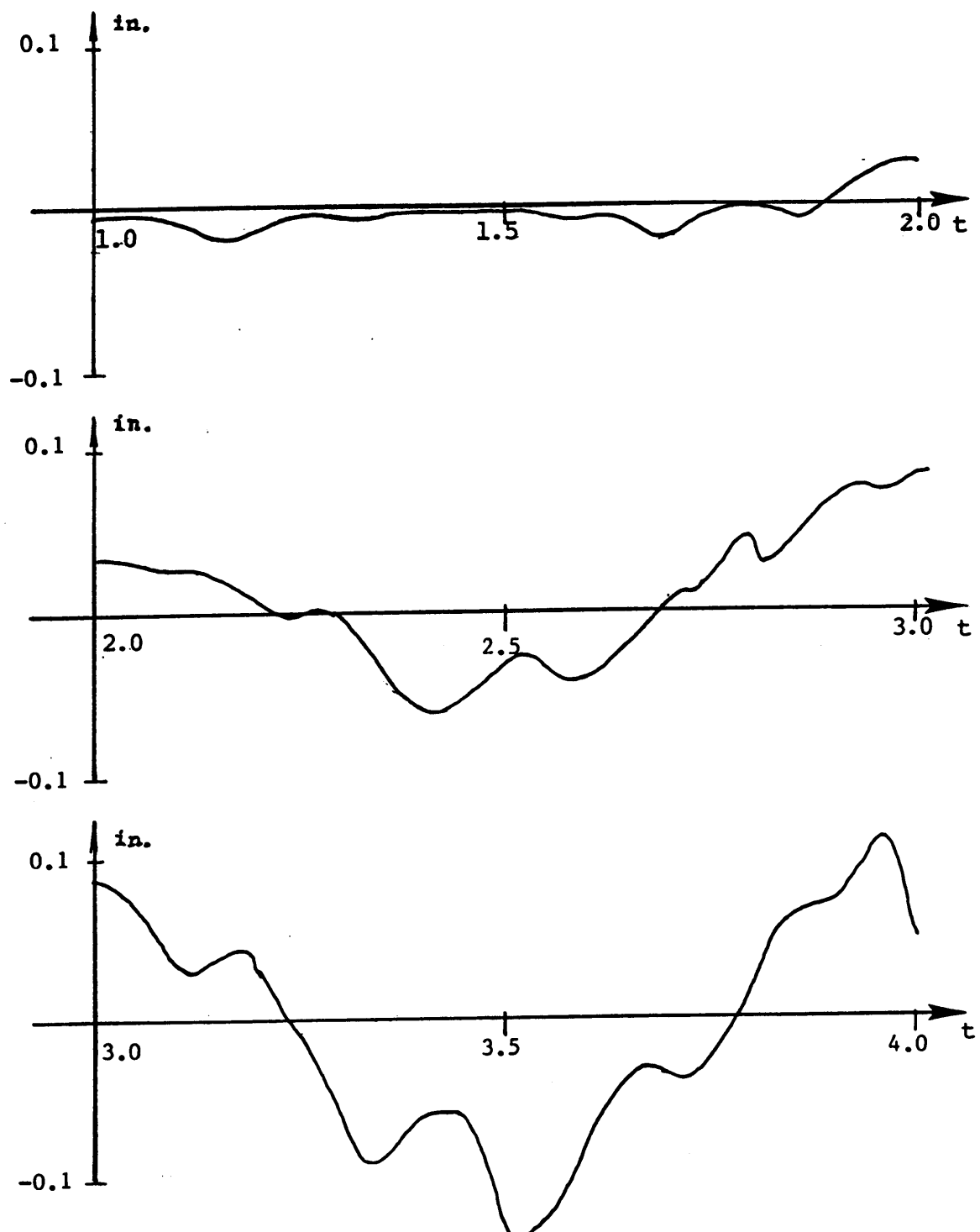


Figure 35: Displacement of joint A for dead load plus 20 lb./ft.<sup>2</sup> on the large dome.

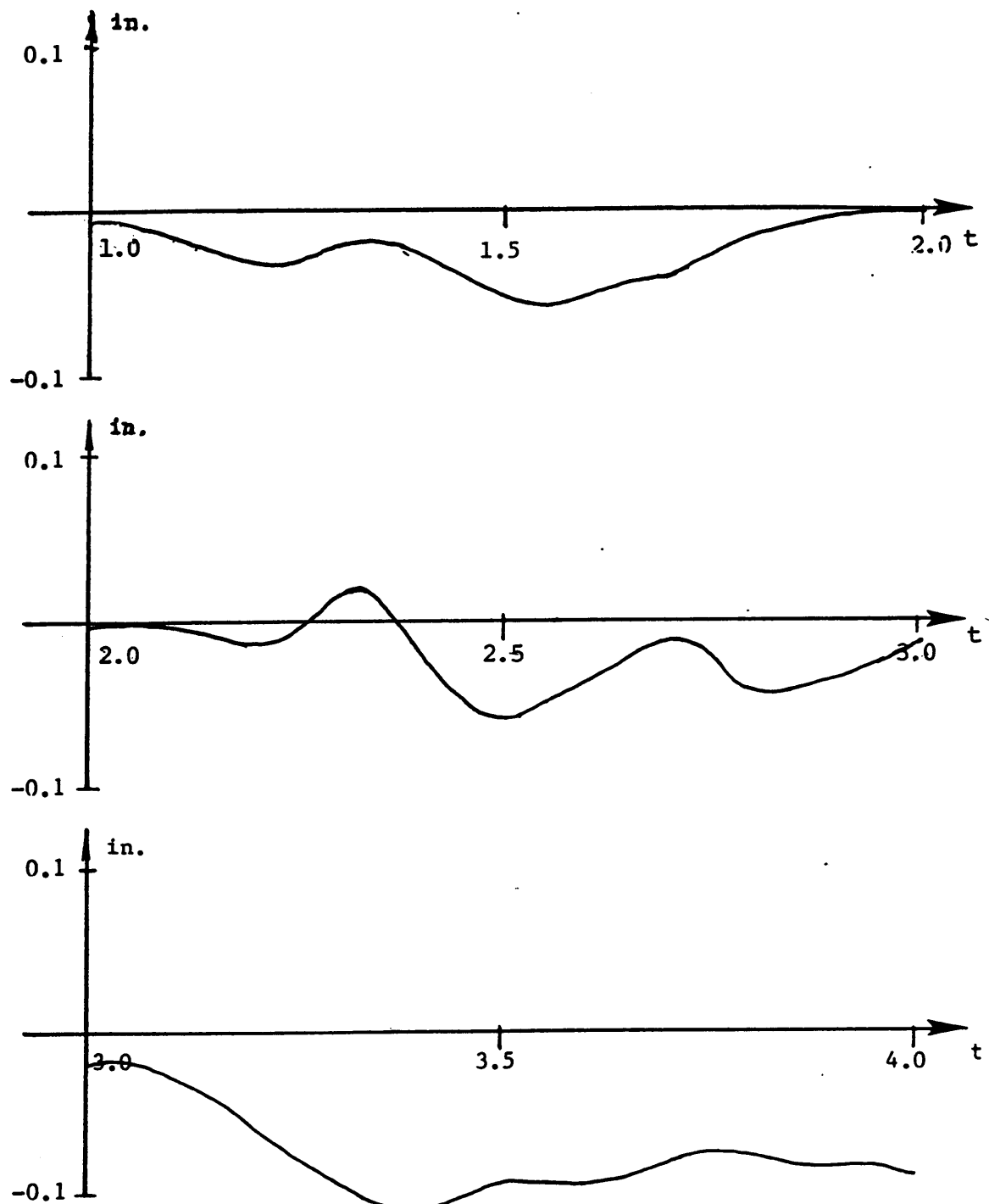


Figure 36: Displacement of joint A for dead load plus 40 lb./ft.<sup>2</sup> on the large dome.

two live loads is presented in Fig. 37. Tables 10 through 12 offer comparisons between the maximum stresses in the numbered elements of both the static and dynamic analyses. The tension ring elements are not included in the dynamic analyses.

#### 5.4 COMPARISONS OF STRESSES FOR BOTH LARGE AND SMALL DOMES

The allowable stress for all members according to the Aluminum Association (49) were calculated. Allowable tensile stress for all members is 19 ksi. Allowable compressive stresses are found in Table 2 for the small dome and in Table 9 for the large dome. These compressive stresses are very low because the members are unusually long for their cross-sectional areas.

For the static analyses all members of the small dome were over-stressed at failure. These over-stresses ranged from 6% in members 1, 2 and 3 to 74% in members 7, 10 and 13. No members, however, reached the buckling load or yield stress prior to failure. For the large dome, half of the members were over-stressed at failure. The over-stresses ranged from 5% in members 1, 2 and 3 to 71% in members of the tension ring. Other over-stressed members were 7, 10, 13, 20, 25, 30, 22, 23, 27, 28 and 32. As with the small dome, no members reached their buckling stress and none reached the yield stress of the material.

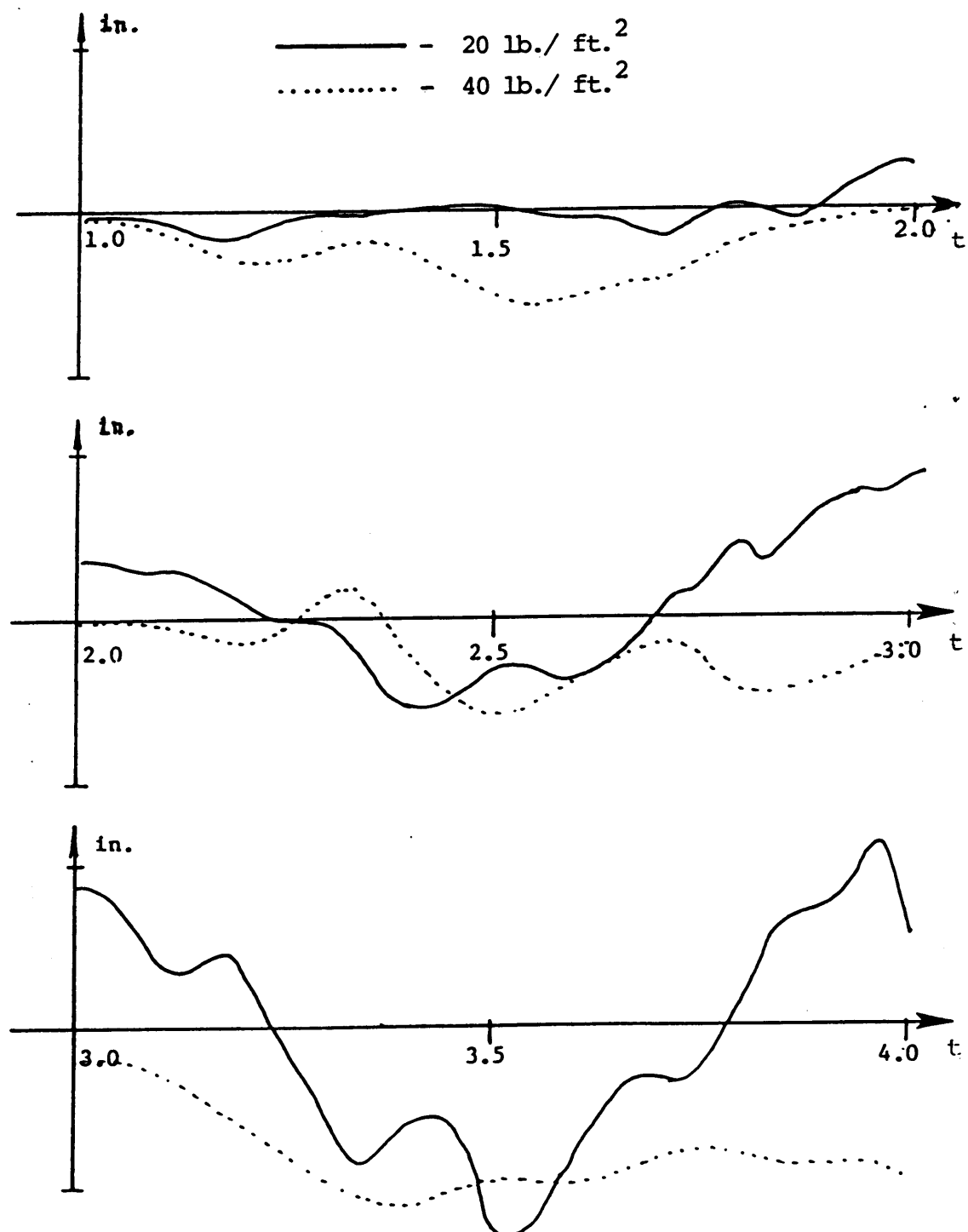


Figure 37: A comparison of the displacements of joint A for the two live loads on the large dome.

TABLE 10

A comparison of maximum stresses in numbered members of the large dome for dead load only.

ELEMENT NUMBER	MAXIMUM STRESSES (KSI)	
	STATIC	DYNAMIC
1	-0.1786	-0.6109
2	-0.1787	-0.6475
3	-0.1787	-0.5835
4	-0.3594	-0.9185
5	-0.3594	-0.9619
6	-0.3594	-0.8995
7	-0.2235	-0.4755
8	-0.1159	-0.4775
9	-0.1159	-0.5595
10	-0.2236	-0.4851
11	-0.1158	-0.4421
12	-0.1158	-0.3582
13	-0.2236	-0.5059
14	-0.1158	-0.4643
15	-0.2558	-0.6264
16	-0.2558	-0.6284
17	-0.2558	-0.7462
18	-0.2558	-0.7373
19	-0.2558	-0.8282

TABLE 10 (cont'd)

ELEMENT NUMBER	MAXIMUM STRESSES (KSI)	
	STATIC	DYNAMIC
20	-0.2264	-0.3024
21	-0.0622	-0.4735
22	-0.1722	-0.4776
23	-0.1721	-0.4713
24	-0.0622	-0.4177
25	-0.2264	-0.2909
26	-0.0624	-0.3460
27	-0.1722	-0.5168
28	-0.1722	-0.4908
29	-0.0624	-0.3659
30	-0.2262	-0.2864
31	-0.0623	-0.3277
32	-0.1722	-0.5147
33	0.9694	N.A.
34	0.9808	N.A.
35	0.9694	N.A.
36	0.9694	N.A.
37	0.9808	N.A.
38	0.9694	N.A.
39	0.9694	N.A.
40	0.9808	N.A.

TABLE 11

A comparison of maximum stresses in numbered members of the large dome for dead load plus 20 lb./ft.<sup>2</sup>.

ELEMENT NUMBER	MAXIMUM STRESSES (KSI)	
	STATIC	DYNAMIC
1	-1.550	-6.4323
2	-1.550	-6.4359
3	-1.550	-6.1703
4	-3.154	-8.3003
5	-3.154	-9.8866
6	-3.154	-8.9202
7	-1.959	-5.8969
8	-1.008	-3.6016
9	-1.008	-4.2084
10	-1.959	-5.1915
11	-1.008	-3.5280
12	-1.008	-4.0336
13	-1.959	-5.9531
14	-1.008	-5.0583
15	-2.263	-7.6324
16	-2.263	-7.5691
17	-2.263	-7.7237
18	-2.263	-7.1507
19	-2.263	-7.2858

TABLE 11 (cont'd)

ELEMENT NUMBER	MAXIMUM STRESSES (KSI)	
	STATIC	DYNAMIC
20	-1.983	-3.5416
21	-0.547	-3.8718
22	-1.508	-4.1010
23	-1.508	-4.3558
24	-0.547	-3.3052
25	-1.983	-3.1945
26	-0.547	-3.3530
27	-1.508	-3.8117
28	-1.508	-3.9527
29	-0.547	-3.1650
30	-1.983	-2.7943
31	-0.547	-2.9507
32	-1.508	-4.8165
33	8.506	N.A.
34	8.506	N.A.
35	8.506	N.A.
36	8.506	N.A.
37	8.506	N.A.
38	8.506	N.A.
39	8.506	N.A.
40	8.506	N.A.

TABLE 12

A comparison of maximum stresses in numbered members of the large dome for dead load plus 40 lb./ft.<sup>2</sup>.

ELEMENT NUMBER	MAXIMUM STRESSES (KSI)	
	STATIC	DYNAMIC
1	-3.021	-8.8923
2	-3.023	-8.7624
3	-3.022	-9.1952
4	-6.430	-13.1460
5	-6.430	-14.6910
6	-6.430	-12.4140
7	-3.973	-8.1468
8	-1.981	-4.3363
9	-1.981	-4.5931
10	-3.975	-8.1657
11	-1.980	-5.1791
12	-1.980	-4.4359
13	-3.975	-8.7122
14	-1.980	-7.0010
15	-4.895	-8.6102
16	-4.895	-8.6628
17	-4.894	-9.6919
18	-4.894	-11.6470
19	-4.894	-13.4650

TABLE 12 (cont'd)

ELEMENT NUMBER	MAXIMUM STRESSES (KSI)	
	STATIC	DYNAMIC
20	-4.033	-5.3766
21	-1.149	-5.2154
22	-3.037	-6.3230
23	-3.035	-6.4656
24	-1.149	-4.6812
25	-4.033	-4.0493
26	-1.153	-4.3976
27	-3.063	-6.5516
28	-3.036	-6.3407
29	-1.119	-5.6663
30	-4.029	-5.7535
31	-1.151	-7.4687
32	-3.036	-8.8391
33	17.387	N.A.
34	17.520	N.A.
35	17.388	N.A.
36	17.388	N.A.
37	17.569	N.A.
38	17.388	N.A.
39	17.388	N.A.
40	17.570	N.A.

In the small dome no members became over-stressed up to and including the static load of  $40 \text{ lb./ft.}^2$ . The highest stress was 6% under allowable. For the large dome, also, no members were over-stressed up to and including  $40 \text{ lb./ft.}^2$ . The highest stress was 8.5% under allowable for the tension ring members.

For the dynamic analyses significant increases in maximum stresses were noticed for all loads on both domes over the stresses in the static analyses. Members of the small dome experienced average increases in maximum stresses of 303%, 121%, 51%, 40% and 47% for the dead load only, dead load plus  $10 \text{ lb./ft.}^2$ , dead load plus  $20 \text{ lb./ft.}^2$ , dead load plus  $30 \text{ lb./ft.}^2$  and dead load plus  $40 \text{ lb./ft.}^2$ , respectively. The maximum increases in stress of any member for the loads given were 514%, 187%, 108%, 84%, and 113%, respectively. The stresses throughout the analyses remained within the allowable range for all cases except  $40 \text{ lb./ft.}^2$  where members 8, 11 and 14 were 8.5% over-stressed but still remained below the buckling stress.

Members of the large dome experienced average stress increases of 236%, 261% and 191% for dead load only, dead load plus  $20 \text{ lb./ft.}^2$  and dead load plus  $40 \text{ lb./ft.}^2$ , while the maximum increases in stress for any member were 661%, 608% and 549%, respectively. These increases resulted in many

over-stressed members and even some buckled members. For 20 lb./ft. members 1, 2, 3, 7, 10, 13, 14 and 32 were over-stressed to a maximum of 26% over allowable but all below the buckling stress. For 40 lb./ft.<sup>2</sup> all members were over-stressed except members 16, 17, 18, 25 and 26 to a maximum of 90%. Ten elements reached buckling, however, all of these elements were outside the quarter region of Fig. 31.

A final note on the results should be given. At no time during the dynamic analyses did either dome become globally unstable. All analyses were able to be carried to completion. This may be because the entries of the force vector due to the earthquake excitation act in a plane parallel to the ground. For shallow domes like the ones used in this study horizontal forces are probably less likely to cause a global instability than vertical downward forces.

## Chapter VI

### CONCLUSIONS AND RECOMMENDATIONS

#### 6.1 CONCLUSIONS

The question to be answered by this study is by how much does an earthquake excitation increase the axial stresses in a reticulated space truss such as the domes in Figs. 2 and 3. The stress increases due to the excitation were significant especially in the large dome where the average increase was about 200% over the stresses of the static analyses. For the small dome the stress increases were smaller but still over 40%. Earthquake excitations cause stress increases that must be considered in the design of a dome in a seismic region.

Even though these stress increases appear to be large, these domes exhibit surprising strength characteristics under dynamic loading. Many studies have shown that these domes are strong for their weight when subjected to static loads and for dynamic loads they again appear to be strong. For example, the large dome was able to withstand a distributed load of nearly six times its own weight before its members became over-stressed under the base excitations. The small dome was able to withstand an additional load of nearly 13 times its own weight. This is impressive and it

demonstrates the strength and usefulness of these domes in seismic regions. Overall, the lamella dome is a strong structure and able to resist base excitations based on the results of this study.

## 6.2 RECOMENDATIONS FOR FUTURE RESEARCH

Although the basic questions of this study were resolved, many other questions were raised during the research that were not answered due to the constraints on time. Several extensions of the thesis topic that address these questions are given. Other students may wish to pursue these topics.

The computer program developed for use in this study may be refined to make it more versatile and economical. It may be modified to include various types of dynamic loads such as blast loads or wind loads to provide more complete dynamic analysis capabilities. The program may be refined to include different material nonlinearities so that different materials may be considered and more accurate results produced. Other direct integration methods may also be included. The Wilson method or the Houbolt method might be suitable for other structures. A study to find the most economical direct integration scheme for these domes is also a possible extension.

The most time consuming step in a typical computer analysis using this program is arranging and inputting the data. The program by Dib (14) produces the necessary data for a lamella dome or a geodesic dome and numbers the elements and joints to provide a reduced bandwidth. The two programs may be combined for a more efficient program.

Additional testing may be performed to answer some intriguing questions. A geodesic dome or other popular dome configuration with the same weight and overall dimensions as the lamella could be tested with the same earthquake data. The results may be compared to the results of this study. Also, the nonuniform loads mentioned in section 5.2.1 may be included and dynamic analyses performed. A comparison with uniform loads would be possible. The methods presented by Rosen and Schmit (47) and (48) to model imperfect members could be included in the program to study the effects of member imperfections.

The frequencies of the structure are calculated using the stiffness matrix of the undeformed structure and the mass matrix of the unloaded structure. By increasing the mass with the live load and changing the stiffness matrix with the initial displacements caused by the live loads, the frequencies should change. A study could be made on how the frequencies change with different live loads. Any changes

in the frequencies would alter the damping coefficients and time steps. The amount of change in these parameters should be determined to see if they are significant and to what degree they affect the analysis. If the time steps would vary significantly for different loads then it may be advantageous to generate an artificial accelerogram to accept the varying time steps.

The last question to be answered is whether the bending strains should be included in the analysis. Perhaps the assumption of the space truss element is not accurate. Including the live loads may require that a space frame element be used. The program may be modified to model a space frame element and comparisons between the frame and the truss can be made.

## REFERENCES

1. Atalik, T. S. and Utku, S., "Stochastic Linearization of Multi-Degree-of-Freedom Nonlinear Systems," Earthquake Engineering and Structural Dynamics, Vol. 4, no. 4, April-June, 1976, pp. 411-420.
2. Baron, F. and Venkatesan, M. S., "Nonlinear Analysis of Cable and Truss Structures," Journal of the Structural Division, ASCE, Vol. 97, no. ST2, Feb., 1971, pp. 679-710.
3. Bathe, K. J., "Solutions of Equilibrium Equations in Static Analysis," Finite Element Procedures in Engineering Analysis, Prentice-Hall, Inc., Englewood Cliffs, New Jersey, 1982, p. 489-491.
4. Bathe, K. J., "Solution of Equilibrium Equations in Dynamic Analysis," Finite Element Procedures in Engineering Analysis, Prentice-Hall, Inc., Englewood Cliffs, New Jersey, 1982, pp. 537-542.
5. Bathe, K. J., "Solution of Equilibrium Equations in Dynamic Analysis," Finite Element Procedures in Engineering Analysis, Prentice-Hall, Inc., Englewood Cliffs, New Jersey, 1982, pp. 527-530.
6. Bathe, K. J. and Cimento, A. P., "Some Practical Procedures for the Solution of Nonlinear Finite Element Equations," Computer Methods in Applied Mechanics and Engineering, Vol. 22, no. 1, April, 1980, pp. 59-85.
7. Bathe, K. J. and Wilson, E. L., "Stability and Accuracy Analysis of Direct Integration Methods," Earthquake Engineering and Structural Dynamics, Vol. 1, no. 3, Jan.-Mar., 1973, pp. 283-291.
8. Berger, B. S. and Shore, S., "Dynamic Response of Lattice-Type Structures," Journal of the Engineering Mechanics Division, ASCE, Vol. 89, no. EM2, April, 1963, pp. 47-69.
9. Bernrueter, D. L., "Estimates of Epicentral Ground Motion in the Central and Eastern United States," Proceedings of the Sixth World Conference on Earthquake Engineering, Earthquake Engineering Research Institute, Vol. 1, 1977, pp. 332-335.

10. Carter, W. L., Dib, G. M. and Mindle, W., "Free and Steady State Vibration of Nonlinear Structures Using a Finite Element Nonlinear Eigenvalue Technique," Earthquake Engineering and Structural Dynamics, Vol. 8, no. 2, Mar.-Apr., 1980, pp. 97-115.
11. Cheung, Y. K. and Lau, S. L., "Incremental Time-Space Finite Strip Method for Nonlinear Structural Vibrations," Earthquake Engineering and Structural Dynamics, Vol. 10, no. 2, Mar.-Apr., 1982, pp. 239-254.
12. Crooker, J. O. and Buchert, K. P., "Reticulated Shell Structures," Journal of the Structural Division, ASCE, Vol. 96, no. ST3, Mar., 1970, pp. 687-700.
13. Der Kiureghian, A., "A Response Spectrum Method for Vibration Analysis of MDF Systems," Earthquake Engineering and Structural Dynamics, Vol. 9, no. 5, Sept.-Oct., 1981, pp. 419-455.
14. Dib, M., "Analysis of Reticulated Domes With Automatic Mesh Generation and Bandwidth Reduction," Thesis presented to Virginia Polytechnic Institute and State University, Blacksburg, Virginia, 1985, in partial fulfillment of the requirements for the degree of Master of Science.
15. Epstein, M. and Tene, Y., "Nonlinear Analysis of Pin-Jointed Space Trusses," Journal of the Structural Division, ASCE, Vol. 97, no ST9, Sept. 1971, pp. 2189-2202.
16. Forman, S. E. and Hutchinson, J. W., "Buckling of Reticulated Shell Structures," International Journal of Solids and Structures, Vol. 6, no. 7, July, 1970, pp. 909-932.
17. Gaylord, E. H. and Gaylord, C. N., ed., Structural Engineering Handbook, Second ed., McGraw-Hill Book Company, New York, 1979, pp. 19-11 to 19-13.
18. Ginsburg, S. and Gilbert, M., "Numerical Solution of Static and Dynamic Nonlinear Multi-Degree-of-Freedom Systems," Computer Methods in Applied Mechanics and Engineering, Vol. 23, no. 1, July 1980, pp. 111-120.
19. Goldberg, J. E. and Richard, R. M., "Analysis of Nonlinear Structures," Journal of the Structural Division, ASCE, Vol. 89, no. ST4, Aug., 1963, pp. 333-351.

20. Hall, J. F., "An FFT Algorithm for Structural Dynamics," Earthquake Engineering and Structural Dynamics, Vol. 10, no. 6, Nov.-Dec., 1982, pp. 797-811.
21. Haroun, M. A., "Corrected Accelerogram and Computed Velocities and Displacements," NISEE, Mail Code, 104-44, California Institute of Technology, Pasadena.
22. Hensley, R. C. and Azar, J. J., "Computer Analysis of Nonlinear Truss Structures," Journal of the Structural Division, ASCE, Vol. 94, no. ST6, Proc. Paper 5997, June 1968, pp. 1427-1439.
23. Hibler, H., Hughes, T. J. R. and Taylor, R. L., "Improved Numerical Dissipation for Time Integration Algorithms in Structural Dynamics," Earthquake Engineering and Structural Dynamics, Vol. 5, no. 3, July-Sept., 1977, pp. 283-292.
24. Hinton, E., Rock, T. and Zienkiewicz, O. C., "A Note on Mass Lumping and Related Processes in the Finite Element Method," Earthquake Engineering and Structural Dynamics, Vol. 4, no. 3, Jan.-Mar., 1976, pp. 245-249.
25. Holzer, S. M., "Notes on Geometrically Nonlinear Analysis," Virginia Polytechnic Institute and State University, Blacksburg, Virginia, 1984.
26. Holzer, S. M., Watson, L. T. and Vu, P., "Stability Analysis of Lamella Domes," Proceedings of a Symposium on Long Span Roof Structures, ASCE, October, 1981, pp. 179-209.
27. Housner, G. W. and Jennings, P. C., "Generation of Artificial Earthquakes," Journal of the Engineering Mechanics Division, ASCE, Vol. 90, no. EM1, February, 1964, pp. 113-150.
28. Iyengar, R. N. and Iyengar, K. T., "Nonstationary Random Process Model for Earthquake Accelerograms," Bulletin of the Seismological Society of America, Vol. 59, no. 3, June 1969, pp. 1163-1188.
29. Jagannathan, S., Epstein, H. I. and Christiano, P., "Nonlinear Analysis of Reticulated Space Trusses," Journal of the Structural Division, ASCE, Vol. 101, no. ST11, November, 1975, pp. 2641-2658.

30. Kameda, H. and Ang, A. H.-S., "Simulation of Strong Earthquake Motions for Inelastic Structural Response," Proceedings of the Sixth World Conference on Earthquake Engineering, Earthquake Engineering Research Institute, Vol. 1, 1977, pp. 483-488.
31. Kubo, T. and Penzien, J., "Simulation of Three-Dimensional Strong Motions Along Principal Axes, San Fernando Earthquake," Earthquake Engineering and Structural Dynamics, Vol. 7, no. 3, May-June, 1979, pp. 279-293.
32. Liou, D. D., "Frequency-Domain Redigitization Method for Seismic Time Histories," Earthquake Engineering and Structural Dynamics, Vol. 10, no. 3, May-June, 1982, pp. 511-515.
33. McConnel, R. E. and Klimke, H., "Geometrically Nonlinear Pin-Jointed Space Frames," Numerical Methods for Nonlinear Problems, C Taylor, E. Hinton and D. R. J. Owen, ed., Vol. 1, p. 333.
34. Newmark, N. M., "A Method of Computation for Structural Dynamics," Journal of the Engineering Mechanics Division, ASCE, Vol. 85, no. EM3, July 1959, pp. 67-94.
35. Nickell, R. E., "Direct Integration Methods in Structural Dynamics," Journal of the Engineering Mechanics Division, ASCE, Vol. 99, no. EM2, April, 1973, pp. 303-317.
36. Nickell, R. E., "Nonlinear Dynamics by Mode Superposition," ASME/SAE/ 15th Structures, Structural Dynamics and Materials Conference, Las Vegas, Nevada, April, 17-19, 1974, Proc. Paper No. 74-341.
37. Nigam, N. C. and Jennings, P. C., "Calculation of Response Spectra from Strong Motion Earthquake Records," Bulletin of the Seismological Society of America, Vol. 59, no. 2, April, 1969, pp. 909-922.
38. Noor, A. K., "Nonlinear Analysis of Space Trusses," Journal of the Structural Division, ASCE, Vol. 100, no. ST3, March, 1974, pp. 533-546.
39. Noor, A. K., "On Making Large Nonlinear Problems Small," Computer Methods in Applied Mechanics and Engineering, Vol. 34, no. 2, Sept., 1982, pp. 955-985.

40. Noor, A. K., Anderson, M. S. and Greene, W. H., "Continuum Models for Beam and Plate-Like Lattice Structures," AIAA Journal, Vol. 16, no. 12, Dec., 1978, pp. 1219-1228.
41. Noor, A. K. and Peters, J. M., "Nonlinear Dynamic Analysis of Space Trusses," Computer Methods in Applied Mechanics and Engineering, Vol. 21, no. 2, February, 1980, pp. 131-151.
42. Park, K. C. and Underwood, P. G., "A Variable-Step Central Difference Method for Structural Dynamics.- Part 1. Theoretical Aspects," Computer Methods in Applied Mechanics and Engineering, Vol. 22, no. 2, May, 1980, pp. 241-258.
43. Penzien, J and Liu, S.-C., "Nonlinear Deterministic Analyses of Nonlinear Structures Subjected to Earthquake Excitations," Earthquake Engineering at Berkeley, Report no. EERC 69-1, Jan. 1969, pp. 210-288.
44. Preumont, A., "Frequency Domain Analysis of the Time Integration Operators," Earthquake Engineering and Structural Dynamics, Vol. 10, no. 5, Sept.-Oct., 1982, pp. 691-697.
45. Renton, J. D., "The Beam-Like Behavior of Space Trusses," AIAA Journal, Vol. 22, no. 2, February, 1984, pp. 273-279.
46. Richter, D. L., "Developments in Tremcor Aluminum Domes," Analysis, Design and Construction of Braced Domes, Z. S. Makowski, ed., 1st ed., Nichols Publishing Company, New York, 1984, pp. 521-539.
47. Rosen, A. and Schmit, L. A. Jr., "Design Oriented Analysis of Imperfect Truss Structures- Part I- Accurate Analysis," International Journal for Numerical Methods in Engineering, Vol. 14, 1979, pp. 1309-1321.
48. Rosen, A. and Schmit, L. A. Jr., "Design Oriented Analysis of Imperfect Truss Structures- Part II- Approximate Analysis," International Journal for Numerical Methods in Engineering, Vol. 15, 1980, pp. 483-484.
49. Specifications for Aluminum Structures, Fourth ed., The Aluminum Association, Inc., New York, N.Y., 1982.

50. St. Balan, Minea, S., Sandi, H. and Seibanescu, G., "A Model for Simulating Ground Motion," Proceedings of the Sixth World Conference on Earthquake Engineering, Earthquake Engineering Research Institute, Vol. 1, 1977, pp. 523-528.
51. Supple, W. J., "Stability and Collapse Analysis of Braced Domes," Analysis, Design and Construction of Braced Domes, Z. S. Makowski, ed., 1st ed., Nichols Publishing Company, New York, 1984, pp. 141-146.
52. Tanabashi, R., "Studies on the Nonlinear Vibrations of Structures Subjected to Destructive Earthquakes," Proceedings of the World Conference on Earthquake Engineering, Earthquake Engineering Research Institute, June 1956, Paper no. 6.
53. Trifunac, M. D., "A Method for Synthesizing Realistic Ground Motion," Bulletin of the Seismological Society of America, Vol. 61, 1971, pp. 1739-1753.
54. Wilson, E. L., Farhoom, I. and Bathe, K. J., "Nonlinear Dynamic Analyses of Complex Structures," Earthquake Engineering and Structural Dynamics, Vol. 1, no. 3, 1973, pp. 241-251.
55. Wong, H. L. and Trifunac, M. D., "Generation of Artificial Strong Motion Accelerograms," Earthquake Engineering and Structural Dynamics, Vol. 7, no. 6, Nov.-Dec., 1979, pp. 509-528.

## Appendix A

### FREQUENCIES OF VIBRATION FOR THE SMALL LAMELLA DOME

FREQUENCY NUMBER	FREQUENCY (HERTZ)	FREQUENCY NUMBER	FREQUENCY (HERTZ)
1.	1.3993	18.	14.6974
2.	1.4014	19.	17.9737
3.	1.7227	20.	17.9742
4.	1.7290	21.	19.8414
5.	1.7523	22.	19.9268
6.	1.7764	23.	19.9268
7.	1.7995	24.	20.6390
8.	1.8205	25.	22.2076
9.	1.8999	26.	22.2037
10.	1.9515	27.	25.3070
11.	2.4822	28.	25.3088
12.	7.6420	29.	25.7914
13.	9.4609	30.	25.7914
14.	9.4612	31.	28.0129
15.	14.4240	32.	28.0133
16.	14.4240	33.	28.9991
17.	14.6974		

Appendix B

FREQUENCIES OF VIBRATION FOR THE LARGE LAMELLA  
DOME

FREQUENCY NUMBER	FREQUENCY (HERTZ)	FREQUENCY NUMBER	FREQUENCY (HERTZ)
1.	1.345	22.	1.752
2.	1.345	23.	1.754
3.	1.359	24.	1.798
4.	1.359	25.	1.798
5.	1.364	26.	1.828
6.	1.367	27.	1.828
7.	1.367	28.	1.841
8.	1.395	29.	1.841
9.	1.395	30.	1.842
10.	1.417	31.	2.687
11.	1.417	32.	4.906
12.	1.423	33.	6.560
13	1.479	34.	6.560
14.	1.730	35.	8.360
15.	1.735	36.	8.360
16.	1.735	37.	8.430
17.	1.742	38.	9.563
18.	1.742	39.	9.563
19.	1.746	40.	11.636
20.	1.746	41.	11.636
21.	1.752	42.	12.384

## Appendix B (Continued)

FREQUENCY NUMBER	FREQUENCY (HERTZ)	FREQUENCY NUMBER	FREQUENCY (HERTZ)
43.	12.384	64..	17.906
44.	12.442	65..	18.062
45.	12.443	66..	18.062
46.	12.443	67..	18.892
47.	13.412	68..	18.892
48.	13.412	69..	19.666
49.	13.775	70..	20.851
50.	14.372	71..	20.851
51.	14.372	72..	21.500
52.	15.038	73..	21.625
53.	15.609	74..	21.625
54.	15.609	75..	21.944
55.	16.891	76..	21.944
56.	17.071	77..	22.370
57.	17.071	78..	22.370
58.	17.359	79..	22.762
59.	17.359	80..	22.762
60.	17.437	81..	23.391
61.	17.437	82..	23.804
62.	17.540	83..	23.804
63.	17.540	84..	24.337

## Appendix B (Continued)

FREQUENCY NUMBER	FREQUENCY (HERTZ)	FREQUENCY NUMBER	FREQUENCY (HERTZ)
85.	24.337	90.	25.592
86.	24.792	91.	25.592
87.	24.792	92.	25.858
88.	25.285	93.	26.198
89.	25.285		

**Appendix C**  
**PROGRAM LISTING**

```

C*****PROGRAM WRITTEN TO SOLVE FOR NODAL DISPLACE-
C*****MENTS, VELOCITIES AND ACCELERATIONS OF A SPACE
C*****TRUSS STRUCTURE SUBJECTED TO BASE EXCITATIONS
C***** (PARTICULARLY EARTHQUAKE MOTIONS). IT ALSO
C*****DETERMINES THE AXIAL STRESSES OF EACH MEMBER
C*****AT EACH TIME STEP. WRITTEN BY DAVID A. ULIANA
C*****FOR USE IN THESIS WORK. SUMMER OF 1984.
C*****DISCRETIZED ACCELERATIONS. USED AS A VECTOR TO
C*****ALLOW FOR READING 8 DIFFERENT ACCELERATIONS AT A
C*****TIME ALLOWING FOR FEWER LINES IN DATA BLOCK.
C*****CROSS-SECTIONAL AREA OF ELEMENT 'I'.
C*****PARAMETER OF THE NEWMARK METHOD RELATED TO THE
C*****TYPE OF ACCELERATION OVER THE TIME STEP DELT.
C*****BETA = •2500 FOR CONSTANT ACCELERATION
C*****= •16666666 FOR LINEARLY INCREASING
C*****ACCELERATION
C*****THE BUCKLING LOAD OF MEMBER 'I'. THE COM-
C*****PRESSIVE STRESS INCREASES LINEARLY WITH STRAIN
C*****UP TO THE BUCKLE('I') LOAD BEYOND WHICH IT IS
C*****CONSTANT AND EQUAL TO BUCKLE('I,1'). INITIALLY

```

C C BUCKLE(I,2)=000, AFTER 'I' BUCKLES IT BECOMES  
 C C EQUAL TO 1000 SO THAT AN ERROR MESSAGE IS NOT  
 C C PRINTED ON EVERY PROCEEDING ITERATION.

C C C(I,J)-----THE DAMPING MATRIX. RAYLEIGH DAMPING IS USED:

I C I = DALPHA\*I M I + DBETA\*I K I

C C C1(I),C2(I),C3(I)-THE DIRECTION COSINES OF THE MEMBER 'I' ALONG  
 C C THE 1,2 AND 3 GLOBAL AXES, RESPECTIVELY.

C C CHOICE-----INTEGER TO DETERMINE IF STATIC OR DYNAMIC ANALYSIS  
 C C IS DESIRED:

C C CHOICE = 1 - STATIC ANALYSIS

C C CHOICE = 2 - DYNAMIC ANALYSIS

C C COMP(3)-----THE COMPONENT OF THE DIRECTION OF THE EARTH-  
 C C QUAKE EXCITATION ALONG THE RESPECTIVE GLOBAL  
 C C AXIS:  
 C C COMP(1) = THE COORDINATE OF EXCITATION ALONG  
 C C THE GLOBAL 1 AXIS  
 ECT.

C C COORD-----THE COORDINATE IN THE GLOBAL REFERENCE FRAME OF  
 C C JOINT 'J':  
 C C COORD(1,J) = THE COORDINATE OF JOINT 'J' IN THE  
 C C GLOBAL 1 DIRECTION  
 ECT.

C C COUNT-----AN INTEGER TO COUNT THE NUMBER OF ITERATIONS OF  
 C C THE NEWTON-RAPHSON PROCEDURE FOR EACH LOAD IN-  
 C C CREMENT (STATIC ANALYSIS) OR EACH TIME STEP  
 C C (DYNAMIC ANALYSIS). IF THE PROCEDURE DOES NOT

```

C CONVERGE AFTER 50 ITERATIONS THE PROGRAM IS
C STOPPED TO AVOID AN INFINITE LOOP.
C
C DAL PHA-----VALUE USED IN RAYLEIGH DAMPING
C OBETA-----VALUE USED IN RAYLEIGH DAMPING
C DELLAM-----THE INCREMENT OF THE LAMBDA PARAMETER IN STATIC
C ANALYSIS.
C
C DELT-----TIME STEP INCREMENT FOR DIRECT INTEGRATION
C
C DSUPT(I)-----A COMBINATION OF TERMS IN THE NEWMARK METHOD THAT
C APPEAR REPEATEDLY IN EACH STEP OF THE NEWTON-
C RAPHSON METHOD FOR COMPACTNESS AND EASE OF
C COMPUTATION.
C
C ELENG(I)-----THE LENGTH OF MEMBER 'I'.
C
C EPMAX(1,2)-----THE MAXIMUM STRAIN
C EPMAX(1,1) IS THE MAXIMUM STRAIN IN MEMBER
C 'I' THROUGHOUT THE ANALYSIS.
C EPMAX(1,2) IS THE LOADING CONDITION 'LAMBDA'
C (STATIC ANALYSIS) OR THE TIME 'T'
C (DYNAMIC ANALYSIS) AT WHICH THE
C MAXIMUM STRAIN OCCURS
C
C EMOD(I)-----THE MODULUS OF ELASTICITY OF MEMBER 'I'.
C
C EPSLON-----THE MAGNITUDE OF THE CHANGE IN DISPLACEMENT
C VECTOR. AN INDICATOR OF CONVERGENCE.

```

C FEFF(I)-----THE VECTOR OF NODAL POINT FORCES CORRESPONDING TO  
 C THE ELEMENT STRESSES AT THE EXISTING CONFIGURATION  
 C (SEE BATHE PG. 309). THE MATERIAL NONLINEARITY OF  
 C THIS FORMULATION APPEARS IN FVECT WHEN CALCULATING  
 C FEFF(I). THE RESISTING STRESSES ARE MODELED USING  
 C A BILINEAR APPROXIMATION. FEFF(I) CAN BE THOUGHT  
 C OF AS THE RESISTING FORCES PRODUCED BY THE STRUC-  
 C TURE IN A CERTAIN CONFIGURATION.

C G(6)-----TEMPORARY STORAGE FOR THE ELEMENT STIFFNESS MATRIX  
 C VALUES. UPDATED FOR EACH ELEMENT CONTRIBUTION TO  
 C THE GLOBAL STIFFNESS MATRIX.

C HOLDK(I,J)-----A STORAGE LOCATION FOR THE STIFFNESS MATRIX  
 C KEFF. USED FOR THREE DIFFERENT PURPOSES IN  
 C THE DYNAMIC ANALYSIS:  
 C 1. ALWAYS-

C AS TEMPORARY STORAGE IN SUBROUTINE  
 C KHT TO STORE THE NON-BANDED STIFFNESS  
 C BEFORE IT IS ADDED TO THE MASS MATRIX  
 C TO FORM KEFF. ALSO USED TO FORM NCN-  
 C BANDED DAMPING MATRIX.

C 2. WHEN STIFFNESS IS NOT MODIFIED (MODIFY = 0)-  
 C AS A PERMANENT STORAGE LOCATION FOR KEFF  
 C SINCE KEFF IS DESTROYED AFTER EACH TIME  
 C 'SOLVE' IS CALLED.

C 3. IN SUBROUTINE LINEAR-  
 C AS A PERMANENT STORAGE FOR THE LINEAR  
 C STIFFNESS MATRIX KEFF SINCE IT IS DES-  
 C TROYED EACH TIME 'SOLVE' IS CALLED.

C ICOUNT-----INTEGER TO COUNT THE NUMBER OF TIME STEPS PER-

C FORMED IN THE CENDIF METHOD. USEFUL WHEN RESULTS  
 C OF ONLY CERTAIN TIME STEPS ARE DESIRED (SINCE  
 C CENDIF TIME STEPS ARE SMALLER).  
 C  
 C IDAMPD-----INDICATES WHETHER DAMPING IS TO BE CONSIDERED  
 C IDAMPD = 1 - DAMPING IS TO BE CONSIDERED  
 C IDAMPD = 0 - NO DAMPING  
 C  
 C JCODE(3,J)-----JOINT CODE MATRIX.  
 C  
 C JDIR-----DIRECTION OF JOINT CONSTRAINT.  
 C  
 C JNUM-----NUMBER OF JOINT WHERE CONSTRAINT OCCURS.  
 C  
 C KEFF(I,J)-----THE EFFECTIVE STIFFNESS MATRIX  
 C  
 C LAMBDA-----INCREMENTED LOADING PARAMETER BY WHICH QBAR(I)  
 C (SEE BELOW) IS MULTIPLIED IN EACH STEP OF THE  
 C STATIC ANALYSIS.  
 C  
 C LUMPD-----TO INDICATE THE TYPE OF MASS MATRIX DESIRED:  
 C LUMPD = 0 - CONSISTENT MASS MATRIX  
 C LUMPD = 1 - LUMPED MASS MATRIX  
 C  
 C MASS(I,J)-----MASS MATRIX  
 C  
 C MAXLAM-----MAXIMUM VALUE OF LAMBDA TO BE CONSIDERED IN  
 C STATIC ANALYSIS.  
 C  
 C MBD-----HALF BAND WIDTH (FOR USE IN \*SOLVE\* ROUTINE)  
 C  
 C MCODE(6,I)-----MEMBER CODE OF ELEMENT 'I'

```

C C MINC(2,1)-----MEMBER INCIDENCE OF ELEMENT #I.

MODIFY-----INDICATES MODIFICATION OF STIFFNESS MATRIX
FOR STATIC ANALYSIS:
MODIFY = 0 - THE STIFFNESS MATRIX WILL BE UPDATED
THROUGHOUT THE ENTIRE ANALYSIS.
MODIFY = 1 - THE STIFFNESS MATRIX WILL BE UPDATED
WHILE THE MAGNITUDE OF THE CHANGE
IN THE DISPLACEMENT VECTOR (REFF)
DEFINED VALUE. WHEN THE MAGNITUDE
IS LESS THE STIFFNESS MATRIX IS NO
LONGER UPDATED.

FOR DYNAMIC ANALYSIS:
MODIFY = 0 - THE STIFFNESS MATRIX WILL NOT BE
UPDATED THROUGHOUT THE TIME STEP.
IT REMAINS CONSTANT OVER DELT
(MODIFIED NEWTON-RAPHSON METHOD).
MODIFY = 1 - THE STIFFNESS MATRIX WILL BE UPDATED
AT EVERY STEP IN THE SOLUTION
PROCESS.

MXNEQ-----MAXIMUM NUMBER OF DEGREES OF FREEDOM

NCOUNT-----INTEGER TO COUNT THE NUMBER OF TIMES QVECT IS
CALLED EVERY TENTH TIME QVECT IS CALLED IT READS
THE NEXT TEN ACCELERATION VALUES. (THIS IS USFD
SO THAT TEN PIECES OF DATA MAY BE USED PER DATA
LINE AS OPPOSED TO ONE)

NE-----NUMBER OF ELEMENTS
C C

```

C NEQ-----NUMBER OF DEGREES OF FREEDOM

C NJ-----NUMBER OF JOINTS

C OLDEP(I)-----THE STRAIN IN MEMBER 'I' AFTER PREVIOUS ITERATION.  
USED IN 'STRESS' SUBROUTINE TO MONITOR THE STRAIN  
FOR USE WITH BILINIFAR STRESS-STRAIN LAW.

C OLDSIG(I)-----THE STRESS IN MEMBER 'I' AFTER THE PREVIOUS  
ITERATION. (USED IN 'STRESS')

C Q(I),QP(I),QDP(I)-----THE DISPLACEMENT, VELOCITY AND ACCELERATION  
(Q, Q-PRIME, Q-DOUBLE PRIME), RESPECTIVELY,  
OF DEGREE OF FREEDOM 'I'.

C QBAR(I)-----STATIC LOADING VECTOR THAT WILL BE INCREMENTED  
BY LAMBDA FOR NONLINEAR ANALYSIS. QBAR(I) IS  
THE LOAD APPLIED TO DEGREE OF FREEDOM 'I' IN THE  
GLOBAL REFERENCE FRAME.

C QEFF(I)-----EFFECTIVE EXTERNAL LOADING VECTOR. FOR EARTH-  
QUAKE EXCITATION IT IS THE NEGATIVE OF THE MASS  
MATRIX MULTIPLIED BY THE GROUND ACCELERATION  
APPLIED AT THE DEGREES OF FREEDOM. OR:

$$Q_{EFF} = - I \text{ MASS } I * ( \begin{matrix} Q \\ \vdots \end{matrix} ) \quad G$$

C QINST(I)-----THE DISPLACEMENT VECTOR OF THE PREVIOUS TIME  
STEP. USED IN THE CENTRAL DIFFERENCE METHOD.

C QPLUS(I)-----THE DISPLACEMENT VECTOR OF THE NEXT (OR DESIRED)

C C TIME STEP. USED IN THE CENTRAL DIFFERENCE METHOD.

C C REFF(I)-----SERVES TWO PURPOSES:

1. AS THE EFFECTIVE NODAL LOAD VECTOR IN BOTH THE LINEAR AND NONLINEAR ANALYSES.

2. AFTER SOLVING, REFF IS EITHER:

    A) THE CHANGE IN DISPLACEMENT VECTOR FOR NON-LINEAR ANALYSIS.

    B) THE ACTUAL DISPLACEMENT VECTOR FOR LINEAR ANALYSIS

(NOTE: DURING "SOLVE" REFF IS DESTROYED)

RHO(I)-----MASS PER UNIT LENGTH OF MEMBER "I".

SIGMAX(I,2)-----MAXIMUM STRESS:

SIGMA(I,1) IS THE MAXIMUM STRESS IN ELEMENT "I" THROUGHOUT ANALYSIS

SIGMA(I,2) IS THE LOADING CONDITION "LAMBDA" (STATIC ANALYSIS) OR THE TIME "T" (DYNAMIC ANALYSIS) AT WHICH THIS MAXIMUM OCCURS.

TLENG(I)-----THE TEMPORARY (DEFORMED) LENGTH OF MEMBER "I" AT ANY POINT IN THE ANALYSIS. USED TO DETERMINE AXIAL STRAIN. IT IS DETERMINED IN SUBROUTINE "LENCOUS" BY ADDING THE NODAL DISPLACEMENTS TO THE APPROPRIATE JOINT COORDINATES AND FINDING THE RELATED LENGTHS.

X1(3),X2(3)-----THE THREE TEMPORARY COORDINATES OF THE DEFORMED STRUCTURE AT THE 1-END AND THE 2-END OF THE STRUCTURE, RESPECTIVELY.



```

C      0,0 (INCLUDE AT END)
C
C      4) DO J=1,NJ
C             (ON NEW LINE FOR EACH J)
C             COORD(1,J),COORD(2,J),COORD(3,J)
C
C      5) DO I=1,NE
C             (ON NEW LINE FOR EACH I)
C             AREA(I),EMOD(I),ZI(I),RHO(I),YLDSTR(I)
C
C      6) CHOICE
C
C             IF CHOICE = 1 (STATIC ANALYSIS)
C
C             7) DO K=1,NEQ
C                   (ON NEW LINE FOR EACH K)
C                   QBAR(K)
C
C             8) DELLAM,MAXLAM,MODIFY
C
C             IF CHOICE = 2 (DYNAMIC ANALYSIS)
C
C             7) METHOD,NONLIN,MODIFY
C
C             IF METHOD = 1 (NEWMARK METHOD)
C
C             8) BETA,DELT,TIME,LUMPD,DAMPD
C
C             IF METHOD = 0 (CENTRAL DIFFERENCE METHOD)
C
C             8) DELT,TIME,DAMPD

```

```

C 9) DALPHA,DBETA
C
C 10) COMP(1),COMP(2),COMP(3)
C
C 11) DO K=1,NEQ
C        INITIAL CONDITIONS OF EACH DEGREE OF FREEDOM
C        (ON NEW LINE FOR EACH K)
C        Q(K),QP(K),QDP(K)
C
C 12) ACCEL(1),ACCEL(2),ACCEL(3),ACCEL(4),ACCEL(5),
C        ACCEL(6),ACCEL(7),ACCEL(8)

C (NOTE: ALWAYS COMPLETE LINE WITH ZEROS AND PROVIDE
C A SUFFICIENT NUMBER OF ACCELERATIONS FOR
C ENTIRE TIME.)
```

```

C*****  

C*****  

C***** IMPLICIT REAL*8 (A-H,O-Z)  

REAL*8 KEFF(150,150),MASS(150,150)
INTEGER CHOICE
DIMENSION AREA(150),C1(150),C2(150),C3(150),COORD(3,150),
* EMOD(150),JCODE(3,150),MCODE(6,150),MINC(2,150),RHO(150),
* DSUP(150),FEFF(150),G(6),Q(150),ACCEL(8),C(150,150),
* QP(150),QDP(150),QBAR(150),QEPP(150),REFF(150),TEMP(150),
* X1(3),X2(3),VSUPT(150),YLDSTR(150),BUCKLE(150,2),ZI(150),
* OLDSIG(150),QMNST(150),QPLUST(150),COMP(3),HOLDK(150,150),
* EPMAX(150,2),SIGMAX(150,2),ELENG(150),TLENG(150),OLDEP(150)
MXNEQ=150
READ,NE,NJ
CALL STRUCT(AREA,BUCKLE,C1,C2,C3,COORD,ELENG,EMOD,JCODE,
* MBD,MCODE,MINC,NE,NEQ,NJ,RHO,YLDSTR,ZI)
READ,CHOICE
IF (CHOICE .EQ. 1) THEN DO
  CALL STATIC(AREA,BUCKLE,C1,C2,C3,COORD,ELENG,EMOD,EPMAX,
  * FEFF,G,HOLDK,JCODE,KEFF,MBD,MCODE,MINC,MXNEQ,
  * NE,NEQ,NJ,OLDEP,OLDSIG,Q,QBAR,REFF,SIGMAX,TEMP,
  * TLENG,X1,X2,YLDSTR)
ELSE DO
  CALL DYNAMIC(ACCEL,AREA,BUCKLE,C,C1,C2,C3,COMP,COORD,
  * DELT,DSUPT,ELFNG,EMOD,EPMAX,FEFF,G,HOLDK,JCODE,
  * KEFF,MASS,MBD,MCODE,MINC,MXNEQ,NE,NEQ,NJ,OLDEP,
  * OLDSIG,Q,QP,QDP,QEPP,QMNST,QPLUST,REFF,RHO,
  * SIGMAX,TEMP,TLENG,X1,X2,VSUPT,YLDSTR)
END IF
STOP
END

```

```

C*
C* **** SUBROUTINE STRUCT ****
C* **** READ AND ECHO THE MEMBER INDICES, MINC(L,I); INITIALIZE
C* THE ELEMENTS OF THE JOINT CODE MATRIX, JCODE, TO UNITY.
C* READ AND ECHO, FOR EACH JOINT CONSTRAINT, THE JOINT NUMBER
C* JNUM, AND THE JOINT DIRECTION, JDIR, AND STORE A ZERO IN
C* THE CORRESPONDING LOCATION OF JCODE (END OF DATA MARKER
C* JNUM=0; CALL CODES, MBAND AND PROP.) }

SUBROUTINE STRUCT (AREA,BUCKLE,C1,C2,C3,COORD,ELENG,EMOD,JCODE,MRD,
* MCODE,MINC,NE,NEQ,NJ,RHO,YLDSTR,ZI)
* IMPLICIT REAL*8 (A-H,O-Z)
DIMENSION AREA(1),BUCKLE(NE,2),C1(1),C2(1),C3(1),COORD(3,1),
* ELENG(1),EMOD(1),JCODE(3,1),MCODE(6,1),MINC(2,1),
* RHO(1),YLDSTR(1),ZI(1)
* PRINT 10
DO 20 I=1,NE
READ,MINC(1,I),MINC(2,I)
PRINT 30,I,MINC(1,I),I,MINC(2,I)
20 CONTINUE
DO 40 L=1,3
DO 50 J=1,NJ
JCODE(L,J)=1
50 CONTINUE
40 CONTINUE

```

```

READ,JNUM, JDIR
PRINT 60
PRINT 70
WHILE(JNUM .NE. 0) DO
  JCODE(JDIR,JNUM)=0
  PRINT 80,JNUM, JDIR
  READ, JNUM, JDIR
END WHILE
CALL CODES(JCODE,MINC,NE,NJ,MCODE,NEQ)
MBD=MBAND(MCODE,NE)
CALL PROP(AREA,BUCKLE,C1,C2,C3,COORD,ELENG,EMOD,MINC,NE,NJ,RHO,
*
      YLDSTR,ZI)
10 FORMAT(//,T20,'THE MINC INPUT')
30 FORMAT(//,T10,'MINC(1',I3,')= ',I3,T30,'MINC(2',I3,')= ',I3)
60 FORMAT(//,T15,'CONSTRAINTS (JOINT NUMBER AND DIRECTION),')
70 FORMAT(//,T10,'NUM',T30,'JDIR')
80 FORMAT(/,T10,I4,T30,I4,T40,'CONSTRAINT')
RETURN
END

```

```

C***** SUBROUTINE CODES *****
C***** GENERATE THE JOINT CODE. JCODE, BY ASSIGNING INTEGERS IN
C THE SEQUENCE, BY COLUMNS, TO ALL NONZERO ELEMENTS OF JCODE
C FROM 1 TO NEQ; GENERATE THE MEMBER CODE, MCODE, BY TRANSFER-
C RING VIA MINC COLUMNS OF JCODE INTO COLUMNS OF MCODE.
C

SUBROUTINE CODES(JCODE,MINC,NF,NJ,MCODE,NEQ)
DIMENSION JCODE(3,1),MCODE(6,1)
NEQ=0
DO 90 J= 1,NJ
  DO 100 L = 1,3
    IF (JCODE(L,J) .NE. 0) THEN DO
      NEQ=NEQ+1
      JCODE(L,J)=NEQ
    END IF
  100  CONTINUE
  90  CONTINUE
  DO 110 I=1,NE
    J=MINC(1,I)
    K=MINC(2,I)
    DO 120 L = 1,3
      MCODE(L,I)=JCODE(L,J)
      MCODE(L+3,I)=JCODE(L,K)
  120  CONTINUE
  110 CONTINUE
  PRINT 130
  PRINT 140
  DO 150 J=1,NJ
    PRINT 160,J,JCODE(1,J),JCODE(2,J),JCODE(3,J)
  150 CONTINUE

```

```

PRINT 170
PRINT 180
DO 190 M=1,NE
PRINT 200,M,MCODE(1,M),MCODE(2,M),MCODE(3,M),MCODE(4,M),
      MCODE(5,M),MCODE(6,M)
*
190 CONTINUE
130 FORMAT(//,T20,'THE JCODE TRANSPOSE MATRIX')
140 FORMAT(/,T28,'-1-',T38,'-2-',T48,'-3-',/)
160 FORMAT(/,T12,T13,T27,T37,T3,T47,T13)
170 FORMAT(//,T20,'THE MCODE TRANSPOSE MATRIX',/)
180 FORMAT(/,T23,'-1-',T28,'-2-',T33,'-3-',T38,'-4-',T43,'-5-',T48,
      *
      '-6-',/)
200 FORMAT(/,T12,T13,T22,T13,T27,T32,T13,T37,T42,T13,T47,T13)
RETURN
END

```

```

C***** FUNCTION MBAND *****
C***** COMPUTE THE HALF BANDWIDTH. MBAND, BY EQ. 6.2 (HOLZER): IN
C EACH COLUMN OF MCODE, THE FIRST AND LAST NONZERO INTEGERS
C ARE THE SMALLEST AND LARGEST NONZERO INTEGERS, RESPECTIVELY,
C OF THAT COLUMN. MBAND IS THE MAXIMUM DIFFERENCE OF NONZERO
C INTEGERS IN ANY COLUMN OF MCODE.

C
FUNCTION MBAND(MCODE,NE)
DIMENSION MCODE(6,1)
MBAND=0
DO 210 I = 1,NE
  L=1
  WHILE (MCODE(L,I) .EQ. 0) DO
    L=L+1
  END WHILE
  IS=MCODE(L,I)
  L=6
  WHILE (MCODE(L,I) .EQ. 0) DO
    L=L-1
  END WHILE
  IL=MCODE(L,I)
  IDIF=IL-IS
  IF (IDIF .GT. MBAND) MBAND=IDIF
210 CONTINUE
RETURN
END

```

```

C***** SUBROUTINE PROP  *****
C***** READ AND ECHO THE JOINT COORDINATES. COORD(I,J); COMPUTE FOR
C EACH ELEMENT BY EQS. C• 21 (HOLZER) THE LENGTH, ELENG(I),
C AND THE DIRECTION COSINES, C1(I),C2(I),C3(I); READ FOR EACH
C ELEMENT THE CROSS SECTIONAL AREA(I), AREA(I), THE MOMENT OF
C INERTIA ABOUT THE LOCAL Z(3)-AXIS, ZI(I), THE MODULUS OF
C ELASTICITY, EMOD(I), MASS PER UNIT LENGTH, RHO(I);
C AND THE YIELD STRESS, YLDSTR(I).
C
C SUBROUTINE PROP(AREA,BUCKLE,C1,C2,C3,COORD,ELENG,EMOD,MINC,NE,NJ,
*      RHO,YLDSTR,ZI)
* IMPLICIT REAL*8 (A-H,O-Z)
DIMENSION AREA(1),BUCKLE(NE•2),C1(1),C2(1),C3(1),COORD(3,1),
*      ELENG(1),EMOD(1),MINC(1),RHO(1),YLDSTR(1),ZI(1)
PRINT 220
PRINT 230
DO 240 J = 1,NJ
      READ,COORD(1,J),COORD(2,J),COORD(3,J)
      PRINT 250,J,COORD(1,J),COORD(2,J),COORD(3,J)
240 CONTINUE
      PRINT 260
      PRINT 270
      DO 280 I = 1,NE
      J=MINC(1,I)
      K=MINC(2,I)
      EL1=COORD(1,K)-COORD(1,J)
      EL2=COORD(2,K)-COORD(2,J)
      EL3=COORD(3,K)-COORD(3,J)
      ELENG(I)=DSQRT((EL1**2+EL2**2+ELENG(I)**2))
      C1(I)=EL1/ELENG(I)

```

```

C2(I)=EL2/ELENG(I)
C3(I)=EL3/ELENG(I)
READ,AREA(I),EMOD(I),ZI(I),RHO(I),YLDSTR(I)
BUCKLE(I,I)=-3.1415927**2*EMOD(I)*ZI(I)/(AREA(I)*ELENG(I)**2)
IF (BUCKLE(I,I) .LT. -YLDSTR(I)) BUCKLE(I,I)=-YLDSTR(I)
PRINT 290,I,AREA(I),EMOD(I),ZI(I),RHO(I),ELENG(I),YLDSTR(I)
280 CONTINUE
PRINT 300
DO 310 I=1,NE
  PRINT 320,I,C1(I),I,C2(I),I,C3(I)
310 CONTINUE
220 FORMAT(//T15,*THE COORDINATES OF THE JOINTS ARE *)
230 FORMAT(//T25,*X-COORDINATE*T40,*Y-COORDINATE*T55,*Z-COORDINATE*)
250 FORMAT(T10,JOINT # *I2,T30,F7.2,T45,F7.2,T60,F7.2)
260 FORMAT(//T30,*THE PROPERTIES OF EACH MEMBER ARE *)
270 FORMAT(T19,*AREA*T26,*MODULUS*T38,*INERTIA*T50,*RHO*
* T62,*ELENG*T74,*YLDSTR*)
290 FORMAT(* MEMBER# *I2,T15,F8.5,T25,F8.2,T35,F11.3,T46,F8.4,
* T59,F9.3,T71,E10.3)
300 FORMAT(//,*T40,*DIRECTION COSINES*)
320 FORMAT(//,T15,*C1(*I3,* )= *T25,F10.6,T40,*C2(*I3,* )= *,*
* T50,F10.6,T65,*C3(*I3,* )= *,T75,F10.6)
* RETURN
END

```

```

C*
C*
C***** SUBROUTINE STATIC *****
C*****      FEFF, G, HOLDK, JCODE, KEFF, MBD, MCODE, MINC, MXNEQ,
C*****      NF, NEQ, NJ, OLDEP, OLDSIG, Q, QBAR, REFF, SIGMAX, TEMP,
C*****      TLENG, X1, X2, YLDSTR)
C*
C*      IMPLICIT REAL*8 (A-H,O-Z)
C*      REAL*8 KEFF(MXNEQ,NEQ)
C*      DIMENSION AREA(1), BUCKLE(NE,2), C1(1), C2(1), C3(1), COORD(3,1),
C*      ELENG(1), EMOD(1), EPMAX(NE,2), FEFF(1), G(6), HOLDK(MXNEQ,1),
C*      JCODE(3,1), MCODE(6,1), MINC(2,1), OLDEP(1), OLDSIG(1), Q(1),
C*      QBAR(1), REFF(1), SIGMAX(NE,2), TEMP(1), TLENG(1),
C*      X1(3), X2(3), YLDSTR(1)
C*
C*      REAL*8 LAMBDA, MAXLAM
C*      INTEGER COUNT, FIRST
C*      PRINT 5
C*      PRINT 10
C*      PRINT 15
C*      PRINT 10
C*      DO 340 I=1,NEQ

```

```

Q(1)=0.0D00
READ,QBAR(1)
PRINT 20,1,QBAR(1)
PRINT 10
340 CONTINUE
DO 350 N=1,NE
  OLDEP(N)=0.0D00
  OLDSIG(N)=0.0D00
  EPMAX(N,1)=0.0D00
  SIGMAX(N,1)=0.0D00
  BUCKLE(N,2)=0.0D00
350 CONTINUE
READ,DELLAM,MAXLAM,MODIFY
PRINT 5
PRINT 30
PRINT 30
PRINT 40,DELLAM
PRINT 30
PRINT 50,MAXLAM
PRINT 30
PRINT 60,MODIFY
PRINT 30
PRINT 30
PRINT 980
980 FORMAT(/,T10,"SMALL LAMELLA DOME • 69 DEGREES OF FREEDOM. /"
*,          "T10."3.615,10.3D3,15.64,3.017D-06,35.00",/
*,          "T10."STIFFNESS NOT UPDATED. BALANCED LOAD.",)
*           LAMBDA=DELLAM
MB01=MBD+1
WHILE (LAMBDA .LE. MAXLAM) DO
C   EPSILON IS SET AT 10.0 SO THAT WHILE-DO CONDITION IS NOT SATISFIED

```

```

C   ON THE FIRST RUN.  THE EFFECTIVE LOAD REFF IS FORMED.
C
C   EPSLON=10.0
C   FIRST=0
C   COUNT=0
C   WHILE (EPSLON .GT. 1.0D-4) DO
C     COUNT=COUNT+1
C     IF (COUNT .GT. 10) THEN DO
C       PRINT 1
C       FORMAT(//,T20,'** CONVERGENCE NOT REACHED **',//)
C       GOTO 999
C     END IF
C     CALL FVECT(AREA,BUCKLE,C1,C2,C3,COORD,ELENG,EMOD,EPMAX,FEFF,
C               * JCODE,MCODE,MINC,NE,NEQ,OLDEP,OLDSIG,Q,SIGMAX,
C               * TEMP,TLENG,X1,X2,YLDSTR,LAMBDA)
C     DO 360 I=1,NEQ
C       REFF(I)=LAMBDA*QBAR(I)-FEFF(I)
C     CONTINUE
C
C     IF MODIFY = 1 THEN THE STIFFNESS MATRIX IS UPDATED AT EACH
C     ITERATION.  ON THE FIRST TIME THROUGH THE STIFFNESS MATRIX IS
C     DETERMINED FOR LINEAR ANALYSIS.  AFTER 10 ITERATIONS IF
C     CONVERGENCE IS NOT REACHED THE STIFFNESS IS UPDATED.
C
C     IF (MODIFY .EQ. 1 .OR. FIRST .EQ. 0 .OR. MOD(COUNT,10)
C     .EQ. 0) THEN DO
C       FIRST=1
C       CALL STIFF(AREA,C1,C2,C3,COORD,ELENG,EMOD,G,JCODE,
C                 KEFF,MBD,MCODE,MINC,MXNEQ,NE,NEQ,Q,TLENG,X1,X2)
C       IF (MODIFY .EQ. 0) THEN DO
C         DO 361 I=1,MBD1
C           DO 362 J=1,NEQ

```

```

362      HOL DK(I,J)=KEFF(I,J)
361      CONTINUE
362      END IF
363      ELSE DO
          DO 363 I=1,MBD1
              DO 364 J=1,NEQ
                  KEFF(I,J)=HOLDK(I,J)
364      CONTINUE
363      CONTINUE
364      END IF
365      CALL SOLVE(KEFF,REFF,NEQ,MBD,MXNEQ,INFO)
366      IF (INFO .NE. 0) GOTO 999
367      VALUE=0.0
368      OVAL=0.0
C
C      REFF IS NOW THE CHANGE IN DISPLACEMENT VECTOR (DELT-A-Q).
C
369      DO 370 I=1,NEQ
              Q(I)=Q(I)+REFF(I)
              VALUE=VALUE+REFF(I)**2
              QVAL=QVAL+Q(I)**2
370      CONTINUE
              EPSLON=DSQRT(VALUE)/DSORT(OVAL)
      END WHILE
C
C      ITERATION IS OVER. PRINT RESULTS.
C
998      PRINT 5
              PRINT 70
              PRINT 80,LAMBDA
              PRINT 70

```

```

DO 371 I=1,NEQ
      PRINT 90,I,Q(I)
371   CONTINUE
      PRINT 70
      PRINT 5
      PRINT 70
      PRINT 71,COUNT
      FORMAT(T19,'* NUM. OF ITERATIONS = ',15,'*')
71
      PRINT 70
      PRINT 5
      PRINT 5
      LAMBDA=LAMBDA+DELLAM
END WHILE

C   ANALYSIS IS OVER.   PRINT MAXIMUM STRESSES AND STRAINS.
C
999  PRINT 5
      PRINT 110
      PRINT 120
      PRINT 110
DO 65 K=1,NE
      PRINT 130,K,EPMAX(K,1),EPMAX(K,2),SIGMAX(K,1),SIGMAX(K,2)
65   CONTINUE
      PRINT 110
      FORMAT(1)
10  FORMAT(T20,'*****')
15  FORMAT(T20,'** QBAR VALUES    **')
20  FORMAT(T20,'* QBAR( ',I3,',') = ',D12.4,'*')
30  FORMAT(T25,'*****')
40  FORMAT(T25,'** DELLAM = ',F8.5,'*')
50  FORMAT(T25,'** MAXLAM = ',F8.5,'*')
60  FORMAT(T25,'** MODIFY = ',I3,'*')
70  FORMAT(T19,'*****')

```

```

80 FORMAT(19,*) LAMBDA = ",F10.3,*")
90 FORMAT(19,*) Q(1,13,0) = ",D15.7,*")
110 FORMAT(15,*****)
1120 FORMAT(15,* ELEMENT * MAXIMUM STRAIN LAMBDA ** MAXIMUM STRES
* S LAMBDA *)
1130 FORMAT(15,* 13,0 * ,D14.5,0 * ,F8.2,0 ** ,D14.5,0 * )
*F8.2,*)
      RETURN
      END

```

```

C***** SUBROUTINE STIFF(AREA,C1,C2,C3,COORD,ELENG,EMOD,G,JCODE,
C***** KEFF,MBD,MCODE,MINC,MXNEQ,NE,NEQ,Q,TLENG,X1,X2)
C***** IMPLICIT REAL*8 (A-H,O-Z)
C***** REAL*8 KEFF(MXNEQ,NEQ)
C***** DIMENSION AREA(1),C1(1),C2(1),C3(1),COORD(3,1),ELENG(1),
C***** EMOD(1),G(6),JCODE(3,1),MCODE(6,1),MINC(2,1),Q(1),
C***** TLENG(1),X1(3),X2(3)
C***** INTEGER INDEX(6,6)/1,4,5,-1,-4,-5, 4,2,6,-4,-2,-6, 5,6,3,-5,-6,-3,
C***** -1,-4,-5,1,4,5, -4,-2,-6,4,2,6, -5,-6,-3,5,6,3/
C DO 165 I=1,NEQ
C   DO 166 J=1,NEQ
C     KEFF(I,J)=0.0D00
C 166 CONTINUE
C 165 CONTINUE
C
C FORM THE ELEMENT STIFFNESS MATRIX CONTRIBUTIONS G(6). FROM
C DEFORMED LENGTH (TLENG) AND THE DIRECTION COSINES (ALREADY
C DETERMINED FOR FVECT).
C
C DO 170 N=1,NE
C   GAMMA=EMOD(N)*AREA(N)/TLENG(N)
C   G(1)=GAMMA*(TLENG(N)/ELENG(N)-(1.-C1(N)**2))
C   G(2)=GAMMA*(TLENG(N)/ELENG(N)-(1.-C2(N)**2))
C   G(3)=GAMMA*(TLENG(N)/ELENG(N)-(1.-C3(N)**2))
C   G(4)=GAMMA*C1(N)*C2(N)
C   G(5)=GAMMA*C1(N)*C3(N)

```

```

C G(6)=GAMMA*C2(N)*C3(N)
C ASSEMBLE INTO BANDED GLOBAL STIFFNESS
C
DO 180 JE=1,6
  J=MCODE(JE,N)
  IF (J .NE. 0) THEN DO
    DO 190 IE=1,JE
      I=MCODE(IE,N)
      IF (I .NE. 0) THEN DO
        K=I-J+MBD+1
        L=INDEX(IE,JE)
        IF (L .GT. 0) THEN DO
          KEFF(K,J)=KEFF(K,J)+G(L)
        ELSE DO
          KEFF(K,J)=KEFF(K,J)-G(-L)
        END IF
      END IF
      CONTINUE
    END IF
  CONTINUE
END IF
190   END IF
180   CONTINUE
170   RETURN
END

```

```

C***** SUBROUTINE LENCOS ***** C
C DETERMINES TLENG AND DIRECTION COSINES BY ADDING Q(I)'S TO THE
C APPROPRIATE COORDINATE TO FORM A NEW DEFORMED STATE. COORDINATES
C OF DEFORMED STATE ARE STORED TEMPORARILY IN X1(3) AND X2(3)
C

SUBROUTINE LENCOS(C1,C2,C3,COORD,JCODE,MINC,N,Q,TLENG,X1,X2)
IMPLICIT REAL*8 (A-H,O-Z)
DIMENSION C1(1),C2(1),C3(1),COORD(3,1),JCODE(3,1),MINC(2,1),
*          Q(1),TLENG(1),X1(3),X2(3)

L=MINC(1,N)
K=MINC(2,N)
DO 200 M=1,3
  IF (JCODE(M,L) .NE. 0) THEN DO
    I=JCODE(M,L)
    X1(M)=COORD(M,L)+Q(I)
  ELSE DO
    X1(M)=COORD(M,L)
  END IF
  IF (JCODE(M,K) .NE. 0) THEN DO
    I=JCODE(M,K)
    X2(M)=COORD(M,K)+Q(I)
  ELSE DO
    X2(M)=COORD(M,K)
  END IF
 200 CONTINUE
EL1=X2(1)-X1(1)
EL2=X2(2)-X1(2)
EL3=X2(3)-X1(3)
TLENG(N)=DSQRT(EL1**2+EL2**2+EL3**2)

```

```
C1(N)=EL1/TLENG(N)
C2(N)=EL2/TLENG(N)
C3(N)=EL3/TLENG(N)
RETURN
END
```

```

C***** SUBROUTINE FVECT *****
C***** SUBROUTINE INE FVECT *****
C***** CALL LENCO TO DETERMINE DEFORMED LENGTH AND DIRECTION COSINES.
C      CALL STRESS TO CALCULATE SIG (AXIAL STRESS).
C
C      SUBROUTINE FVECT(AREA,BUCKLE,C1,C2,C3,COORD,ELENG,EMOD,EPMAX,FEFF,
*      JCODE,MCODE,MINC,NE,NEQ,OLDEP,OLDSIG,Q,SIGMAX,TEMP,
*      TLENG,X1,X2,YLDSTR,Z)
C      IMPLICIT REAL*8 (A-H,O-Z)
C      DIMENSION AREA(11),BUCKLE(NE+2)*C1(1),C2(1),C3(1),COORD(11),ELENG(11)
*      ,EMOD(1),EPMAX(NE+2)*FEFF(1),JCODE(3,1),MCODE(6,1),
*      MINC(2,1)*OLDEP(11)*OLDSIG(11)*Q(11),SIGMAX(NE+2),TEMP(11),
*      TLENG(1),X1(3),X2(3),YLDSTR(1)
DO 310 I=1,NEQ
  FEFF(I)=0.0D00
310 CONTINUE
DO 320 I=1,NE
  CALL LENCO(C1,C2,C3,COORD,JCODE,MINC,I,Q,TLENG,X1,X2)
  CALL STRESS(BUCKLE,ELENG,EMOD,EPMAX,EPSLON,I,NE,OLDEP,OLDSIG,
*      SIG,SIGMAX,TLENG,YLDSTR,Z)
C      CALCULATE END FORCES.
C
C      TEMP(1)=-C1(1)*SIG*AREA(1)
C      TEMP(2)=-C2(1)*SIG*AREA(1)
C      TEMP(3)=-C3(1)*SIG*AREA(1)
C      TEMP(4)=-TEMP(1)
C      TEMP(5)=-TEMP(2)
C      TEMP(6)=-TEMP(3)

```

C MATCH APPROPRIATE END FORCES WITH GLOBAL DISPLACEMENTS

```
DO 330 J=1,6
  N=MCODE(J,I)
  IF (N .NE. 0) THEN DO
    FEFF(N)=FEFF(N)+TEMP(J)
  END IF
330  CONTINUE
320  CONTINUE
      RETURN
END
```

```

C***** DETERMINE AXIAL STRESS USING BILINEAR STRESS-STRAIN RELATION
C
C***** SUBROUTINE STRESS(BUCKLE,ELENG,EMOD,EPMAX,EPSLON,I,NE,OLDEP,
C*****          OLDSIG,SIG,SIGMAX,TLENG,YLDSTR,Z)
C
C***** IMPLICIT REAL*8 (A-H,O-Z)
C***** DIMENSION BUCKLE(NE,2),ELENG(1),EMOD(1),EPMAX(NE,2),OLDEP(1),
C*****          OLDSIG(1),SIGMAX(NE,2),TLENG(1),YLDSTR(1),
C*****          EPSLON=(TLENG(1)-ELENG(1))/ELENG(1)
C
C***** IF EPSLON IS POSITIVE THEN THE LINEAR LIMIT FOR THE BILINEAR
C***** LAW IS THE YIELD STRESS. IF EPSLON IS NEGATIVE THEN THE LIMIT
C***** IS THE BUCKLING STRESS.
C
C***** IF (EPSLON .GE. 0.0000) THEN DO
C*****     SIG=OLDSIG(1)+EMOD(1)*(EPSLON-OLDFP(1))
C*****     IF (SIG .GT. YLDSTR(1)) SIG=YLDSTR(1)
C***** ELSE DO
C*****     SIG=EMOD(1)*EPSLON
C*****     IF (SIG .LT. BUCKLE(1,1)) THEN DO
C
C*****         IF THE MEMBER BUCKLES PRINT ERROR MESSAGE AND RECORD THAT IT
C*****         BUCKLED SO THAT THE MESSAGE WILL NOT BE REPEATED.
C
C*****         SIG=BUCKLE(1,1)
C*****         IF (BUCKLE(1,2) .EQ. 0.0D00) THEN DO
C*****             PRINT 1,I,SIG
C*****             FORMAT(T15, MEMBER 'I3.' BUCKLED AT STRESS 'F10.3')
C*****             BUCKLE(I,2)=1.0D00
C

```

```
      END IF
      END IF
    END IF

C   STORE MAXIMUM STRESS AND STRAIN AND THE LAMBDA OR TIME AT
C   WHICH THEY OCCUR
C
IF (DABS(SIG) .GT. DABS(SIGMAX(I,1))) THEN DO
  SIGMAX(I,1)=SIG
  SIGMAX(I,2)=Z
END IF
IF (DABS(EPSLON) .GT. DABS(EPMAX(I,1))) THEN DO
  EPMAX(I,1)=EPSLON
  EPMAX(I,2)=Z
END IF

C   STORE STRESS AND STRAIN OF THIS ITERATION TO COMPARE IN
C   NEXT ITERATION.
C
OLDEP(I)=EPSLON
OLDSIG(I)=SIG
RETURN
END
```

```

C*
C***** SUBROUTINE DYNAMIC *****
C***** THEY ARE THE NEWMARK METHOD AND THE CENTRAL DIFFERENCE METHOD.
C***** A LINEAR OR NONLINEAR ANALYSIS OPTION IS AVAILABLE FOR EACH
C***** METHOD.
C*
C*
      SUBROUTINE DYNAMIC(ACCEL,ARFA,BUCKLE,C,C1,C2,C3,COMP,COORD,
     * DELT,DSUPT,ELENG,EMOD,EPMAX,FEFF,G,HOLDK,JCODE,
     * KEFF,MASS,MBD,MCODE,MINC,MXNEQ,NE,NEQ,NJ,OLDEP,
     * OLDSIG,Q,QP,QDP,QEFF,QINST,QPLUST,REFF,RHO,
     * SIGMAX,TEMP,TLENG,X1,X2,VSUPT,YLDSTR)
      IMPLICIT REAL*8 (A-H,O-Z)
      REAL*8 KEFF(MXNEQ,NEQ),MASS(NEQ,NEQ)
      DIMENSION ACCEL(1),AREA(1),BUCKLE(NE*2),C(NEQ,NEQ),C1(1),C2(1),
     * C3(1),COMP(3),COORD(3,1),DSUPT(1),ELENG(1),EMOD(1),
     * EPMAX(NE,2),FEFF(1),G(6),HOLDK(MXNEQ,NEQ),JCODE(3,1),
     * MCODE(6,1),MINC(2,1),OLDEP(1),OLDSIG(1),Q(1),QP(1),
     * QDP(1),QEFFF(1),QINST(1),QPLUST(1),REFF(1),RHO(1),
     * SIGMAX(NE,2),TEMP(1),TLENG(1),X1(3),X2(3),VSUPT(1),
     * YLDSTR(1)
      DO 501 I=1,NE
     *     OLDEP(I)=0.0000
     *     OLDSIG(I)=0.0000
     *     EPMAX(I,1)=0.0000
      501

```

```

SIGMAX(1,1)=0.0
BUCKLE(1,2)=0.0
501 CONTINUE
READ, METHOD, NONLIN, MODIFY
PRINT 502, METHOD, NONLIN, MODIFY
502 FORMAT(/T10, 'METHOD = ', I2, ' MODIFY = ', I2)

C
C IF METHOD = 1 THE NEWMARK SCHMID IS IMPLEMENTED. IT CONSISTS OF
C SUBROUTINES 'INFO' AND EITHER 'NEWTON' (NONLINEAR) OR 'LINEAR'.
C IF METHOD = 0 'CENTDIF' (CENTRAL DIFFERENCE) IS CALLED

C
C IF (METHOD .EQ. 1) THEN DO
CALL INFO( AREA, BETA, C, C1, C2, C3, COMP, COORD, DELT, ELENG, EMOD, G, HOLDK,
* JCODE, KEFF, MASS, MBD, MCODE, MINC, MXNEQ, NE, NEQ, Q, QP, QDP,
* RHO, TIME, TLENG, X1, X2)
*
T=DELT

C
C FOR NONLINEAR ANALYSIS 'NEWTON' (NEWTON-RAPHSON) IS CALLED.
C FOR LINEAR ANALYSIS THE INITIAL STIFFNESS MUST BE FORMED TO BE
C USED THROUGHOUT THE ANALYSIS. IT IS THEN STORED IN A PERMANENT
C MATRIX 'HOLDK' FOR FUTURE RETRIEVAL. LINEAR IS THEN CALLED.

C
C IF (NONLIN .EQ. 1) THEN DO
CALL NEWTON(ACCEL, AREA, BETA, BUCKLE, C, C1, C2, C3, COMP, COORD, DELT,
* DSUPT, ELENG, EMOD, EPHAX, FEFF, G, HOLDK, JCODE, KEFF, MASS,
* MBD, MCODE, MINC, MXNEQ, NE, NEQ, NJ, NUNLIN,
* OLDEP, OLDSIG, Q, QP, QDP, QEFF, REFF, SIGMAX, T, TEMP,
* TIME, TLENG, VSUPT, X1, X2, YLDSTR)
*
ELSE DO
CALL KHT( AREA, BETA, C, C1, C2, C3, COORD, DELT, ELENG, EMOD, G, HOLDK,
* JCODE, KEFF, MASS, MBD, MCODE, MINC, MXNEQ, NE, NEQ, NONLIN, Q,
* TLENG, X1, X2)
*
```

```

M=MBD+1
DO 161 I=1,M
  DO 162 J=1,NEQ
    HOLDK(I,J)=KEFF(I,J)
    CONTINUE
162
    CONTINUE
    CALL LINEAR(AREA,ACCEL,BETA,BUCKLE,C,C1,C2,C3,COORD,COMP,
               *      DELT,DSUPT,ELENG,FMOD,EPMAX,FEFF,HOLDK,JCODE,
               *      KEFF,MASS,MBD,MCODE,MINC,MXNEQ,NE,NEQ,NJ,OLDEP,
               *      OLDSIG,O,QP,QDP,QEFF,REFF,SIGMAX,T,TEMP,TLEN,
               *      TIME,X1,X2,VSUPT,YLDSTR)
    END IF
  ELSE DO
    CALL CENDIF(ACCEL,AREA,C1,C2,C3,COMP,COORD,ELENG,FMOD,G,
               *      HOLDK,JCODE,KEFF,MASS,MCODE,MINC,MXNEQ,NE,NEQ,NJ,
               *      NONLIN,O,QP,QDP,QEFF,QMINST,QPLUST,RHO,TEMP,TLEN,
               *      X1,X2)
  END IF
  RETURN
END

```

```

C***** SUBROUTINE INFO *****
C***** C***** C***** C***** C***** C***** C***** C*****
C***** READ INFORMATION NEEDED IN DYNAMIC ANALYSIS. FORMULATE DESIRED
C***** MASS MATRIX AND DAMPING MATRIX.
C***** C***** C***** C***** C***** C***** C***** C*****
C***** SUBROUTINE INFO(AREA,BETA,C,C1,C2,C3,COMP,COORD,DELT,ELENG,EMOD,
* G,HOLDK,JCODE,KEFF,MASS,MBD,MCODE,MINC,MXNEQ,NE,NEQ,
* Q,OP,QDP,RHO,TIME,TLENG,X1,X2)
* IMPLICIT REAL*8 (A-H,O-Z)
REAL*8 KEFF(MXNEQ,NEQ),MASS(NEQ,NEQ)
DIMENSION AREA(1),C(NEQ,NEQ),C1(1),C2(1),C3(1),COMP(3),COORD(3,1),
ELENG(1),EMOD(1),G(6),HOLDK(MXNEQ,NEQ),JCODE(3,1),
MCODE(6,1),MINC(2,1),Q(1),QDP(1),RHO(1),TLENG(1),
X1(3),X2(3)
READ,BETA,DELT,TIME,LUMPD,IDAMPD
READ,DALPHA,DBETA
READ,COMP(1),COMP(2),COMP(3)
PRINT 105
PRINT 110
PRINT 110
PRINT 120,BETA
PRINT 130,DELT
PRINT 140,TIME
PRINT 110
PRINT 150,COMP(1)
PRINT 160,COMP(2)
PRINT 170,COMP(3)
PRINT 110
PRINT 180,DALPHA
PRINT 190,DBETA

```

```

PRINT 110
PRINT 110
PRINT 105
PRINT 200
PRINT 210
PRINT 200
PRINT 220
PRINT 200
PRINT 100 I=1,NEQ
READ,Q(I),QP(I),QDP(I)
PRINT 230,I,Q(I),QP(I),QDP(I)
PRINT 200
100 CONTINUE
C
C FORMS LUMPED OR CONSISTENT MASS MATRICES
C
IF (LUMPD .EQ. 1)THEN DO
  CALL LUMPED(TLENG,MASS,MCODE,NE,NEQ,RHO)
ELSE DO
  CALL MASMAT(TLENG,G,MASS,MCODE,NE,NEQ,RHO)
END IF
NONLIN=0
C
C FORM DAMPED MATRIX WITH *HOLDK* SINCE IT IS UNBANDED. DAMPING
C MATRIX REMAINS SAME THROUGHOUT ANALYSIS SO THAT NO UPDATING IS
C NECESSARY.
C
CALL DAMPED(AREA,BETA,C,C1,C2,C3,COORD,DALPHA,DBETA,DELT,ELENG,
*      EMOD,G,HOLDK,IDAAMPD,JCODE,KEFF,MASS,MBD,MCODE,MINC,
*      MXNEQ,NF,NEQ,NONLIN,Q,TLENG,X1,X2)
105 FORMAT(//)
110 FORMAT(T20,'*****')

```

```
120 FORMAT(T20,***      BETA    = 'F8.5.' ***)
130 FORMAT(T20,***      DELT    = 'F8.5.' ***)
140 FORMAT(T20,***      TIME    = 'F8.2.' ***)
150 FORMAT(T20,***      COMP(1) = 'F8.5.' ***)
160 FORMAT(T20,***      COMP(2) = 'F8.5.' ***)
170 FORMAT(T20,***      COMP(3) = 'F8.5.' ***)
180 FORMAT(T20,***      DALPHA = 'F8.5.' ***)
190 FORMAT(T20,***      DBETA   = 'F8.5.' ***)
200 FORMAT(T5,*****      ***** *****)
```

\*\*\*\*\*

```
210 FORMAT(T5,***      INITIAL CONDITIONS OF DEGREES OF FREEDOM
*      **)
220 FORMAT(T5,* D.O.F. * DISPLACEMENT * VELOCITY * ACCELERATIO
*N **)
230 FORMAT(T5,* I4,* * ,D13.5,* * ,D13.5,* * ,D13.5,* *)
RETURN
END
```

```

C***** SUBROUTINE MASMAT ***** C
C***** C
C***** FORMULATE ELEMENTS G(3) OF THE CONSISTENT ELEMENT MASS MATRIX.
C
      SUBROUTINE MASMAT (ELENG,G,MASS,MCODE,NE,NEQ,RHO)
      IMPLICIT REAL*8 (A-H,O-Z)
      REAL*8 MASS(NEQ,NEQ)
      DIMENSION ELENG(11),G(6),MCODE(6,1),RHO(11)
      DO 110 I=1,NEQ
      DO 120 J=1,NEQ
         MASS(I,J)=0.0D0
120   CONTINUE
110   CONTINUE
      DO 130 N=1,NE
         G(1)=0.0D0
         G(2)=RHO(N)*ELENG(N)*.333333333333333
         G(3)=G(2)/2.0D0
         CALL ASSEM(G,MASS,MCODE,N,NEQ)
130   CONTINUE
      RETURN
      END

```

```

C***** SUBROUTINE ASSEM *****
C***** SUBROUTINE ASSEM(G,MASS,MCODE,N,NEQ)
C***** IMPLICIT REAL*8 (A-H,O-Z)
C***** REAL*8 MASS(NEQ,NEQ)
C***** DIMENSION G(6),MCODE(6,1)
C***** INTEGER INDEX(6,6)/2,1,1,3,1,1, 1,2,1,1,3,1, 1,1,2,1,1,3,1,1,2,1/
C***** *
C      C ASSEMBLE CONSISTENT GLOBAL MASS MATRIX.
C
      DO 140 JE=1,6
         J=MCODE(JE,N)
         IF (J .NE. 0) THEN 10
            DO 150 IE=1,6
               I=MCODE(IE,N)
               IF (I .NE. 0) THEN 10
                  L=INDEX(IE,JE)
                  MASS(I,J)=MASS(I,J)+G(L)
               END IF
            END IF
         CONTINUE
      END IF
140  CONTINUE
      RETURN
      END

```

```

C***** SUBROUTINE LUMPED *****
C***** COMPUTE HALF THE MASS OF EACH ELEMENT AND ADD IT TO THE MASS OF
C      EACH DEGREE OF FREEDOM OF THE ELEMENT.
C
      SUBROUTINE LUMPED(ELENG,MASS,MCODE,NE,NEQ,RHO)
      IMPLICIT REAL*8 (A-H,O-Z)
      REAL*8 MASS(NEQ,NEQ)
      DIMENSION ELENG(1),MCODE(6,1),RHO(1)
      DO 151 I=1,NEQ
      DO 152 J=1,NEQ
      MASS(I,J)=0.0D00
      152 CONTINUE
      151 CONTINUE
      DO 154 N=1,NE
      HAFMAS=5.0D-1*RHO(N)*ELENG(N)
      DO 155 J=1,6
      I=MCODE(J,N)
      IF (I .NE. 0) MASS(I)=MASS(I)+HAFMAS
      155 CONTINUE
      154 CONTINUE
      RETURN
      END

```

```

C***** SUBROUTINE DAMPED *****
C***** DAMPED *****
C***** C*
C* FORMS THE DAMPING MATRIX BY RAYLEIGH DAMPING. THE 'HOLDK'
C* MATRIX IS USED FOR THE STIFFNESS MATRIX BECAUSE IT IS NOT
C* BANDED AT THIS TIME.
C*
C* SUBROUTINE DAMPED( AREA, BETA, C, C1, C2, C3, COORD, DALPHA, DBETA, DELT,
C* ELEN, EMOD, G, HOLDK, IDAMPD, JCODE, KEFF, MASS, MBD, MCODE,
C* MINC, MXNEQ, NE, NEQ, NONLIN, Q, TLENG, X1, X2)
C* IMPLICIT REAL*8 (A-H,O-Z)
C* REAL*8 KEFF(MXNEQ,NEQ), MASS(NEQ,NEQ)
C* DIMENSION AREA(1), C(NEQ,1), C1(1), C2(1), C3(1), COORD(3,1), ELEN(1),
C* EMOD(1), G(6), HOLDK(MXNEQ,NEQ), JCODE(3,1), MCODE(6,1),
C* MINC(2,1), Q(1), TLENG(1), X1(3), X2(3)
DO 160 I=1,NEQ
  DO 165 J=1,NEQ
    C(I,J)=0.0D00
 165 CONTINUE
 160 CONTINUE
C*
C* FORMS MATRIX IF IT IS REQUESTED. ELSE C(I,J)=0D00
C*
IF (IDAMPD .EQ. 1) THEN
  CALL KHAT(AREA,BETA,C,C1,C2,C3,COORD,DELT,ELEN,EMOD,G,HOLDK,
  *          JCODE,KEFF,MASS,MBD,MCODE,MINC,MXNEQ,NE,NONLIN,Q,
  *          TLENG,X1,X2)
  DO 170 I=1,NEQ
    DO 175 J=1,NEQ
      C(I,J)=DALPHA*MASS(I,J)+DBETA*HOLDK(I,J)
    175 CONTINUE
  170 CONTINUE
 175 CONTINUE

```

170 CONTINUE  
END IF  
RETURN  
END

```

C***** SUBROUTINE NEWTON
C***** THIS SUBROUTINE PERFORMS THE NEWTON-RAPHSON METHOD IN ORDER
C DETERMINE THE SOLUTION OF THE EFFECTIVE STATIC FORMULATION.
C
C SUBROUTINE NEWTON(ACCEL,AREA,BUCKLE,C,C1,C2,C3,COMP,COORD,
C * DELT,DSUPT,ELENG,EMOD,EPMAX,FEFF,G,HOLDK,JCODE,KEFF,
C * MASS,MBD,MCODE,MINC,MODIFY,MXNEQ,NEQ,NJ,NONLIN,
C * OLDEP,OLDSIG,Q,QP,QEFF,REFF,SIGMAX,T,TEMP,
C * TIME,TLENG,VSUPT,X1,X2,YLDSTR)
C
C IMPLICIT REAL*8 (A-H,O-Z)
C REAL*8 KEFF(MXNEQ,NEQ),MASS(NEQ,NEQ)
C
C DIMENSION ACCEL(1),AREA(1),BUCKLE(NE,2),C(NEQ,1),C1(1),C2(1),C3(1),
C * COMP(3),COORD(3,1),DSUPT(1),ELENG(1),EMOD(1),EPMAX(NE,2),
C * ,FEFF(1),G(6),HOLDK(MXNEQ,NEQ),JCODE(3,1),MCODE(6,1),
C * MINC(2,1),OLDEP(1),OLDSIG(1),Q(1),QP(1),QEFF(1),
C * REFF(1),SIGMAX(NE,2),TEMP(1),TLENG(1),VSUPT(1),X1(3),
C * X2(3),YLDSTR(1)
C
C INTEGER COUNT
NCOUNT=0
WHILE (T .LE. TIME) DO
COUNT=0
EPSLON=1.0D00
C
C AT THE BEGINNING OF EACH TIME STEP DSUPT, VSUPT, KHT AND QEFF
C MUST BE DETERMINED TO START THE ITERATIVE PROCESS. IF THE
C STIFFNESS IS NOT TO BE CHANGED (MODIFIED NEWTON-RAPHSON METHOD)
C THEN IT MUST BE STORED IN •HOLDK• SINCE IT IS DESTROYED IN •SOLVE•.
C
DO 160 I=1,NEQ

```

```

DSUP(T(I))=Q(I)+DELT*OP(I)+(.5D00-BETA)*(DELT**2)*QDP(I)
VSUP(T(I))=QP(I)+QDP(I)*DELT/2*D00
160  CONTINUE
      CALL KHTA(ARFA,BETA,C,C1,C2,C3,COORD,DELT,ELENG,EMOD,G,HOLDK,
      JCODE,KEFF,MASS,MBD,MCODE,MINC,MXNEQ,NE,NEQ,NOLIN,Q,
      TLENG,X1,X2)
      *
      CALL QVECT(ACCEL,COMP,JCODE,MASS,NCOUNT,NEQ,NJ,QEFF,TEMP)
      IF (MODIFY .EQ. 0) THEN DO
      M=MBD+1
      DO 161 I=1,M
          DO 162 J=1,NFQ
              HOLDK(I,J)=KEFF(I,J)
      162      CONTINUE
      161      CONTINUE
      END IF

C   BEGIN NEWTON-RAPHSON ITERATION
C
      WHILE(EPSON .GT. 1.0D-3) DO
          COUNT=COUNT+1
          IF (COUNT .GT. 20) THEN DO
              PRINT 1
              1      FORMAT(///,T10,*** CONVERGENCE NOT REACHED***)
              STOP
          END IF

C   THE EFFECTIVE STIFFNESS AND THE EFFECTIVE LOAD MUST BE DETERMINED.
C   IF THE STIFFNESS IS NOT UPDATED (MODIFY = 0) THE ORIGINAL STIFF-
C   NESS COMES FROM "HOLDK".
C
      IF (MODIFY .EQ. 1 ) THEN DO
          CALL RVECT(AREA,BETA,BUCKLE,C,C1,C2,C3,COORD,DELT,DSUPT,

```

```

* * * ELENG, EMOD, EMAX, FEFF, JCODE, MASS, MCODE, MINC, NE, NEQ, NJ,
* * * OLDEP, OLDSIG, Q, QP, QDP, QEFF, REFF, SIGMAX, T, TEMP, TLENG,
* * * VSUP T, X1, X2, YLDSSTR)
* * * CALL KHAT( AREA, BETA, C, C1, C2, C3, COORD, DELT, ELENG, EMOD, G,
* * * HOLDK, JCODE, KEFF, MASS, MBD, MCODE, MINC, MXNEQ, NE, NEQ,
* * * NONLIN, Q, TLENG, X1, X2)
* * ELSE DO
* *   CALL RVECT( AREA, BUCKLE, C, C1, C2, C3, COORD, DELT, DSUPT,
* *   ELENG, EMOD, EMAX, FEFF, JCODE, MASS, MCODE, MINC, NE, NEQ, NJ,
* *   OLDEP, OLDSIG, Q, QP, QDP, QEFF, REFF, SIGMAX, T, TEMP, TLENG,
* *   VSUP T, X1, X2, YLDSSTR)
* *   DO 171 I=1,M
* *     DO 172 J=1,NEQ
* *       KEFF(I,J)=HOLDK(I,J)
* *     CONTINUE
* *   CONTINUE
* * END IF
* * CALL SOLVE(KEFF,REFF,NEQ,MBD,MXNEQ,INFO)
* * C
* * REFF IS CHANGE IN DISPLACEMENT VECTOR THAT MUST BE ADDED TO
* * Q(I) TO GET THE NEW Q(I).
* * C
* * 172
* * 171
* * C
* * VALUE=0.0D00
* * QVAL=0.0D00
* * DO 240 I=1,NEQ
* *   Q(I)=Q(I)+REFF(I)
* *   VALUE=VALUE+REFF(I)**2
* *   QVAL=QVAL+Q(I)**2
* * CONTINUE
* * EPSLON=DSQRT(VALUE)/DSORT(QVAL)
* * END WHILE
* * PRINT 10

```

```

PRINT 20,T,COUNT
PRINT 10
PRINT 30
PRINT 10

C   QP(I) AND QDP(I) BY NEWMARK METHOD (SEE BATHE PG. 512)
C

DO 260 I=1,NEQ
  QDP(I)=(1/(BETA*DELT**2))*Q(I)-DSUPT(I)
  QP(I)=VSUPT(I)+.5*DELT*QDP(I)
  PRINT 40,I,Q(I),QP(I),QDP(I)
  PRINT 10

260   CONTINUE
      T=T+DELT
END WHILE
PRINT 5
PRINT 50
PRINT 60
PRINT 50
PRINT 50
DO 65 K=1,NE
  PRINT 70,K,EPMAX(K,1),EPMAX(K,2),SIGMAX(K,1),SIGMAX(K,2)

65 CONTINUE
PRINT 50
5 FORMAT(1)
10 FORMAT(T5,1*****)
*****)
20 FORMAT(T5,* TIME = *F8.2.* NUMBER OF ITERATIONS TO CONVERGE-
*          *I3,* *)
30 FORMAT(T5,* D.O.F.* DISPLACEMENT * VELOCITY * ACCELERATION
*N *)
40 FORMAT(T5,* I4,* * ,D13.5,* ,D13.5,* ,D13.5,* )
50 FORMAT(T5,1*****)

```

```
*****  
60 FORMAT(T5, " ELEMENT * MAXIMUM STRAIN TIME ** MAXIMUM STRES  
*S TIME * )  
70 FORMAT(T5, " ,I3, " * ,014.5, " ,F8.2, " ** ,D14.5, " .  
*F8.2, * )  
RETURN  
END
```

```

C***** SUBROUTINE KHAT *****
C DETERMINE THE VALUES OF THE EFFECTIVE STIFFNESS MATRIX FOR THE
C NEWMARK-BETA METHOD (SEE BATHE P. 512). *HOLDK* WILL BE USED
C AS A TEMPORARY FULL STORAGE FOR THE STIFFNESS BEFORE IT IS
C ADDED TO THE MASS AND DAMPING MATRICES AND BANDED.
C
      SUBROUTINE KHAT(AREA,BETA,C,C1,C2,C3,COORD,DELT,ELENG,EMOD,G,
      *      HOLDK,JCODE,KEFF,MASS,MBD,MCODE,MINC,MXNEQ,NE,NEQ,
      *      NONLIN,Q,TLENG,X1,X2)
      *
      IMPLICIT REAL*8 (A-H,O-Z)
      REAL*8 KEFF(MXNEQ,NEQ),MASS(NEQ,NEQ)
      DIMENSION AREA(1),C(NEQ,1),C1(1),C2(1),C3(1),COORD(3,1),ELENG(1),
      *      EMOD(1),G(6),HOLDK(MXNEQ,NEQ),JCODE(3,1),MCODE(6,1),
      *      MINC(2,1),Q(1),TLENG(1),X1(3),X2(3)
      INTEGER INDEX(6,6)/1,4,5,-1,-4,-5, 4,2,6,-4,-2,-6, 5,6,3,-5,-6,-3,
      *      -1,-4,-5,1,4,5, -4,-2,-6,4,2,6, -5,-6,-3,5,6,3/
      DO 165 I=1,NEQ
      DO 166 J=1,NEQ
         KEFF(I,J)=0.0D00
         HOLDK(I,J)=0.0D00
 166   CONTINUE
 165 CONTINUE
      DO 170 N=1,NE
      *
      CALL "LENCO" TO DETERMINE THE DEFERRED LENGTH OF ELEMENT *N*
      C (REFER TO CHAPTER 2 OF THESIS FOR DERIVATION).
      C
      CALL LENCO(C1,C2,C3,COORD,JCODE,MINC,N,Q,TLENG,X1,X2)
      IF (NONLIN .EQ. 0) THEN DO

```

```

C FOR A LINEAR ANALYSIS THE DIAGONAL ELEMENTS ARE NOT A FUNCTION
C OF THE DEFORMED LENGTH. THEREFORE THE FOLLOWING ARE CALCULATED.
C
C GAMMA=EMOD(N)*AREA(N)/TLENG(N)
C G(1)=GAMMA*C1(N)**2
C G(2)=GAMMA*C2(N)**2
C G(3)=GAMMA*C3(N)**2
C ELSE DO
C
C GAMMA=EMOD(N)*AREA(N)/TLENG(N)
C G(1)=GAMMA*( TLENG(N)/ELENG(N)-(1.000-C1(N)**2))
C G(2)=GAMMA*( TLENG(N)/ELENG(N)-(1.000-C2(N)**2))
C G(3)=GAMMA*( TLENG(N)/ELENG(N)-(1.000-C3(N)**2))
C END IF
C G(4)=GAMMA*C1(N)*C2(N)
C G(5)=GAMMA*C1(N)*C3(N)
C G(6)=GAMMA*C2(N)*C3(N)
C
C ASSEMBLE THE "UNBANDED" STIFFNESS.
C
C DO 180 JE=1,6
C     J=MCODE(JE,N)
C     IF (J .NE. 0) THEN DO
C        190 IE=1,JE
C        I=MCODE(IE,N)
C        IF (I .NE. 0) THEN DO
C           L=INDEX(IE,JE)

```

```

IF (L .GT. 0) THEN DO
  HOLDK(I,J)=HOLDK(I,J)+G(L)
ELSE DO
  HOLDK(I,J)=HOLDK(I,J)-G(-L)
END IF
  190  CONTINUE
END IF
  180  CONTINUE
  170 CONTINUE

C FORM EFFECTIVE STIFFNESS MATRIX AND STORE INTO "BANDED" "KEFF".
C
DO 191 J=1,NEQ
  DO 192 I=1,J
    K=I-J+MBD+1
    IF (K .GT. 0) THEN DO
      KEFF(K,J)=HOLDK(I,J)+MASS(I,J)/(BETA*DELT*#2)
      *          +C(I,J)/(2.000*BETA*DELT)
    END IF
  192 CONTINUE
  191 CONTINUE
RETURN
END

```

```

C***** SUBROUTINE RVECT ***** C
C DETERMINE THE EFFECTIVE NODAL LOAD VECTOR 'R' OF THE NEWMARK-BETA
C METHOD. (SEE BATHE P. 512)
C
C SUBROUTINE RVECT( AREA,BUCKLE,C,C1,C2,C3,COORD,DELT,DSUPT,
*      ELEN,EMOD,EPMAX,FEFF,JCODE,MASS,MCODE,MINC,NE,
*      NEQ,NJ,OLDEP,OLDSIG,Q,QP,QDP,REFF,SIGMAX,
*      T,TEMP,TLENG,VSUPT,X1,X2,YLDSTR)
*
* IMPLICIT REAL*8 (A-H,O-Z)
REAL*8 MASS(NEQ,NEQ)
DIMENSION AREA(1),BUCKLE(NE,2),C(NEQ,1),C1(1),C2(1),C3(1),
*      COORD(3,1),DSUPT(1),ELEN(1),EMOD(1),EPMAX(NE,2),FEFF(1),
*      JCODE(3,1),MCODE(6,1),MINC(2,1),OLDEP(1),OLDSIG(1),
*      Q(1),QP(1),QDP(1),REFF(1),SIGMAX(NE,2),TEMP(1),
*      TLENG(1),VSUPT(1),X1(3),X2(3),YLDSTR(1)
C
C FOR THE NEWTON-RAPHSON METHOD THE NODAL FORCE VECTOR, 'FEFF',
C MUST BE DETERMINED. IT IS PART OF THE ITERATIVE PROCESS.
C
CALL FVECT( AREA,BUCKLE,C1,C2,C3,COORD,ELEN,EMOD,EPMAX,FEFF,JCODE,
*      MCODE,MINC,NE,NEQ,OLDEP,OLDSIG,Q,SIGMAX,TEMP,TLENG,
*      X1,X2,YLDSTR,T)
DO 270 I=1,NEQ
  QDP(I)=(1/(BETA*DELT**2))*(Q(I)-DSUPT(I))
270 CONTINUE
C
C THE RESIDUAL FORCE VECTOR 'REFF' OF THE NEWTON-RAPHSON TECHNIQUE
C IS FORMED.
C

```

```
DO 280 I=1,NEQ
  STORE=0.0D00
  DO 290 J=1,NEQ
    STORE=STORE+(MASS(I,J)+.5D00*DELT*C(I,J))*QDP(J)
    *          +C(I,J)*VSUPT(J)
    290  CONTINUE
      REFF(I)=QEFF(I)-FEFF(I)-STORE
  280  CONTINUE
      RETURN
      END
```

```

C **** SUBROUTINE QVECT ****
C **** THE NODAL LOAD VECTOR CAUSED BY THE EARTHQUAKE EXCITATION IS
C ****
C ****
C **** (QEFF) = -1 M I*( Q )
C ****
C **** SUBROUTINE QVECT(ACCEL,COMP,JCODE,MASS,NCOUNT,NEQ,NJ,QEFF,TEMP)
C **** IMPLICIT REAL*8 (A-H,O-Z)
C **** REAL*8 MASS(NEQ,NEQ)
C **** DIMENSION ACCEL(1),COMP(3),JCODE(3,1),QEFF(1),TEMP(1)
C **** IF (MOD(NCOUNT,8) .EQ. 0) THEN DO
C **** READ,ACCEL(1),ACCEL(2),ACCEL(3),ACCEL(4),ACCEL(5),ACCEL(6),
C **** * ACCEL(7),ACCEL(8)
C **** NCOUNT=0
C **** END IF
C **** NCOUNT=NCOUNT+1
C **** PRINT 100,ACCEL(NCOUNT)
C **** 100 FORMAT(/,T5,'** ACCELERATION IS ',D15.7,' MM/SEC**2 **')
C ****
C **** THE ACCELERATION ( Q ) IS THE BASE ACCELERATION IN THE APPRO-
C **** PRIATE DIRECTION. (IT IS DIVIDED BY 304.8 BECAUSE THE DATA IS
C **** GIVEN IN MM/SEC**2). EACH JOINT IS CONSIDERED AND A FORCE OF
C **** MASS TIMES THE ACCELERATION IS APPLIED IN THE DIRECTION OF
C **** THE DEGREE OF FREEDOM.
C ****
C **** DO 200 J=1,NJ
C ****
C **** TO INCLUDE GRAVITY EFFECTS ADD AN ACCELERATION OF 32.21 FT/SEC**2
C **** IN THE POSITIVE VERTICAL DIRECTION.
C ****

```

```
M=JCODE(1,J)
IF (M .NE. 0) THEN DO
  TEMP(M)=32.21
END IF
DO 210 K=2,3
  N=JCODE(K,J)
  IF (N .NE. 0) THEN DO
    TEMP(N)=ACCEL(NCOUNT)*COMP(K)/304.8
  END IF
210  CONTINUE
200 CONTINUE
  DO 220 I=1,NEQ
    QEFF(I)=0.0
  DO 230 J=1,NEQ
    QEFF(I)=QEFF(I)-MASS(I,J)*TEMP(J)
230  CONTINUE
220 CONTINUE
  RETURN
END
```

```

C***** SUBROUTINE LINEAR *****
C PERFORMS A LINEAR ANALYSIS OF THE STRUCTURE. THE STIFFNESS IS
C ALREADY DETERMINED AND STORED IN 'HOLDK'. IT IS NOT UPDATED
C THROUGHOUT THE ANALYSIS.
C
C SUBROUTINE LINEAR(AREA,ACCEL,BUCKLE,C,C1,C2,C3,COORD,COMP,
* DELT,DSUPT,ELENG,EMOD,EPMAX,FEFF,HOLDK,JCODE,
* KEFF,MASS,MBD,MCODE,MINC,MXNEQ,NE,NEQ,NJ,OLDEP,
* OLDSIG,Q,OP,QDP,QEFP,REFF,SIGMAX,T,TEMP,TLENG,
* TIME,X1,X2,VSUPT,YLDSTR)
*
* IMPLICIT REAL*8 (A-H,O-Z)
REAL*8 KEFF(MXNEQ,NEQ),MASS(NEQ,NEQ)
DIMENSION AREA(1),ACCEL(8),BUCKLE(NE,2),C(NEQ,NEQ),C1(1),C2(1),
* C3(1),COORD(3,1),COMP(3),DSUPT(1),ELENG(1),EMOD(1),
* EPMAX(NE,2),FEFF(1),HOLDK(MXNEQ,NEQ),JCODE(3,1),
* MCODE(6,1),MINC(2,1),OLDEP(1),OLDSIG(1),Q(1),OP(1),
* QDP(1),QEFP(1),REFF(1),SIGMAX(NE,2),TEMP(1),TLENG(1),
* X1(3),X2(3),VSUPT(1),YLDSTR(1)
NCOUNT=0
WHILE (T .LE. TIME) DO
PRINT 1
1 FORMAT(//)
C
C THE STIFFNESS MATRIX IS COPIED INTO KEFF. THE STIFFNESS IS
C ALTERED IN THE 'SOLVE' ROUTINE SO IT MUST BE REFRESHED AT
C EVERY TIME STEP.
C
M=MBD+1
DO 171 I=1,M

```

```

DO 172 J=1,NEQ
  KEFF(I,J)=HOLDDK(I,J)
172  CONTINUE
171  DO 160 I=1,NEQ
    DSUPT(I)=Q(I)+DELT*QP(I)+(5D00-BETA)*(DELT**2)*QDP(I)
    VSUP(I)=QP(I)+QDP(I)*DELT/2.D00
160  CONTINUE
    CALL QVFC(ACCEL,COMP,JCODE,MASS,NCOUNT,NEQ,NJ,OEFF,TEMP)
C
C FORMULATE THE EFFECTIVE LOAD VECTOR ( SEE BATHE P. 512 ). IT
C IS "REFF".
C
DO 590 I=1,NEQ
  STORE=0.0D00
  REFF(I)=0.0D00
  DO 595 J=1,NEQ
    STORE=STORE+(MASS(I,J)*DSUPT(J))/(BETA*DELT**2)
595  CONTINUE
  REFF(I)=OEFF(I)+STORE
590  CONTINUE
    CALL SOLVE(KEFF,REFF,NEQ,MBD,MXNEQ,INFO)
C
C THE DISPLACEMENT VECTOR IS NOW REFF. PRINT RESULTS.
C
      PRINT 5
      PRINT 10
      PRINT 20,T
      PRINT 10
      PRINT 30
      PRINT 10
      DO 600 I=1,NEQ

```

```

C Q(I)=REFF(I)
C
C   VELOCITIES AND ACCELERATION FROM THE NEWMARK METHOD.
C
      QDP(I)=(Q(I)-DSUPT(I))/(BETA*DELT**2)
      QP(I)=VSUPT(I)+.5*DELT*QDP(I)
      PRINT 40,I,Q(I),QP(I),QDP(I)
      PRINT 10
      CONTINUE
      600
C
C   SUBROUTINE FVECT IS CALLED TO DETERMINE THE STRESSES AND STRAINS
C   AT EVERY TIME AND RECORD THE MAXIMUMS. IT IS NOT USED IN THE
C   SOLUTION PROCESS AS IT IS IN THE NEWTON-RAPHSON TECHNIQUE.
C
      CALL FVECT(AREA,BUCKLE,C1,C2,C3,COORD,ELENG,EMOD,EPMAX,FEFF,
      *          JCODE,MCODE,MINC,NE,NEQ,OLDEP,OLDSIG,Q,SIGMAX,TEMP,
      *          TLENG,X1,X2,YLDSTR,T)
      T=T+DELT
      END WHILE
      PRINT 5
      PRINT 50
      PRINT 60
      PRINT 50
      DO 65 K=1,NE
      PRINT 70,K,EPMAX(K,1),EPMAX(K,2),SIGMAX(K,1),SIGMAX(K,2)
      PRINT 50
      CONTINUE
      65
      5 FORMAT(//)
      10 FORMAT(T5,******)
      *** */
      20 FORMAT(T5,**
      * *)
      TIME = *,FB.2,

```

```
30 FORMAT(T5,'* D.O.F. * DISPLACEMENT * VELOCITY * ACCELERATION  
*N *')  
40 FORMAT(T5,'* I14,* * ,D13.5,* * ,D13.5,* * ,D13.5,* *)  
50 FORMAT(T5,'*****'*'*****'*'*****'*'*****'*'*****'*')  
*****'*')  
60 FORMAT(T5,'* ELEMENT * MAXIMUM STRAIN TIME ** MAXIMUM STRES  
*S TIME *')  
70 FORMAT(T5,'* I13,* * ,D14.5,* * ,F8.2,* * ,D14.5,* *)  
*F8.2,* *)  
RETURN  
END
```

```

C*****SUBROUTINE SOLVE ****
C* FOR THE FIRST LOAD CONDITION, LC=1, CALL SPBFA AND SPBSL;
C* FOR SUBSEQUENT LOAD CONDITIONS, LC>1, CALL SPBSL.
C*
C* SUBROUTINE SOLVE (KEFF,REFF,NEQ,MBD,MXNEQ,INFO)
C* IMPLICIT REAL*8 (A-H,O-Z)
C* REAL*8 KEFF(MXNEQ,1)
C* DIMENSION REFF(1)
C* INFO=0
C* CALL SPBFA(KEFF,MXNEQ,NEQ,MBD,INFO)
C* IF (INFO .NE. 0) THEN
C*   PRINT 320
C*   FORMAT(//,T20,'K MATRIX IS SINGULAR',//,T20,
C*          *'NO SOLUTION CAN BE FOUND',//)
C*   STOP
C* END IF
C* I=0
C* CALL SPBSL (KEFF,MXNEQ,NEQ,MBD,REFF)
C* RETURN
C* END

```

```

C***** SUBROUTINE SPBFA ****
C***** SUBROUTINE SPBFA(ABD,LDA,N,M,INFO)
INTEGER LDA,N,M,INFO
REAL*8 ABD(LDA,1)
REAL*8 SDOT,T
REAL*8 S
INTEGER IK,J,JK,K,MU
DO 30 J = 1, N
INFO = J
S = 0.0D0
IK = M + 1
JK = MAX0(J-M,1)
MU = MAX0(M+2-J,1)
IF (M .LT. MU) GO TO 20
DO 10 K = MU, M
T = ABD(IK,J) - SDOT (K-MU, ABD(IK,JK),1, ABD(MU,J),1)
T = T/ABD(M+1,JK)
ABD(IK,J) = T
S = S + T*T
IK = IK - 1
JK = JK + 1
CONTINUE
CONTINUE
S = ABD(M+1,J) - S
IF ( S .LE. 0.0D0) GO TO 40
ABD(M+1,J) = DSQRT(S)
30 CONTINUE
INFO = 0
40 CONTINUE
RETURN

```

END

```

C***** SUBROUTINE SPBSL *****
C***** SPBSL *****
C***** SPBSL ( ABD, LDA, N, M, B )
C***** SPBSL ( ABD(LDA,1), B(1) )
C***** SPBSL ( ABD(LA,1), B(LA) )
C***** SPBSL ( ABD(LB,1), B(LB) )
C***** SPBSL ( ABD(LM,1), B(LM) )
C***** SPBSL ( ABD(M,1), B(M) )
C***** SPBSL ( ABD(K,1), B(K) )
C***** SPBSL ( ABD(T,1), B(T) )

SUBROUTINE SPBSL(ABD,LDA,N,M,B)
  INTEGER LDA,N,M
  REAL*8 ABD(LDA,1),B(1)
  REAL*8 SDOT,T
  INTEGER K,KB,LA,LB,LM
  DO 10 K = 1, N
    LM = MINO(K-1,M)
    LA = M + 1 - LM
    LB = K - LM
    T = SDOT(LM,ABD(LA,K)*1,B(LB),1)
    B(K) = (B(K) - T)/ABD(M+1,K)
10 CONTINUE
  DO 20 KB = 1, N
    K = N + 1 - KB
    LM = MINO(K-1,M)
    LA = M + 1 - LM
    LB = K - LM
    B(K) = B(K)/ABD(M+1,K)
    T = -B(K)
    CALL SAXPY(LM,T,ABDI(LA,K),1,B(LB),1)
20 CONTINUE
  RETURN
END

```

```

C***** SUBROUTINE SAXPY *****
C***** SUBROUTINE SAXPY(N, SA, SX, INCX, SY, INCY)
REAL*8 SX(1), SY(1), SA
INTEGER I, INCX, INCY, IX, IY, M, MP1, N
IF(N.LE.0)RETURN
IF((SA .EQ. 0.0D00)) RETURN
IF(INCX.EQ.1.AND.INCY.EQ.1)GO TO 20
IX = 1
IY = 1
IF(INCX.LT.0)IX = (-N+1)*INCX + 1
IF(INCY.LT.0)IY = (-N+1)*INCY + 1
DO 10 I = 1,N
SY(IY) = SY(IY) + SA*SX(IX)
IX = IX + INCX
IY = IY + INCY
10 CONTINUE
RETURN
20 M = MOD(N, 4)
IF(M .EQ. 0 ) GO TO 40
DO 30 I = 1,M
SY(I) = SY(I) + SA*SX(I)
30 CONTINUE
IF(N .LT. 4 ) RETURN
40 MP1 = M + 1
DO 50 I = MP1,N,4
SY(I) = SY(I) + SA*SX(I)
SY(I + 1) = SY(I + 1) + SA*SX(I + 1)
SY(I + 2) = SY(I + 2) + SA*SX(I + 2)
SY(I + 3) = SY(I + 3) + SA*SX(I + 3)
50 CONTINUE

```

180

RETURN  
END

```

C***** FUNCTION SDOT *****
C***** SDOT(N,SX,INCX,SY,INCY)
REAL FUNCTION SDOT*(N,SX,INCX,SY,INCY)
REAL*8 SX(1),SY(1),STEMP
INTEGER I,INCX,INCY,IX,IY,M,MP1,N
SDOT = 0.0D0
STEMP = 0.0D0
IF(N.LE.0)RETURN
IF(INCX.EQ.1.AND.INCY.EQ.1)GO TO 20
IX = 1
IY = 1
IF(INCX.LT.0)IX = (-N+1)*INCX + 1
IF(INCY.LT.0)IY = (-N+1)*INCY + 1
DO 10 I = 1,N
STEMP = STEM + SX(IX)*SY(IY)
IX = IX + INCX
IY = IY + INCY
10 CONTINUE
SDOT = STEM
RETURN
20 M = MOD(N,5)
IF( M .EQ. 0 ) GO TO 40
DO 30 I = 1,M
STEMP = STEM + SX(I)*SY(I)
30 CONTINUE
IF( N .LT. 5 ) GO TO 60
40 MP1 = M + 1
DO 50 I = MP1,N,5
STEMP = STEM + SX(I)*SY(I) + SX(I + 1)*SY(I + 1) +
* SX(I + 2)*SY(I + 2) + SX(I + 3)*SY(I + 3) + SX(I + 4)*SY(I + 4)
50 CONTINUE

```

60 SDOT = STEMP  
RETURN  
END

```

C***** SUBROUTINE CENDIF *****
C***** SUBROUTINE CENDIF(ACCEL, AREA, C1, C2, C3, COMP, COORD, ELENG, EMOD, G,
*      HOLDK, JCODE, KEFF, MASS, MCODE, MINC, MXNEQ, NE, NEQ, NJ,
*      NONLIN, Q, QP, QDP, QEFF, QMINST, QPLUST, RHO, TEMP, TLENG,
*      X1, X2)
C
C      IMPLICIT REAL*8 (A-H,0-Z)
C      REAL*8 KEFF(MXNEQ,NEQ), MASS(MEQ,NEQ)
C      DIMENSION ACCEL(1), AREA(1), C1(1), C2(1), C3(1), COMP(3), COORD(3,1),
*      ELENG(1), EMOD(1), G(6), HOLDK(MXNEQ,NEQ), JCODE(3,1),
*      MCODE(6,1), MINC(2,1), Q(1), QP(1), QDP(1), QEFF(1), QMINST(1)
*      , QPLUST(1), RHO(1), TEMP(1), TIME(1), X1(3), X2(3)
C
C      MBD=0
C      READ,DELT,TIME
C
C      CONSTANTS OF THE METHOD .
C
C      A0=1/DELT**2
C      A1=1/(2*DELT)
C      A2=2*A0
C      A3=1/A2
C      READ,COMP(1),COMP(2),COMP(3)
C      DO 600 I=1,NEQ
C          READ,Q(I),QP(I),QDP(I)
C
C      INITIAL CONDITIONS .
C
C      QPLUST(1)=0.0000
C      QMINST(1)=Q(1)-DELT*QP(1)+A3*QDP(1)
C      PRINT 510,I,Q(I),QP(I),QDP(I)
C      FORMAT(15,1,I13,' Q = ',F7.3,' QP = ',F7.3,' QDP = ',F7.3)
510

```

```

*      F7.3)
600 CONTINUE
PRINT 97,DELT,TIME
97 FORMAT(T10.,* DELT = *,F10.5,* TIME = *,F10.5)

C ONLY THE LUMPED MASS CAN BE USED FOR HIGH SPEED COMPUTATION.
C IF CONSISTENT MASS IS USED, THE *SOLVE* ROUTINE MUST BE CALLED.
C
CALL LUMPED(ELENG,MASS,MCODE,NE,NEQ,RHO)
T=DELT

C ICOUNT IS A COUNTER FOR THE PRINTOUT. ONLY DESIRED TIME STEPS
C ARE PRINTED. NCOUNT IS USED IN *QVECT* TO DETERMINE WHICH ACCEL-
C ERATION TO USE.

C ICOUNT=0
NCOUNT=0
IF (NONLIN .EQ. 0) THEN DO
C FOR A LINEAR ANALYSIS (NONLIN=0) THE STIFFNESS IS FORMULATED ONLY
C ONCE.

C CALL KMAT(AREA,C1,C2,C3,COORD,ELENG,EMOD,G,JCODE,
*          KEFF,MBD,MCODE,MINC,MXNEQ,NE,NEQ,Q,TLENG,X1,X2)
END IF

C BEGIN ANALYSIS.

C WHILE (T .LE. TIME) DO
CALL QVECT(ACCEL,COMP,JCODE,MASS,NCOUNT,NEQ,NJ,QEFF,TEMP)
IF (NONLIN .EQ. 1) THEN DO
    CALL KMAT(ARFA,C1,C2,C3,COORD,ELENG,EMOD,G,JCODE,KEFF,

```

```

*      END IF
DO 610 I=1,NEQ
  TEMP(I)=0.0
C
C FORM EFFECTIVE LOAD VECTOR.
C
DO 620 J=1,NEQ
  TEMP(I)=TEMP(I)+(KEFF(I,J)-A2*MASS(I,J))*Q(J)
*          +A0*MASS(I,J)*QMINST(J)
  CONTINUE
  QEFF(I)=QEFFF(I)-TEMP(I)
C
C DISPLACEMENTS (QPLUST) ARE FOUND. THEN VELOCITIES AND ACCELER-
C ATIONS FROM EQN. 9.10 BATHE.
C
QPLUST(I)=QEFFF(I)*DELT**2/MASS(I,I)
QDP(I)=A0*(QMINST(I)-2*Q(I)+QPLUST(I))
QP(I)=A1*I-QMINST(I)+QPLUST(I)
  CONTINUE
DO 630 K=1,NEQ
  QMINST(K)=Q(K)
  Q(K)=QPLUST(K)
  CONTINUE
  ICOUNT=ICOUNT+1
C
C PRINT DESIRED RESULTS.
C
IF(MOD(ICOUNT,1).EQ.0) THEN DO
  PRINT 5
  PRINT 10
  PRINT 20,T

```



```

C***** SUBROUTINE KMAT *****
C FORMULATES THE EFFECTIVE STIFFNESS MATRIX TO BE USED IN FINDING
C THE EFFECTIVE NODAL LOAD VECTOR. (SEE BATHE P. 502)
C
C SUBROUTINE KMAT(AREA,C1,C2,C3,COORD,ELENG,EMOD,G,JCODE,
*      KEFF,MBD,MCODE,MINC,MXNEQ,NE,NEQ,Q,TLENG,X1,X2)
C
C IMPLICIT REAL*8 (A-H,O-Z)
C
C REAL*8 KEFF(MXNEQ,NEQ)
C
C DIMENSION AREA(1),C1(1),C2(1),C3(1),COORD(3,1),ELENG(1),
*      EMOD(1),G(6),JCODE(3,1),MCODE(6,1),MINC(2,1),Q(1),
*      TLENG(1),X1(3),X2(3)
C
C INTEGER INDEX(6,6)/1,4,5,-1,-4,-5, 4,2,6,-4,-2,-6, 5,6,3,-5,-6,-3,
*      -1,-4,-5,1,4,5, -4,-2,-6,4,2,6, -5,-6,-3,5,6,3/
C
DO 165 I=1,NEQ
  DO 166 J=1,NEQ
    KEFF(I,J)=0.0D00
166  CONTINUE
165  CONTINUE
  DO 170 N=1,NE
C
C CALL 'LENCO'S* TO DETERMINE THE DEFORMED LENGTH OF ELEMENT 'N'.
C (REFER TO CHAPTER 2 OF THESIS FOR DERIVATION).
C
C
CALL LENCO(C1,C2,C3,COORD,JCODE,MINC,N,Q,TLENG,X1,X2)
  GAMMA=EMOD(N)*AREA(N)/TLENG(N)
  G(1)=GAMMA*(TLENG(N)/ELENG(N)-(1.-C1(N)**2))
  G(2)=GAMMA*(TLENG(N)/ELENG(N)-(1.-C2(N)**2))
  G(3)=GAMMA*(TLENG(N)/ELENG(N)-(1.-C3(N)**2))
  G(4)=GAMMA*C1(N)*C2(N)

```

```

G(5)=GAMMA*C1(N)*C3(N)
G(6)=GAMMA*C2(N)*C3(N)

C ASSEMBLE FULL "UNBANDED" MATRIX "KEFF".
C

DO 180 JE=1,6
  J=MCODE(JE,N)
  IF (J .NE. 0) THEN DO
    DO 190 IE=1,6
      I=MCODE(IE,N)
      IF (I .NE. 0) THEN DO
        L=INDEX(IE,JE)
        IF (L .GT. 0) THEN DO
          KEFF(I,J)=KEFF(I,J)+G(L)
        ELSE DO
          KEFF(I,J)=KEFF(I,J)-G(-L)
        END IF
      END IF
    END IF
  CONTINUE
  END IF
190  CONTINUE
END IF
180  CONTINUE
170 CONTINUE
RETURN
END

```

**The vita has been removed from  
the scanned document**

THE EFFECTS OF EARTHQUAKE EXCITATIONS  
ON RETICULATED DOMES

by

David A. Uliana

(ABSTRACT)

Comparisons were made on the behavior of two full-sized reticulated domes subjected to uniform static loads only and uniform static loads with earthquake excitations. Space truss elements were used in the dome models. The stiffness matrix of the space truss element allows for the nonlinear strain-displacement behavior and the stress-strain behavior of the material is modeled with a bilinear approximation. The nonlinear solution technique is the Newton-Raphson method while the direct integration technique is the Newmark-Beta method.

The joint displacements for the static and the dynamic analyses were compared for both domes along with the axial stresses in all members. The percentage increases in the axial stresses of the dynamic analyses as compared to those of the static analyses were determined.

The reticulated domes used in the study were found to be capable of withstanding the earthquake excitations when subjected to various uniform loads without failure.